1-1-2007

Study of impact of sonic energy waves on the rate of precipitation of particles in liquid

Abdisamed Sheik-Qasim
Ryerson University

STUDY OF IMPACT OF SONIC ENERGY WAVES ON THE RATE OF PRECIPITATION OF PARTICLES IN LIQUID

by

Abdisamed Sheik-Qasim, BSc

Somali National University, Lafole College of Education, Mogadishu, 1982

A thesis

presented to Ryerson University

in partial fulfillment of the

requirements for the degree of

Master of Applied Science

in the program of

Chemical Engineering

Toronto, Ontario, Canada, 2007

Author's Declaration

I hereby declare that I am the sole author of this thesis.

I authorize Ryerson University to lend this thesis to other institutions or individuals for the purpose of scholarly research.

Abdisamed Sheik-Qasim

I further authorize Ryerson University to reproduce this thesis by photocopying or by other means, in total or in parts, at the request of other institutions or individuals for the purpose of scholarly research.

Abdisamed Sheik-Qasim

Study of Impact of Sonic Energy Waves on the Rate of Precipitation of Particles in Liquid.

Master of Applied Science (MASc), 2007

Abdisamed Sheik-Qasim

Chemical Engineering

Ryerson University

Abstract

The effects of sonic energy waves on the settling velocity of small particles in water were studied. A design of experiment (DOE) with five variables (frequency, amplitude, particle diameter, particle density and fluid viscosity) at two or three levels was conducted to obtain the particle settling velocity as the response. The DOE data were analyzed both experimentally and by a statistical multiple regression software. It was concluded that when sound frequency and amplitude in the range of 0 to 500 Hz and 2 to 3 Vrms (root mean square) respectively were applied to plastic particles of three different diameters (2,381 μm, 3,175 μm and 4,763 μm) and two different densities (1.14 g/cm^3 and 1.40 g/cm^3), their effects on the particle settling velocity in hydroxypropyl cellulose (HPC) solutions of three different viscosities (1.30×10^{-2} g/cm.s, 4.57×10^{-2} g/cm.s and 7.02×10^{-2} g/cm.s) were insignificant. The regression analysis gave an equation that is in good agreement with the experimental data.

Acknowledgement

I would like to express my sincere appreciation to Dr. Farhad Ein-Mozaffari (RU) and Dr. Hwee Ng (XRCC) for their professional support and understanding. A much added thanks for the time spent in addressing the numerous questions and concerns of the author. The tireless encouragement of Dr. Stephan Drappel (XRCC) is also unforgettable. The services offered by Mr. Gaetano Lavigne and Mr. Johann Junginger for their support services in building the equipment at Xerox Research Centre of Canada were greatly appreciated.

My thanks also go to the faculty members and staff of the Department of the Chemical Engineering for their contribution to my career development during my program in the University.

This thesis is dedicated to the late Dr. Muhammad E. Fayed who selected this topic for me and supervised most of my time in the University.

It is also dedicated to my wife and children who gave me support and joy whenever I needed it.

Table of Content

List of Tables

List of Figures

Nomenclature

Symbols Description

λ Sound Wavelength

μ, η Viscosity of the fluid ($g.cm^{-1}.s^{-}1$ or poise)

a Particle acceleration ($cm.s^{-2}$)

A, A_p Frontal area of the particle (cm^2)

C_D Drag coefficient

d_f Density of the fluid ($g.cm^{-3}$)

d_s Density of the sphere ($g.cm^{-3}$)

D_p Diameter of the sphere (cm)

D_r Drag

g Acceleration due to gravity ($cm.s^{-2}$)

Hz Hertz, unit of frequency

m Mass of the sphere (g)

N_D Dimensionless number

ρ_f Density of the fluid ($g.cm^{-3}$)

ρ_p Density of the particle ($g.cm^{-3}$)

r Radius of the sphere (cm)

Re Reynolds number

v, v_s fall velocity of the sphere ($cm.s^{-1}$)

V Terminal velocity ($cm.s^{-1}$)

V_p Volume of the sphere (cm^{-3})

V_{rms} root mean square, unit of amplitude

V_y Particle settling velocity at y direction ($cm.s^{-1}$)

w Dimensionless number

W Weight, Gravity force ($g.cm.s^{-2}$)

Chapter 1

1. INTRODUCTION

Numerous fields of modern technology require that materials which are being carried by a fluid system be separated from the liquid. For example, many industrial processes generate waste water which is contaminated by particulate matter. Separation of the particulate matter from the fluid allows the water to be easily disposed of and the particulate matter, if valuable, put to a good use. Furthermore, it is often desirable to separate an immiscible liquid or undissolved gas from a liquid.

The number of occasions in which it is necessary to separate particulates from a fluid medium is so pervasive that an extraordinary amount of attention has been devoted to the development of methods and apparatus to affect such separations.

1.1 Classical Methods for Particle Segregation

One of the most rudimentary, yet pervasive, of separation techniques involves simple sedimentation. Sedimentation is the natural settling process wherein the particulates or immiscible liquids are separated due to gravitational force. The medium may then be removed by decanting or suction, while taking care not to disturb the particulates which have settled out of the medium.

Sedimentation techniques have the advantage of being simple and inexpensive. Unfortunately, the characteristics of the medium and the particles to be separated are often the same such that the time required for separation by sedimentation can be so long as to make this technique entirely impractical. Furthermore, if the particles are of a very

small size, the particles will never "settle out" due to the Brownian motion of the molecules. Still further, if the carrying liquid is not kept free of any turbulence until sedimentation is complete, the particles will become re-suspended. As a result, simple sedimentation techniques are practical only in certain limited situations.

In recognition of the fact that gravitational forces are too weak to effect rapid sedimentation in many instances, a frequent approach utilized in the prior art in order to increase the sedimentation rate of the material is to increase the gravitational force. This may be accomplished by subjecting the particle and medium mixture to centrifugation.

Centrifugation is a technique in which a container holding the particle and medium mixture is spun about a central axis in order to create centrifugal forces extending radially from the central axis. Increasing the speed of rotation will increase the centrifugal force applied to suspended particles, thereby increasing the rate of sedimentation. Modern centrifuges are capable of generating forces many thousands of times greater than gravity (Allen et.al 1981).

Yet another general technique used to separate some types of particles from a medium is filtration. Filtration involves the use of a porous filter that allows passage of the medium, while forming a barrier to the particles to be separated out. The speed of filtration can be enhanced by the application of pressure. However, the speed of filtration markedly decreases as a layer of filtered material builds up against the filter. For optimum performance, the filter must be replaced or cleaned frequently.

Each of the foregoing techniques is widely practiced and is extremely useful in many applications. Yet, each technique suffers significant drawbacks which limits its application to many situations.

For example, as mentioned above, gravitational sedimentation is not effective in many instances when the particles or the medium exhibit particular characteristics, such as when the medium is extremely viscous. Although centrifugation often speeds up the process of separation in such cases, centrifugation is often not completely effective; moreover, centrifugation is ill suited either for processing large quantities of a medium and particle mixture or for processing in continuous flow systems.

Filter techniques also suffer ineffectiveness when the particles to be separated from the medium begin to significantly build up on the filter. This build-up, or "caking", reduces the efficiency of the filter; at some point in the filtration process, this caking may completely stop the flow of the medium through the filter. If additional pressure is applied to the medium in order to improve the flow through the filter, damage to some types of separated material could possibly happen.

A brief review of the current technologies for particle separation is given in Table 1.1 along with some of the advantages and disadvantage of each method.

Table 1.1 Reviews of Current Technologies for Particle Segregation (Johnson et.al 1995)

Methods	Examples	Mechanics	Advantages	Disadvantages
Physical Methods	Filters	Particle size <0.75 mm	Inexpensive	High Pressure drops. Filter clogging. Fouling of filter material.
	Screens	Particle size <0.75 mm	Easy	Long time processing.
Size/density differences	Sedimentation	Settlement of particles at the bottom with higher density than fluid	Inexpensive	Long hold-up time. Not possible when density of particle and fluid are same.
	Centrifuge	Centrifugal force to settle the particles	Faster than sedimentation	Mechanical failure. Small quantities.
Electric and Magnetic fields	Electric charge	Electrical or magnetic attraction or repulsion between the particles and suspended fluid	Fast, depending on chemical reactions. Easy	Requires high electric or magnetic fields. Induced or natural charges. High power consumption.

1.2 Gravity Sedimentation and Stokes Diameter

In gravity sedimentation methods for characterizing fine particles, the falling speeds of fine particles settling in a viscous fluid under the influence of gravity are measured. The measured speeds are transformed by using Stokes' equation into a size parameter known as Stokes diameter. The various sources of uncertainty in the measured Stokes' diameter distribution of a fine particle system arise from the various compromises that have to be made in the design of systems for studying the group dynamics of the fine particles.

In the published literature of sedimentation procedures for characterizing fine particles, there is considerable confusion over the interpretation of sedimentation data for irregularly shaped fine particles. It is sometimes claimed that "increasing error" occurs if sedimentation procedures are used to study highly irregular fine particles. This is a misleading statement. If irregular fine particles are allowed to sediment in a fluid, there is uncertainty range for the Stokes' diameter of the fine particle because different orientations of the fine particle are possible. For example, if an irregular fine particle falls with its largest dimension perpendicular to the direction of motion, it will fall more slowly than if its maximum dimension is aligned with the direction of fall. It has been shown that under laminar flow conditions the initial orientation of an irregular fine particle falling under gravity is maintained throughout the complete trajectory of the fine particle. Therefore, an irregular fine particle will have a range of settling speeds that will be interpreted as a range of Stokes' diameters. Furthermore, the average Stokes diameter of an irregular fine particle will differ from the diameter of the dense smooth sphere of the same material because the irregular fine particle drags stagnant fluid with it during its fall. The difference between the measured Stokes' diameter calculated by considering the dynamics of a sphere of equal volume is a measure of the shape of the fine particle. Before the physical reasons for this discrepancy were fully appreciated, the discrepancy was sometimes classified as an 'error'; it is now seen to be information concerning the structure of the fine particle. The containing vessel walls can interfere with the free fall of a fine particle. The presence of other fine particles in a suspension can also interfere with the free fall of a particle. Disturbances caused by the presence of other fine particles are referred to as concentration effects.

When measuring the Stokes' diameter distribution of a sedimenting suspension, two basic suspension systems can be used. In the simplest system the fine particles to be characterized are placed at the top of a column of fluid and the movement of the fine particles down the column is studied. Historically, this system has been referred to be in literature as a two-layer sedimentation system. This name is misleading since it implies that there are two layers in the column whereas there is only one layer of suspension on top of a column of fluid. The modern term for this type of system is line start procedure.

The movement of the fine particles down the column can be monitored as they pass through a given zone at a certain depth, a technique referred as incremental sampling of suspension. Characterization procedures that monitor the arrival of the fine particles at the base of a column of fluid are known as cumulative sedimentation methods.

The line start procedure has the advantage that each size of fine particle presents itself to an incremental measuring zone or cumulative rate-measuring device in decreasing order of magnitude, thus enabling the output of the instrument to be interpreted as a size distribution function with minimum data manipulation. The disadvantage of the procedure is ensuring the stability of the layer of suspension used in the line start sedimentation dynamics (Allen et.al 1981).

1.3 Need for a New Technology

Because of the limitations of conventional techniques for separating particles from a medium, a great deal of effort has been directed to developing new techniques as well as improving the conventional techniques. One technique of relatively recent origin is the application of ultrasound energy to particles in the medium to cause acoustic cavitation.

Cavitation enhances the ability of the particles to be exposed to oxygen and thus accelerate the action of aerobic bacteria. The term "cavitation" refers to the creation of disturbances in a fluid caused by formation of gas bubbles by the application of acoustic energy (Porath-Furedi et.al., 1997).

According to the Porath-Furedi (1997), ultrasonic standing waves are used to cause flocculation of small particles, such as blood or algae, so that they will settle out of the carrying liquid. The Porath-Furedi patent describes a separation process which submerges an ultrasonic wave generator within a liquid having particles suspended therein and energizing it so that standing wave is established.

The establishment of a standing wave in the medium results in formation of pressure nodes to which the particles tend to migrate; these nodes and antinodes are at right angles to the direction of propagation of the ultrasonic waves, and the nodes are spaced from adjacent nodes by a distance equal to one-half of the wavelength of the ultrasonic wave. The Porath-Furedi patent utilizes the accumulation of solid particles at the nodes or antinodes to cause flocculation, thereby assisting in simple gravitational sedimentation of the suspended particles when the ultrasonic standing wave is discontinued.

Ultra-fine particles and particles with neutral buoyancy, or a uniform electromagnetically charged surface pose difficulties with fractionation. Existing methods require excessive time, prohibitive pressure drops, or extremely high electric or magnetic fields. Also, in the case of particles having very narrow ranges of sizes and densities, none of the above methods can be used. Based on the above discussion there is a need for cost effective

technology for studying the characteristics of particles. In this study we investigated the impact of sonic energy waves on the rate of precipitation of particles in a liquid.

1.3.1 Basic Definitions

In order to understand this technology, brief introductions of various terms used in this proposed technology are given below.

1.3.2 Acoustic. The science that deals with production, control, transmission, reception, and effects of sound is called Acoustics.

1.3.3 Sound. Sound is generated by pressure variation in a medium. Sound waves can be produced in a medium when there is continuous expansion and contraction of the medium by a mechanical excitation of a sound source.

1.3.4 Piezoelectric. A common sound source is vibrating piezoelectric crystals. Piezo is derived from a Greek word, "to press", thus, piezoelectric means pressure electric. A plate cut from piezoelectric crystal with an applied electrical signal, serves as a device for converting electrical energy to mechanical energy.

1.3.5 Transducer. A sound source usually made of piezoelectric crystals for generating sound waves is called a transducer. When an electrical signal with a given frequency is sent to the transducer, electrical energy is converted to mechanical energy. This mechanical energy causes the medium to vibrate; expanding when the electrical voltage is positive and contracting when the electric voltage is negative. The expansion and contraction of the transducer causes compression and contraction of the medium, producing acoustic sound waves in the medium. If the frequency of vibration is higher than 18,000 cycles per second, it is not audible and is called ultrasound (Holland R.1969)

1.3.6 Standing waves. When the traveling waves meet a perpendicular boundary, they are reflected back to the source. These reflected waves carry some amount of energy. If waves are continuously sent out and reflected back, the two waves reach a state of equilibrium, when the distance between the source and the reflector is a multiple of a half-wavelength, $n\lambda/2$, where n is an integer number and λ is the sound wavelength. This type of wave field is called an acoustic standing wave field. Thus, the necessary and sufficient condition for the formation of a standing wave is that the distance between the source and the reflecting source (L) is $L=n\lambda/2$. The standing wave with n=1 is called the fundamental or first harmonic. The wave for n=2 is the second harmonic, the wave for n=3 is the third harmonic and so forth. This is shown in figure 1.1 with corresponding wavelength λ and the distance between the two boundaries.

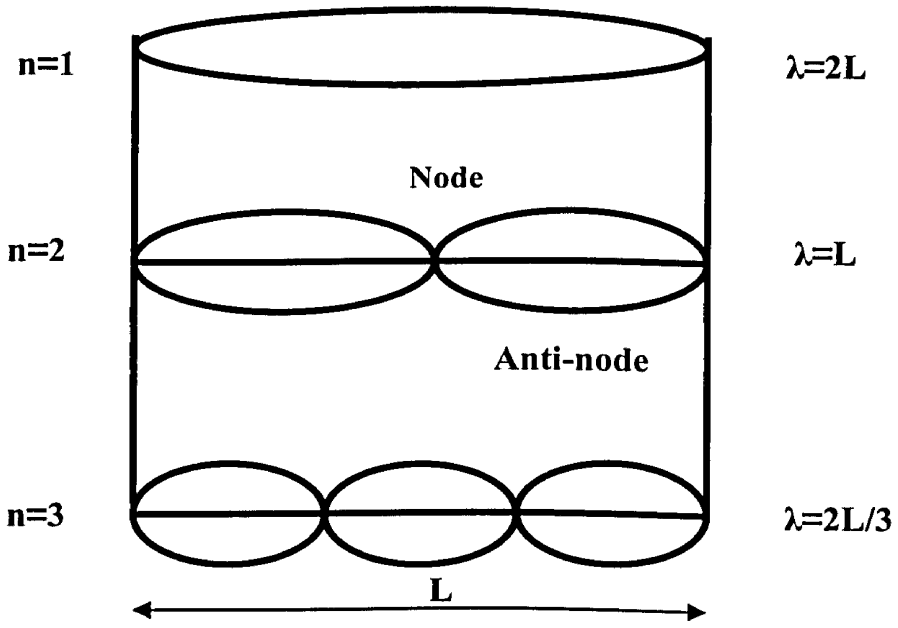

Figure 1.1 Standing Waves

1.3.7 Acoustic Radiation and Energy. The total energy in a sound wave is always the summation of the kinetic and potential energies. The waves of energy, which travel at the speed of sound in an acoustic field, are the acoustic radiation. Under a stable situation in a standing wave, the amount of energy at various points in the path of travel for a standing wave may differ and points of maximum and minimum energy occur. If the frequency is changed, the wavelength changes cause a shift in the position of maximum and minimum energy. The force exerted by an acoustic standing wave field on the medium is called the acoustic radiation force.

1.3.8 Acoustic Pressure and Velocity Amplitudes in an Acoustic Field. A plane standing-wave field arises from the superposition of two waves of equal wavelength and amplitude traveling in opposite directions. Equal wavelengths are necessary for reflection of the waves, and equal amplitudes are required to have constant pressure values at any time along the wave-guide. Figure 1.2 shows the formation of stationary planes of maximum velocity or zero pressure (anti-node planes) and zero velocity or maximum pressure (node planes) in the medium. The node planes lie at half wavelength intervals, with the antinode planes lying equidistant between them. The pressure nodes coincide with the velocity antinodes and vice versa.

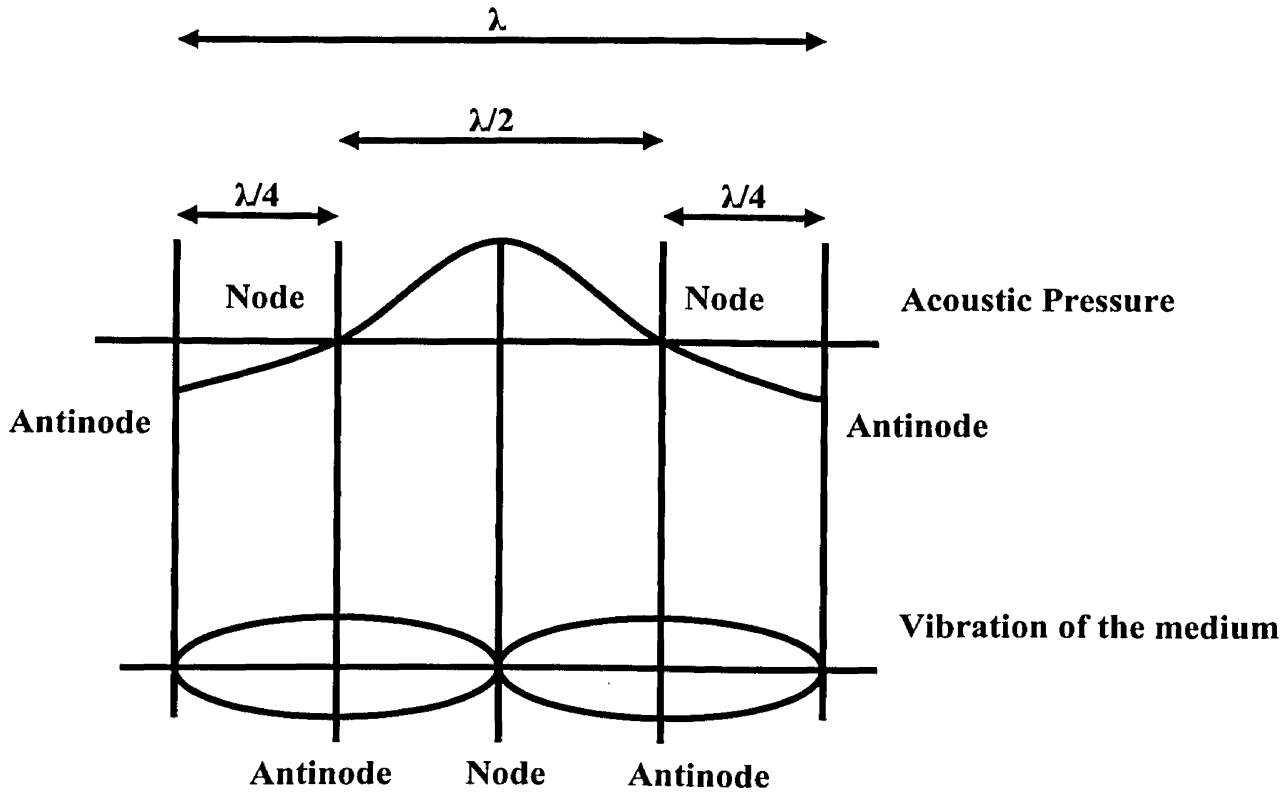

Figure 1.2 Planes of Nodes and Antinodes

1.4 Research Objective

The primary objective of this research is to study the behaviour of particulates based on the effect of acoustic waves, which is a function of particle densities, particle diameter, fluid viscosity and compressibilities of fluid. Compressibility is a measure of the amount of volume reduction due to pressure. Compressibility is sometimes expressed by the "bulk modulus," which is the reciprocal compressibility of acoustic forces generated by acoustic pressure and can drive particles to locations of zero acoustic pressure within the acoustic standing wave field. The magnitude of acoustic forces acting on a particle in a medium depends on the acoustic contrast.

For particles with little or no density contrast, the proposed technique is able to discriminate them on the basis of their compressibility. Particles with different size,

density, or compressibility respond at different rates to the imposed acoustic wave field. The ultimate separation between the fluid and the particles is achieved by either removing the fluid while the particles are held stationary by applying force or pressure which can act on the particles only, or by transporting the particles through the fluid while keeping the fluid stationary by applying a special type of acoustic force on the particles.

The application of an acoustic field in order to change the terminal velocity of a settling particle will be studied in this research. The acoustic effect studied in this research will help providing an alternative to the classical fractionation methods for sediments. Only a few separation or purification methods exist for the discrimination of particulate materials based on their compressibility. Conventional methods rely upon differences in particles density (centrifugation or sedimentation), size (sieve or filtration), thermodynamic properties (selective solubility), electrical charge (electrophoresis), or interfacial properties (floatation). However, particles that have traits such as small size, neutral buoyancy, or uniform electromagnetic characteristics pose difficult fractionation problems. As stated before, the existing methods usually require excessive time, prohibitive pressure drops, or extremely high electric or magnetic fields.

Some of the advantages of using this technology of acoustic energy separation are to increase the resolution of the separation of the sediments, high production rates by continuous acoustic treatment, and low energy requirement. Unique separation of neutral buoyant particles and particles exhibiting compressibility differences can be achieved.

Chapter 2

2. Literature Search

The potential of separation techniques utilizing acoustic radiation pressure on suspended particles is known but has been relatively less developed. A surprising result was obtained during the sonication of *E.coli* in that the size of the particles increased.

Initially the *E.coli* bacteria suspension showed particles less than 1μm, i.e. too small to be detected accurately by the particle size analyzer. The particle size of the suspension increased to a maximum size of 10.6 μm after 15 minutes sonication. These particles were then separated from the remaining suspension which contains viable (live) *E.coli* cells by centrifugation. The particles were then washed with saline solution and resuspended in nutrient agar and incubated for 24 hours to see if any viable bacteria were present. After 24 hours it was seen that no *E.coli* colonies grew on the agar. Ultrasound appears to kill some of the *E.coli* cells as expected and then aggregates the dead cells into larger clumps. (Phull, et.al., 1997)

Micron size particles do aggregate when subjected or exposed to an acoustic standing wave field and was first observed by Kundt and Lehmann (1874). This theory was not implemented practically until very recently. The search for solving problems relating to particle-liquid separation has enhanced a fresh interest in systems that make use of the acoustic forces on particles suspended in a standing wave field. During the last decade, there has been a tremendous interest in studying the characteristics of particulates, droplets or bubbles suspended in liquid or gases by forces associated with a resonant

acoustic field. When a particle suspended in a medium in the presence of an acoustic field, it will experience force associated with the field. It was recognized by Kundt (1874) that the acoustic pressure in a medium having waves propagating in one direction, is normal to the waves and is numerically equal to the energy per unit volume. He also observed the effect of acoustic forces through measurements of the motion of dust particles in resonant tubes. The first detailed theoretical formulation of acoustic forces for a rigid sphere in a plane standing or progressive wave field in an ideal fluid was presented by King (1934). He calculated the radiation forces by adding the effect of acoustic pressures acting on each surface element of the rigid sphere. Yosioka and Kawasima *(1955)* extended this method to include the effects on compressible spheres. King's theory was verified experimentally for liquid (Klein, 1938) and gaseous (Rudnick, 1977) media. King's (1934) approach was later extended by Embleton (1956) to the case of a rigid sphere in a progressive spherical or cylindrical wave field. Gor'kov (1962) derived a simple method to determine the forces acting on a particle in an arbitrary acoustic field using a different approach than that proposed by King *(1934).* He illustrated that his expression was equivalent to King's expression for a plane standing wave. Nyborg (1967) also derived simple expressions for the acoustic force by extending the methods of King and Embleton. In the case of standing waves, Nyborg's expression was reduced to that of Gor'kov.

When particles are suspended in an acoustic field, the medium exerts hydrodynamic forces on them. In an acoustic field, forces exerted on particles in the medium are proportional to the local velocities of the fluid and their average becomes zero. In an

acoustic standing wave field, the average of the forces acting on a particle are not zero and play an important part as they arise from second order effects (Gor'kov, 1962).

As the diameter of the bubble approaches the pipe diameter, the shape of the bubble is deformed into a lengthwise ellipse and rising velocity slows due to the pipe wall. The velocities and shapes of single bubbles are obtained for both standing waves formed in the axial direction of pipes and in the radial direction. When an initial spherical bubble rises through the node of the radially formed standing wave in pipes, it is deformed into a lengthwise elliptical shape by the acoustic radiation force even if the wall effect is small, and the velocity of the bubble is faster than that for when there is no ultrasonic field. In other cases, the average terminal velocity of bubbles is slower than that for when there is no ultrasonic field.

2.1 Theory

2.1.1 Settling Velocity and Stokes' Law

Settling velocities used in the sedimentation analysis of silt and clay are usually computed from the now-famous settling law developed by Stokes in 1851. Stokes' law pertains to the terminal fall velocity of a sphere in a fluid and is explained as follows:

VRF (the viscous resistance to fall of a sphere in fluid) = $6\pi r\mu\upsilon$ 2.1

Where r, μ, and υ are the radius of the sphere in cm, the viscosity of the fluid in dyne.sec.cm^{-2} (poises) or g.cm^{-1}s^{-1} and the fall velocity of the sphere in cm/s, respectively.

NDF (the net downward force on a sphere in a fluid) = the force of gravity on the sphere minus the buoyant force of the fluid

$$NDF = \frac{4}{3}(\pi r^3 d_S g) - \frac{4}{3}(\pi r^3 d_f g) \qquad 2.2$$

Where r, d_S, d_f and g are the radius of the sphere in cm, the density of the sphere in g/cm^3, the density of the fluid in g/cm^3 and the acceleration due to gravity in cm/sec^2, respectively.

However, the terminal fall velocity is reached when *VRF* = *NDF*, that is, when

$$6\pi r \mu \upsilon = \frac{4}{3}(\pi r^3 d_S g) - \frac{4}{3}(\pi r^3 d_f g) \qquad 2.3$$

or when

$$\upsilon = \frac{2(d_S - d_f) g r^2}{9\mu}, \qquad 2.4$$

which is Stokes' law, where υ is now the terminal fall velocity of the sphere in cm/s.

Stokes' law as used in sedimentation analysis at a particular temperature is commonly simplified to

$$\upsilon = CD^2 \qquad 2.5$$

where C is a constant equal to:

$$C = \frac{(d_s - d_f) g}{18\mu}, \qquad 2.6$$

Stokes' law cannot be applied indiscriminately to all particles settling in a fluid. In the strictest theoretical sense, it is only valid under the following conditions and limitations.

1. Particles must have reached terminal fall velocity. For particles within the size range of applicability of Stokes' law, the terminal fall velocity is reached almost instantaneously. Weyssenhoff (1920) has shown that for a sphere with a diameter of 50 μm, the terminal fall velocity is reached in about 0.003 second. For smaller particles, the time is even less.
2. Particles must be rigid. All particles analyzed sedimentologically fulfill this condition.
3. Particles must be smooth. Most particles analyzed sedimentologically are not smooth. Arnold (1911) has shown that within the size range of applicability of Stokes' law, grains with irregular surfaces do not have any appreciable difference in settling velocity from smooth grains and the theoretical condition has no practical validity.
4. No slippage or shear may take place between the particle and the fluid. This depends on the wettability of the particle in the fluid, and the condition is fulfilled when water is used as the fluid.
5. The fluid must be of infinite extent in relation to the particles. A particle settling near the wall of a container will have its settling velocity decreased by an amount dependent on the nearness of the wall and the size of the particle. In the size range of Stokes' law, the wall effects are negligible if the sedimentation vessel is greater than 4 cm in diameter. Most 1000 ml graduated cylinders used in the pipette analyses of silt and clay are larger than this.

2.1.2 Forces on Falling Object

The three basic forces that act on an immiscible particle suspended in a liquid are: **Weight** is the gravitational force acting on the particle. It acts downward.

Buoyancy is the lifting or upward force that a carrying liquid imparts on a floating or submerged body. It is equal to the weight of the displaced volume of the carrying liquid.

Drag, D_r, is the resistance to motion that the carrying fluid imparts on a particle. It is opposite to the direction of motion of the particle relative to the liquid, and is basically due to frictional effects.

For a sphere rising at constant velocity, the buoyant force is dominant and acts upward. The gravity force (weight) acts downward and the drag force acts opposite to the direction of motion. Thus for a rising sphere, Buoyancy = Weight + Drag

Drag

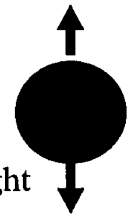

Weight

Weight is constant: $W=mg$ 2.7

Resistance (Drag) = $C_D \frac{rV^2A}{2}$ 2.8

Motion of object (Newton's second law)

$F=ma$ 2.9

$$a = \frac{F}{m} = \frac{(W - D_r)}{m} \quad 2.10$$

When Drag, D_r, is equal to Weight, acceleration is zero.

Velocity becomes constant (terminal velocity).

2.1.3 Shape effects on Drag

The shape of an object has a very great effect on the amount of drag.

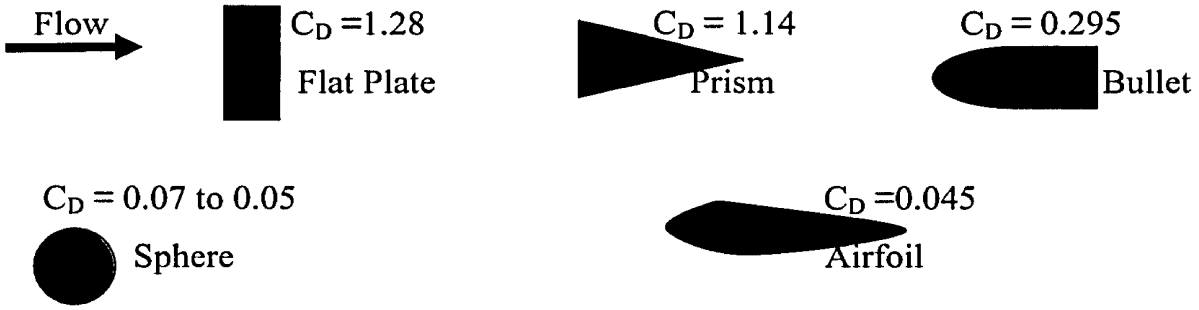

$$C_D = \frac{D_r}{rAV^2/2} \qquad 2.11$$

where A is the frontal area; All objects have the same frontal area.

2.1.4 Cavitation

Cavitation is created in a fluid by highly intensive ultrasonic waves. Cavitation bubbles increase and subsequently implode within a very short time. The implosion results in high pressures and temperatures and in liquid jet streams with up to 400km/h. The jets hit against the surface of particles or materials and remove the impurities or de-agglomerate powders. Cavitation is the formation, expansion, and implosion of microscopic gas bubbles in liquid as the molecules in the liquid absorb ultrasonic energy. Compression and rarefaction waves rapidly move through the liquid media. If the waves are sufficiently intense they will break the attractive forces in the existing molecules and create gas bubbles. As additional ultrasound energy enters the liquid, the gas bubbles grow until they reach a critical size.

Ultrasound represents mechanical waves, i.e. a variation of pressure or density, with frequencies above the human hearing threshold (≈ 18 kHz). As it is not perceived high sound intensities are feasible, where non-linear phenomena like acoustic cavitation occur. Due to high sound intensities the tensile stress of the liquid is exceeded. Little gas bubbles are formed during the expansion cycle of the sound wave and grow over one or several cycles. When having reached a critical size they collapse intensively during the compression cycle. During the collapse a lot of energy is set free inducing extreme thermodynamic conditions of several thousand Kelvin and a few hundred bars in the vicinity of imploding bubbles. Near solid surfaces cavitation bubbles collapse asymmetrically, forming so called micro-jets, which reach speeds up to 500 m/s. Depending on frequency and intensity, different mechanical, thermal and radical effects arising from cavitation dominate (Mason, 1991).

When an ultrasonic wave propagated into fluid is obstructed by a plate, a standing wave is formed between the ultrasonic transducer and the plate. Owing to the force induced by acoustic radiation pressure, small particles in a medium move to the node and anti-node of the standing wave. Lately, manipulation and levitation using ultrasoncic waves are being studied actively as non-contact technique (Aboobaker et al., 2001, Danilov et al., 1984)

On the other hand, cavitation bubbles and acoustic streaming are generated in a liquid by applying ultrasonic vibration above a certain sound pressure. It has been well documented that these effects induce agitation and fluidization, and increase the heat transfer coefficient remarkably (French, 1971, Gould et al., 1991).

Ultrasound has also found important uses for initiation or enhancement of catalytic reactions, in both homogenous and heterogeneous systems. These "cavities" or areas of low pressure provide a sink of low concentration or partial pressure of the most important factor for determining dispersion and de-aggregation of soil in ultrasonic systems (Watson, 1971).

The disintegration of sewage by means of ultrasound is based on the effects of acoustic cavitations in the liquid sewage sludge. Cavitation is "the formation, growth, and implosive collapse of bubbles in a liquid. Cavitational collapse produces intense local heating "hotspot" (~5000 K), high pressures (~1000 atm), and enormous heating and cooling rates (>10^9 K/sec)" and liquid jet streams (~400 km/h) (Suslick 1998). These very intense conditions serve for the destruction of the biological materials, such as sewage.

2.1.5 Drag on spherical particles and steady settling velocities

Most textbooks present results for the dependence of the drag coefficient for a smooth sphere, C_D, on the Reynolds number, Re, in the form of a curve. Such curves are difficult to read accurately especially without a fine grid. Also, finding of the terminal settling velocity of a sphere in a fluid using this curve is a repeating process. Clift (1978) provided correlations based on experimental data that can be used to determine either the drag coefficient or the settling velocity directly. Their results are reproduced below for using solving problems. The standard definitions of the Reynolds number and the drag coefficient are given below.

$$\mathrm{Re} = \frac{D_p V \rho}{\mu} \qquad 2.12$$

$$C_D = \frac{8 D_r}{\pi \rho D_p^{\,2} V^2} \qquad 2.13$$

$$V = \left[\frac{8 D_r}{\pi C_D \rho_f D_P^{\,2}} \right]^{\frac{1}{2}} \qquad 2.14$$

Here,

D_P, V, ρ_f, μ, and D_r are the diameter of the sphere, the velocity of the sphere, the density of the fluid, the viscosity of the fluid and the drag on the sphere, respectively

2.1.6 Drag Coefficient

The entire range of Reynolds numbers has been divided into 10 intervals and in each, the curve for the drag coefficient versus the Reynolds number is fitted to a suitable expression by Clift (1978).

In the results given below, $w = \log \mathrm{Re}$ 2.15

Table 2.1 Reynolds Number and Drag Coefficient Correlations (Clift et.al 1978)

Reynolds Number Range	**Drag Coefficient**
For $\mathrm{Re} \leq 0.01$	$C_D = \frac{9}{2} + \frac{24}{\mathrm{Re}}$
For $0.01 < \mathrm{Re} \leq 20$	$C_D = \frac{24}{\mathrm{Re}} + \left[1 + 0.1315\,\mathrm{Re}^{(0.82-0.05w)}\right]$
For $20 \leq \mathrm{Re} \leq 260$	$C_D = \frac{24}{\mathrm{Re}} + \left[1 + 0.19355\,\mathrm{Re}^{(0.6305)}\right]$
For $260 \leq \mathrm{Re} \leq 1.5\times10^3$	$\log_{10} C_D = 1.6435 - 1.1242w + 0.1558w^2$
For $1.5\times10^3 \leq \mathrm{Re} \leq 1.2\times10^4$	$\log_{10} C_D = -2.4571 + 2.5558w + 0.9295w^2 + 0.1049w^3$
For $1.2\times10^3 \leq \mathrm{Re} \leq 4.4\times10^4$	$\log_{10} C_D = -1.9181 + 0.6370w - 0.0636w^2$
For $4.4\times10^4 \leq \mathrm{Re} \leq 3.38\times10^5$	$\log_{10} C_D = -4.3390 + 1.5809w - 0.1546w^2$
For $3.38\times10^5 \leq \mathrm{Re} \leq 4\times10^5$	$C_D = 29.78 - 5.3w$
For $4\times10^5 \leq \mathrm{Re} \leq 10^6$	$C_D = 0.1w - 0.49$
For $10^6 < \mathrm{Re}$	$C_D = 0.19 - \frac{8\times10^4}{\mathrm{Re}}$

It can be find that this velocity appears in both the drag coefficient and in the Reynolds number and the terminal settling velocity of a sphere can be calculated by performing a repetitive calculation to find the answer. To avoid doing this, Clift (1978) also provided results that permit the direct calculation of the terminal settling velocity. It must be mentioned that for terminal settling, the drag on the sphere is equal to its net weight, which is the weight minus the buoyant force on the sphere.

Buoyancy Force

$$F_G = (\rho_p - \rho_f) g V_p \qquad 2.16$$

Where ρ_P, ρ_f, g, and V_P are the density of the particle, the density of the fluid, the gravitational constant, and the volume of the particle,

Drag Force

$$F_D = \frac{C_D A_P \rho_f v_S^2}{2} \qquad 2.17$$

Where C_D, A_P, ρ_f, and v_S are the drag coefficient, the area of the particle, the density of the fluid, and the settling velocity,

Combining the above two equations gives,

$$v_S = \sqrt{\frac{2(\rho_P - \rho_f) g V_P}{C_D A_P \rho_f}} \qquad 2.18$$

The Reynolds number was defined in the same way as before, but with the understanding that it now applies with $V = V_{terminal}$. A new dimensionless group $N_D = C_D \mathrm{Re}^2$ is introduced in which the terminal settling velocity does not appear. This group could be calculated and use the equations given below to calculate the value of the Reynolds number corresponding to a given value of N_D as stated by Clift (1978).

From the Reynolds number, the terminal settling velocity could be immediately evaluated.

In the equations, $W = \log N_D$ 2.19

Table 2.2 Correlations for Re as a function of N_D (Clift et.al 1978)

Range	Correlation
For $N_D \leq 73$; $\mathrm{Re} \leq 2.37$	$\mathrm{Re} = \frac{N_D}{24} - 1.7569\times10^{-4}\ N_D^2 + 6.9252\times10^{-7}\ N_D^3 - 2.3027\times10^{-10}\ N_D^4$
For $73 < N_D \leq 580$; $2.37 < \mathrm{Re} \leq 12.2$,	$\log_{10}\mathrm{Re} = -1.7095 + 1.33438w - 0.11591w^2$
For $580 < N_D \leq 1.55\times10^7$; $12.2 < \mathrm{Re} \leq 6.35\times10^3$	$\log_{10}\mathrm{Re} = -1.81391 + 1.34671w - 0.12427w^2 + 0.006344\,w^3$
For $1.55\times10^7 < N_D \leq 5\times10^{10}$; $16.35\times10^3 < \mathrm{Re} \leq 3\times10^5$	$\log_{10}\mathrm{Re} = 5.33283 - 1.217281\,w + 0.19007w^2 - 0.007005\,w^3$

The objective of this research is to study the settling velocity of particulates based on the effect of acoustic waves regarding the particle density, the particle diameter, the fluid viscosity and compressibilities.

Chapter 3

3. Experimental Set-Up and Procedures

In this chapter, details of the experimental design and procedures are discussed. This includes the electrical equipment required to produce the acoustic wave field, the design of transparent glass that holds the fluid, the selection of particles, the electrical equipment connections, and the image capturing techniques and analysis.

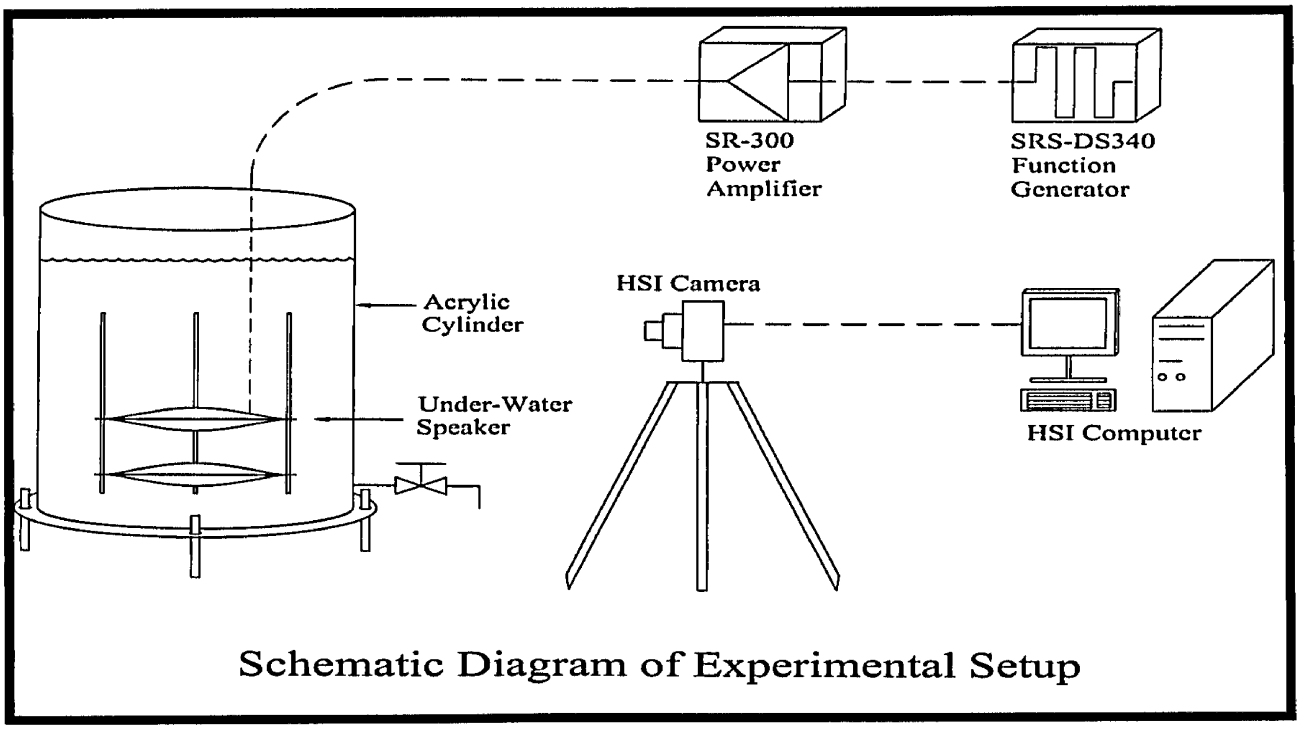

Figure 3.1 Schematic Diagram of the Experimental Setup
HSI (High Speed Imaging Camera)

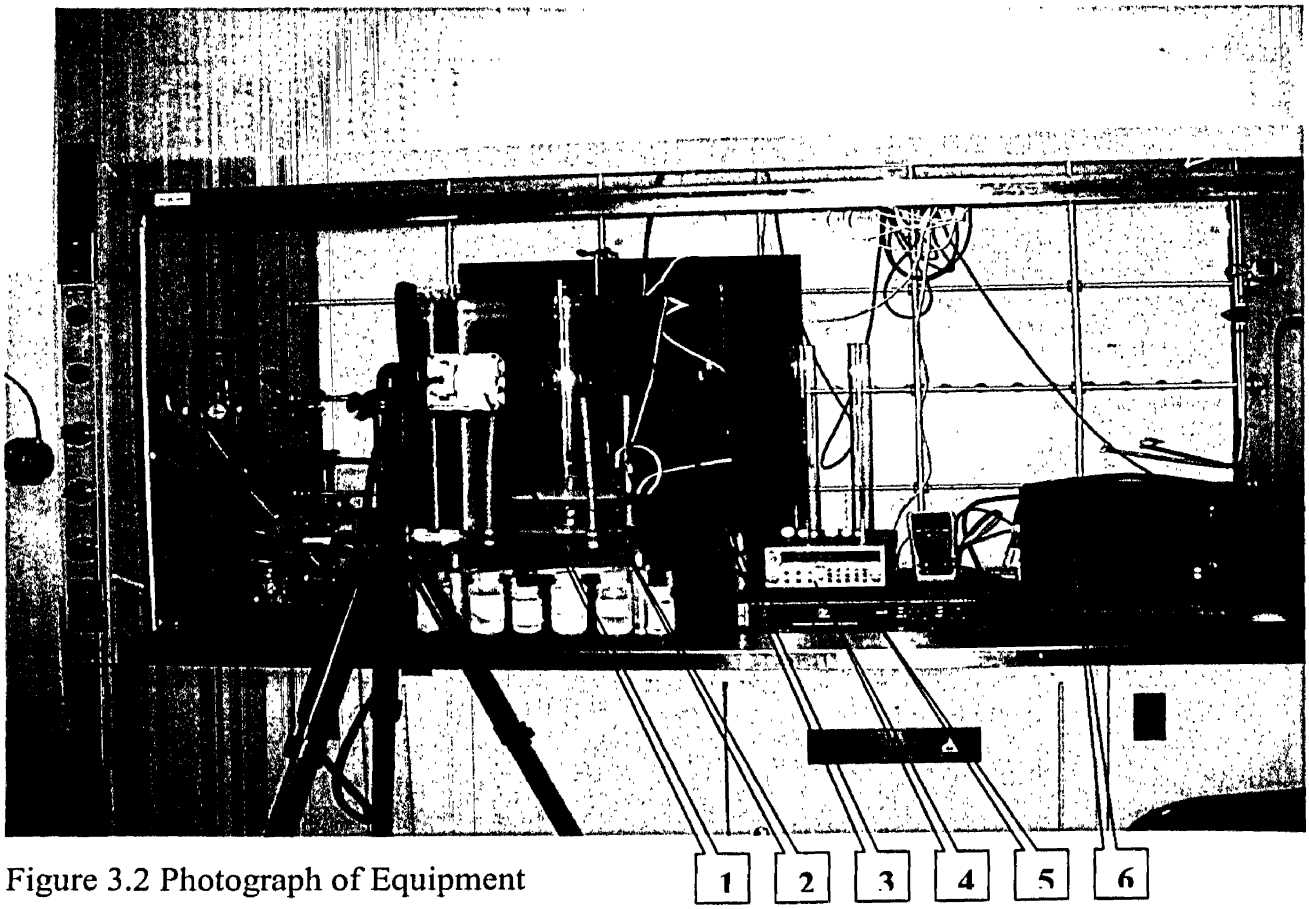

Figure 3.2 Photograph of Equipment

The experimental setup in the lab (1: HSI Camera; 2: Under-water Speaker; 3: Tank; 4: Function generator; 5: Amplifier; 6: HSI Computer)

3.1 Electrical Equipment

To implement this technology, the above physical model was built and electrical equipment was acquired to provide resonance in the chamber. The electrical equipment, which was used in this research, includes: a function generator and power amplifier. The function of each unit and their connections are given below.

3.2 Function Generator

The DS340 is a 15 MHz function and arbitrary waveform generator based on Direct Digital Synthesis (DDS). Sine waves and square waves can be generated at frequencies up to 15.1 MHz, and ramps and triangles up to 100 kHz. Frequency resolution is 1 μHz for all functions. In this research only sine waves were used.

Table 3.1 Function generator Specifications

Specifications: **Frequency Range**		
	Max. Frequency	Resolution
Sine	**15.1 MHz**	**1 μHz**
Square	15.1 MHz	1 μHz
Ramp	100 kHz	1 μHz
Triangle	100 kHz	1 μHz
Noise	10 MHz	(Gaussian weighting)
Arbitrary	10 MHz	40 MHz/N (sample rate)
Output		
Source impedance	50 Ohms	
Grounding	Output may float up to ±40 V (AC + DC)	
Amplitude		
Range	50 mVpp to 10 Vpp into 50 Ohms, 100 mVpp to 20 Vpp into High-Z	
Resolution	3 digits (DC offset = 0 V)	
Offset	±5 VDC (50 Ohms), ±10 VDC (High-Z)	
Offset resolution	3 digits	
Accuracy	0.1 dB (sine output)	

Table 3.1 Function generator Specifications.....continued

Sine Wave	
Spurious response	<-65 dBc to 1 MHz, increases by 6 dB/oct above 1 MHz
Harmonic distortion	
DC to 20 kHz	<-70 dBc
20 kHz to 100 kHz	<-60 dBc
100 kHz to 1 MHz	<-50 dBc
1 MHz to 15 MHz	<-40 dBc
Phase noise	<-55 dBc (30 kHz band centered on carrier)
Square Wave	
Rise/fall time	<15 ns ± 5 ns (10 % to 90 %)
Asymmetry	<3 ns + 1 % of period
Overshoot	<2 % of amplitude (full output)
Ramps and Triangles	
Rise/fall time	45 ns (10 MHz Bessel filter)
Linearity	±0.1 % of full scale
Settling time	200 ns (0.5 % of final value)
Arbitrary Waveforms	
Sample rate	40 MHz or integer sub-multiples
Waveform length	8 to 16,300 points
Vertical resolution	12 bits
Rise/fall time	45 ns (10 MHz Bessel filter)
FSK Modulation	
Modes	Internal, External
Max. rate	50 kHz, internal
External FSK	TTL input, 1 MHz (max.)
Sweeps	
Type	Linear and logarithmic (phase continuous)
Span	Linear (full frequency range), log (6 decades)
Sweep rate	0.01 Hz to 1 kHz

Table 3.1 Function generator Specifications.....continued

Timebase Accuracy	
Standard	±5 ppm (20 °C to 30 °C)
Optional	TCXO, 2 ppm stability, 2 ppm aging (20 °C to 50 °C)
General	
Interfaces	Optional RS-232 and GPIB with DOS based arbitrary waveform software (AWC). All instrument functions can be controlled over interfaces.
Non-volatile memory	9 sets of instruments settings can be stored and recalled
Dimensions	8.5" x 3.5" x 13" (WHL)
Weight	8 lbs.
Power	35 W, 100/120/220/240 VAC, 50/60 Hz

3.3 Power Amplifier

The SR300 is the first member of series power amplifiers. A built in peak and average limiter protects studio monitors or other speakers from potentially harmful signals and keeps the output of the amplifier clean when operating near maximum power. The heat sinks are mounted on the side of the amplifier where the unit can dissipate heat up the side of the rack, away from other heat sinks in the rack.

All connectors are located on the back panel. Front mounted volume knobs, silent convection cooling, low induced hum toroidal transformer, binding post and 1/4" outputs, switchable limiter, clip, activity, and limiter indicators, switchable HP filter, and precision balanced inputs are all features that make the SR300 stand apart from the rest.

Figure 3.3 SR300 Power Amplifier

Power Amplifier Specifications:

Amplifier class A / B

Continuous Average Power @ 8 Ohms BCD (Watts) 110 (x2)

Continuous Average Power @ 4 Ohms BCD (Watts) 150 (x2)

Continuous Average Power @ 2 Ohms BCD (Watts) NA

Continuous Average Power Bridged BCD (Watts) NA

Burst Average Power @ 8 Ohms BCD (Watts) 125 (x2)

Burst Average Power @ 4 Ohms BCD (Watts) 195 (x2)

Burst Average Power @ 2 Ohms BCD (Watts) NA

Burst Average Power Bridged BCD (Watts) NA

Frequency Response (Hz, +/- 1dB) 20-20,000

Hum and Noise (un / Aweighted -dB) -95 / -98

THD -1kHz- 4 OHMS less than 0.015%

THD - 20Hz-20kHz, 4 Ohms less than 0.15%

Slew Rate (V/uS) 20

Slew Rate Bridged (V/uS) NA

Damping Factor (30 Hz - 400 Hz @ 8 Ohms) 400

Crosstalk (1kHz / 20Hz-20kHz) -60 / -40

Input Impedance - Bal/Unbal (Ohms) 20,000/10,000

Input Sensitivity (Vrms) For Full Power Out 1.4 V

Max Voltage Gain (dB) 25

CMRR @ 60Hz (min/typ) 54/66 dB

Stereo / Mono / Bridge (S/M/B) S

Protection DC,Load,Thermal

Limiter Peak / Average

High Pass Filter 35Hz, 12dB Octave

Cooling Passive Convection

Inputs - 1/4" Jacks 2

Outputs - Binding Post 2

Outputs - 1/4" Jacks 2

Power Consumption (typ/max) 200/500 Watts

Rack Spaces 2

Transformer Type Toroidal

Exterior Finish Baked, Black Painted

Dimensions (DWH /D fm ears, inches) 19 x 13.1 x 3.5 x 12.1

Dimensions (DWH /D fm ears, cm) 48.3 x 33.3 x 8.9 x 31

Weight (lbs / kg) 22.5 / 10.25

3.4 Tactile Sound Transducers

Clark Synthesis Tactile Transducer is an electromechanical device designed to drive large surfaces, such as seats, risers, and floors, with tactile information ranging from 1Hz to 800Hz. Audible from 20 Hz to 20 KHz. Sounds are generally audible to the human ear if their frequency (number of vibrations per second) lies between 20 and 20,000 vibrations per second, but the range varies considerably with the individual. Sound waves with frequencies less than those of audible waves are called subsonic; those with frequencies above the audible range are called ultrasonic.

Table 3.2 Tactile Sound Transducer Specifications

Magnetic Assembly	20 oz., 42 MGO Neo.
Transduction Force	2.9 lb-ft/watt
Tactile Force Peak	392 lb-ft
Peak Power Handling	400 watts
Continuous Power handling	135 watts
Frequency range (Tactile)	10 Hz to 800 Hz
Frequency Range (overall)	20 Hz to 17 kHz
Impedance	4 ohms
Overload Protection	Polyswitch
Electrical Connection	3', 14 AWG OFC
Dimensions	8" Diam. x 2.25"H (sealed)

3.5 High Speed Camera

Photron's 512 PCI is designed to operate at full 512×512-pixel resolution as fast as 2,000 frames per second (fps), and with reduced resolution operation to 32,000 fps. High light sensitivity is achieved using a 10-bit monochrome (30-bit color) CMOS sensor with a large 16 µm pixel size. This enables the user to program the system to record the initial stages of an event at one frame rate, and the later stages at a different frame rate, achieving the best possible combination of recording speeds and available memory.

Features:

- 512 x 512-pixel resolution up to 2,000 fps
- Electronic global shutter to 4 µs
- Records at speeds up to 32,000 fps
- Large 16µm pixels provide maximum sensitivity and color fidelity
- Four camera systems can operate in a single PC; Photron Motion Tools™ software

CMOS: CMOS is an abbreviation for Complementary Metal Oxide Semiconductor. Linear image sensors are self-scanning photodiode arrays designed as sensors for multi-channel spectrophotometer and other industrial applications. The CMOS signal processing circuit includes an internal integration amplifier and clamping circuit. This enables the user to construct a simple external driver circuit. The 5 V single power supply makes for simple operation. The photodiode array has a broad spectral response and a high level of ultraviolet sensitivity with stable characteristics under ultraviolet illumination. The low dark current and large charge saturation enables signals to be obtained with a high signal to noise ratio.

3.6 Clear Cast Acrylic Tube (Cylinder)

This tube is purchased from Johnston Industrial Plastics ltd and the base and support is built in Xerox Research Centre of Canada.

The dimensions of the Cylinder are: The height, the diameter, and the thickness of the cylinder are 60 cm, 60 cm, and 1.27 cm respectively.

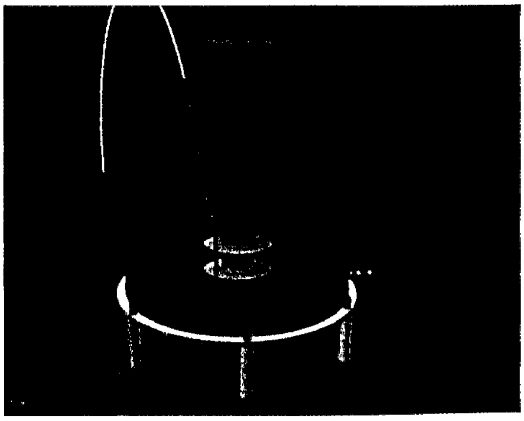

Figure 3.4 Cylinder

3.7 RFS3 Fluids Rheometer

Hydroxypropyl Cellulose, Mw = 10^6, material was prepared in different concentrations and measured the viscosity using RFS3 Fluids Rheometer.

1. Dynamic Viscosity of Water at 10^0C = 1.30 x 10^{-2} g/cm.s
2. 500 g of Hydroxypropyl Cellulose (0.35%) in 145 liters of Water (Viscosity = 4.56 x 10^{-2} g/cm.s)
3. 750 g of Hydroxypropyl Cellulose (0.50%) in 145 liters of Water (Viscosity = 7.02 x 10^{-2} g/cm.s)

The visco-elastic properties were performed on the RFS3 Fluids Rheometer available from TA Instruments both in the steady shear and the dynamic modes, using the 50 mm cone and a nominal gap of 53 microns. The temperature was kept constant and the tests performed were frequency sweeps in the dynamic mode from 0.1 Hz to 15 Hz or steady state rate sweeps from 1000 s^{-1} to 0.1 s^{-1}.

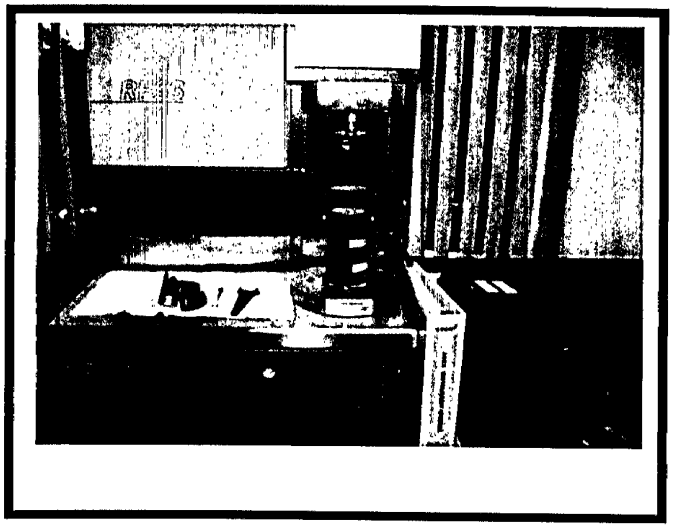

Figure 3.5 RFS3 Fluids Rheometer

3.8 Spherical particles

3.8.1 Plastic Balls - Delrin® Acetal Delrin® - Polished

Acetal (Delrin®) Balls have all the great mechanical properties of the fine quality acetal resins they are made from, including high intensity strength, rigidity, outstanding resistance to abrasion and most solvents. As an acetal homopolymer, Delrin has the highest fatigue endurance of any unfilled commercial thermoplastic. It is opaque white with specific gravity of 1.4.

3.8.2 Balls – Nylon 6/6

Extremely tough, resistant to alkalis, weak acids and most organic solvents. It has very low water absorption. Nylon Balls are useful in check valves and blood transfusion equipment or any application where abrasion or wear is a factor. It is non-polished with specific gravity of 1.14.

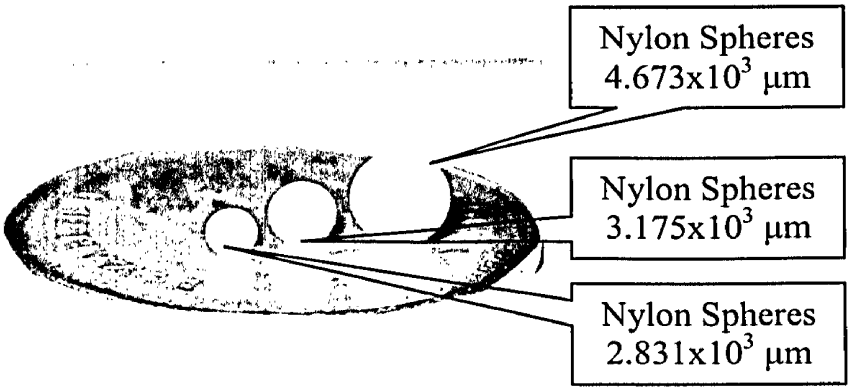

Figure 3.6 Photography of Nylon Particles compared with a coin

Chapter 4

4. Results and discussion

This chapter contains detailed investigations of the settling velocity of particles suspended in an acoustic field. The settling of the suspended particles subjected to acoustic radiation force was investigated utilizing a tactile sound transducer mounted at the bottom of the Plexiglas tank. The tactile sound transducer is activated at different power input levels and the motion of the suspended particle is observed, tracked and recorded. The results were then compared to the mathematical prediction model.

4.1 Experimental Observations

A calibrated Plexiglas tank was filled with 145 liters of water and a particle was dropped at the centre of the container without the application of sound waves. This procedure was repeated three times and recorded the average data of the three runs. A next set of experiments were implemented using sound waves at different levels of frequency (50 Hz, 100 Hz and 500Hz), amplitude (2 V_{rms}, 3 V_{rms}) and viscosity (1.30 x 10^{-2} g/cm.s, 4.57 x 10^{-2} g/cm.s and 7.02 x 10^{-2} g/cm.s)

The images of the particle were captured by a High Speed Imaging Camera, HSI, as frame-by-frame motion characteristics (e.g. position, velocity, etc.) over time, with respect to the plane of the image. This camera had a Simple Analysis Module with photron motion tools such as analysis tab that contained playback controls, tracking controls, calibration controls and export to Microsoft excel controls.

Playback Controls - These controls were useful for seeking through frames and temporally pinpointing key features for tracking.

Tracking Controls - This was the heart of the Analysis Tab.

- Choosing among up to four independent feature markers
- Locating and marking features on individual frames
- Selecting regions for Auto Tracking
- Executing the Photron Motion Tools Auto Tracking algorithm.

Calibration Controls - Calibration gives meaning to the measurements generated by the tracking process. It defines scales, units of measurement, and coordinate system parameters.

Export **to Microsoft Excel or Text** - It exports the tracking data to Microsoft Excel format but only the coordinates as a data and then the distance, displacement, velocity, and velocity at Y direction, $V_{y,}$ were calculated.

BB FlashBack Express software was used –a screen recorder - it makes movies of what was observed on the PC screen and gave a visual analysis and numerical values of the particle motion.

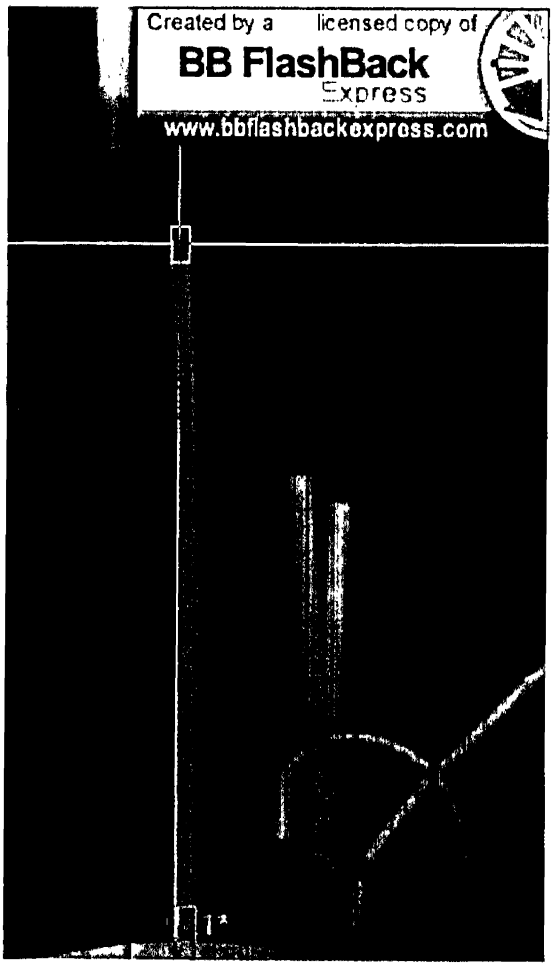

Figure 4.1.1 Image of particle without sound wave

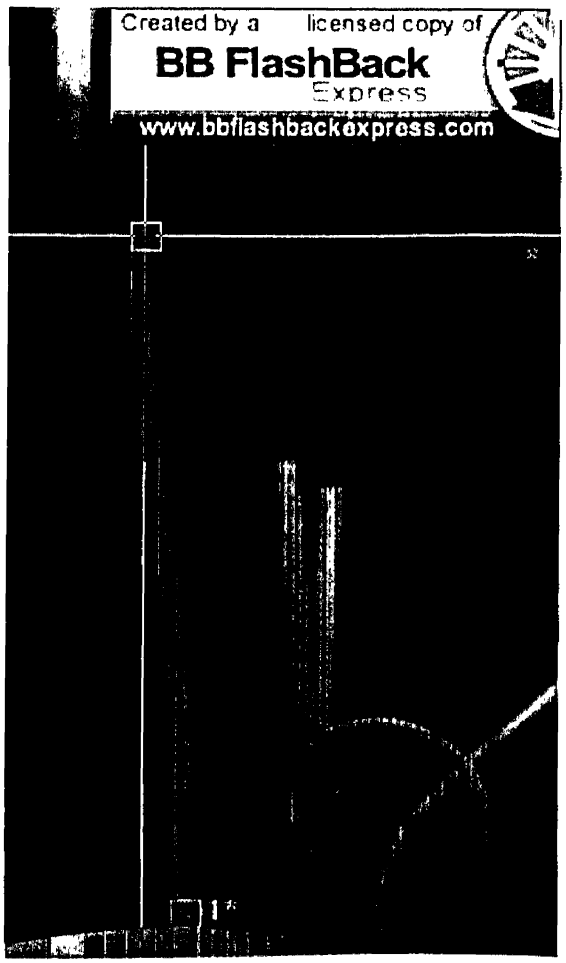

Figure 4.1.2 Image of particle with sound wave

Figure 4.1.1 shows the trajectory of falling Acetal particle in water without applying sound waves.

Figure 4.1.2 shows the trajectory of falling particle in water with the presence of sound waves. The frame-by-frame settling of the particle was recorded by the high speed imaging (HSI) camera and than used the BB Flash Back software to track and picture the particle settling.

Table 4.1 shows four factors used in the Design of Experiments (DOE). These sets of experiments were repeated at three different viscosities:

1) 1.30×10^{-2} g/cm.s at 10 ^{0}C – water viscosity - 42 experiments x 3 repeats.

2) 4.57×10^{-2} g/cm.s at 10 ^{0}C - 42 experiments x 3 repeats.

3) 7.02×10^{-2} g/cm.s at 10 ^{0}C- 42 experiments x 3 repeats.

Viscosity of water was changed by mixing 145 liters of water with 500g of hydroxypropyl cellulose, Mw = 10^6 which gave a concentration of 0.35% and a viscosity of 4.57×10^{-2} g/cm.s. Separately, 750g of hydroxypropyl Cellulose, Mw = 10^6 was dissolved in 145 liters of water which gave a concentration of 0.50% and a viscosity of 7.02×10^{-2} g/cm.s.

There were 42 sets of experiments that have been conducted for every particular viscosity and each one was repeated three times to give the average velocities at Y direction, settling distance at Y direction, settling distance at Y direction per frame, distance and displacement. Frame-by-Frame settling velocities of particles can be seen in Appendix B. The average velocities at Y direction were calculated and the results were tabulated in Table 4.2. These velocities were then plotted against the particle size, viscosity, frequency and amplitude as shown in Figure 4.1 to Figure 4.12. More figures can also be found in Appendix A

Table 4.1 Design of Experiments (DOE)

Particle size Diameter (10^3 µm)	Particle Density (g/cm^3)	Acoustic Energy Freq (Hz)	Amplitude (V_{rms})	
2.38 (Acetal)	1.40	0	0	
3.17	1.40	0	0	
4.76	1.40	0	0	
2.38 (Nylon)	1.14	0	0	
3.17	1.14	0	0	
4.76	1.14	0	0	
2.38 (Acetal)	1.40	50 Hz	2 V_{rms}	3 V_{rms}
3.17	1.40	50 Hz	2 V_{rms}	3 V_{rms}
4.76	1.40	50 Hz	2 V_{rms}	3 V_{rms}
2.38 (Nylon)	1.14	50 Hz	2 V_{rms}	3 V_{rms}
3.17	1.14	50 Hz	2 V_{rms}	3 V_{rms}
4.76	1.14	50 Hz	2 V_{rms}	3 V_{rms}
2.38 (Acetal)	1.40	100 Hz	2 V_{rms}	3 V_{rms}
3.17	1.40	100 Hz	2 V_{rms}	3 V_{rms}
4.76	1.40	100 Hz	2 V_{rms}	3 V_{rms}
2.38 (Nylon)	1.14	100 Hz	2 V_{rms}	3 V_{rms}
3.17	1.14	100 Hz	2 V_{rms}	3 V_{rms}
4.76	1.14	100 Hz	2 V_{rms}	3 V_{rms}
2.38 (Acetal)	1.40	500 Hz	2 V_{rms}	3 V_{rms}
3.17	1.40	500 Hz	2 V_{rms}	3 V_{rms}
4.76	1.40	500 Hz	2 V_{rms}	3 V_{rms}
2.38 (Nylon)	1.14	500 Hz	2 V_{rms}	3 V_{rms}
3.17	1.14	500 Hz	2 V_{rms}	3 V_{rms}
4.76	1.14	500 Hz	2 V_{rms}	3 V_{rms}

Table 4.2 DOE Summary Data

Factor	A	B	C	D	E	Velocity	
Row #	Diameter	Density	Frequency	Amplitude	Viscosity	Y1	Y bar
1	4760	1.4	0	0	0.0130	13.36	13.36
2	4760	1.4	50	2	0.0130	12.07	12.07
3	4760	1.4	100	2	0.0130	13.64	13.64
4	4760	1.4	500	2	0.0130	13.51	13.51
5	4760	1.4	50	3	0.0130	13.92	13.92
6	4760	1.4	100	3	0.0130	13.56	13.56
7	4760	1.4	500	3	0.0130	13.54	13.54
8	3170	1.4	0	0	0.0130	12.68	12.68
9	3170	1.4	50	2	0.0130	12.29	12.29
10	3170	1.4	100	2	0.0130	12.21	12.21
11	3170	1.4	500	2	0.0130	12.23	12.23
12	3170	1.4	50	3	0.0130	12.37	12.37
13	3170	1.4	100	3	0.0130	12.46	12.46
14	3170	1.4	500	3	0.0130	12.3	12.3
15	2380	1.4	0	0	0.0130	10.84	10.84
16	2380	1.4	50	2	0.0130	10.97	10.97
17	2380	1.4	100	2	0.0130	10.96	10.96
18	2380	1.4	500	2	0.0130	10.87	10.87
19	2380	1.4	50	3	0.0130	10.99	10.99
20	2380	1.4	100	3	0.0130	10.98	10.98
21	2380	1.4	500	3	0.0130	10.97	10.97
22	4760	1.14	0	0	0.0130	6.29	6.29
23	4760	1.14	50	2	0.0130	6.24	6.24
24	4760	1.14	100	2	0.0130	6.25	6.25
25	4760	1.14	500	2	0.0130	6.33	6.33
26	4760	1.14	50	3	0.0130	6.32	6.32
27	4760	1.14	100	3	0.0130	6.18	6.18
28	4760	1.14	500	3	0.0130	6.38	6.38
29	3170	1.14	0	0	0.0130	6.2	6.2
30	3170	1.14	50	2	0.0130	6.17	6.17
31	3170	1.14	100	2	0.0130	6.14	6.14
32	3170	1.14	500	2	0.0130	6.11	6.11
33	3170	1.14	50	3	0.0130	6.06	6.06
34	3170	1.14	100	3	0.0130	6	6
35	3170	1.14	500	3	0.0130	5.98	5.98
36	2380	1.14	0	0	0.0130	5.91	5.91
37	2380	1.14	50	2	0.0130	6.05	6.05
38	2380	1.14	100	2	0.0130	5.85	5.85
39	2380	1.14	500	2	0.0130	5.91	5.91
40	2380	1.14	50	3	0.0130	5.97	5.97
41	2380	1.14	100	3	0.0130	5.83	5.83

Table 4.2 DOE Summary Data.....Continued

Factor	A	B	C	D	E	Velocity	
Row #	Diameter	Density	Frequency	Amplitude	Viscosity	Y1	Y bar
42	2380	1.14	500	3	0.0130	5.89	5.89
43	4760	1.4	0	0	0.0457	11.51	11.51
44	4760	1.4	50	2	0.0457	11.01	11.01
45	4760	1.4	100	2	0.0457	11.37	11.37
46	4760	1.4	500	2	0.0457	11.23	11.23
47	4760	1.4	50	3	0.0457	11.18	11.18
48	4760	1.4	100	3	0.0457	11.11	11.11
49	4760	1.4	500	3	0.0457	11.09	11.09
50	3170	1.4	0	0	0.0457	9.63	9.63
51	3170	1.4	50	2	0.0457	9.16	9.16
52	3170	1.4	100	2	0.0457	8.73	8.73
53	3170	1.4	500	2	0.0457	8.95	8.95
54	3170	1.4	50	3	0.0457	9.02	9.02
55	3170	1.4	100	3	0.0457	9.13	9.13
56	3170	1.4	500	3	0.0457	9	9
57	2380	1.4	0	0	0.0457	6.11	6.11
58	2380	1.4	50	2	0.0457	6.18	6.18
59	2380	1.4	100	2	0.0457	5.5	5.5
60	2380	1.4	500	2	0.0457	5.42	5.42
61	2380	1.4	50	3	0.0457	5.66	5.66
62	2380	1.4	100	3	0.0457	5.13	5.13
63	2380	1.4	500	3	0.0457	5.52	5.52
64	4760	1.4	0	0	0.0702	8.24	8.24
65	4760	1.4	50	2	0.0702	8.18	8.18
66	4760	1.4	100	2	0.0702	8.1	8.1
67	4760	1.4	500	2	0.0702	7.99	7.99
68	4760	1.4	50	3	0.0702	7.95	7.95
69	4760	1.4	100	3	0.0702	7.81	7.81
70	4760	1.4	500	3	0.0702	7.8	7.8

The following figures show the outcomes of the experimental analysis.

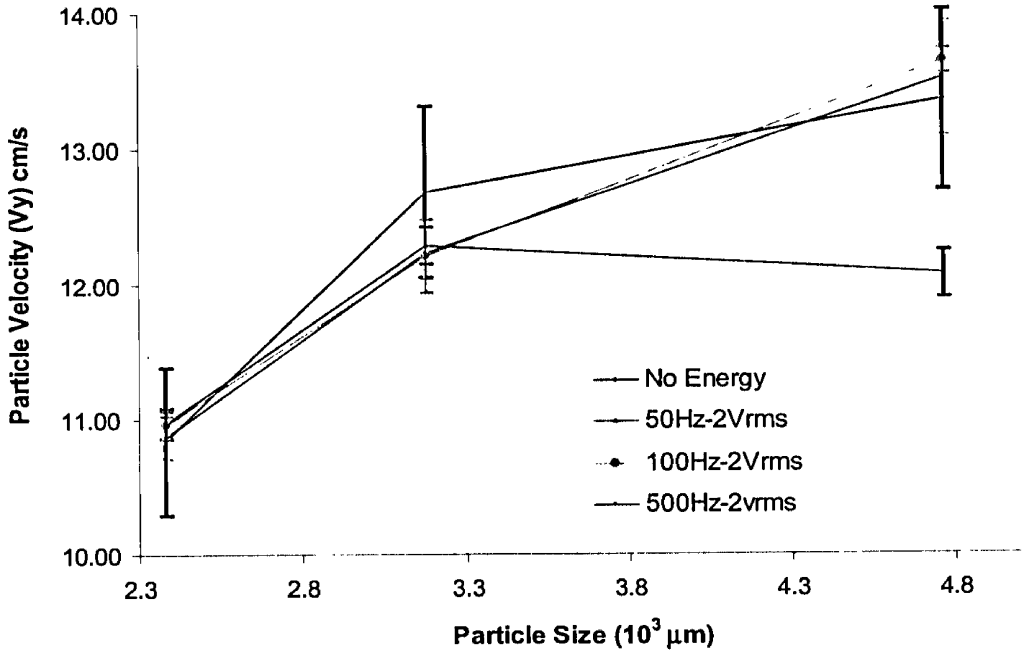

	No Energy		50 Hz		100 Hz		500 Hz	
Size	Average V_y (cm/s)	Standard deviation	Average V_y (cm/s)	Standard deviation	Average V_y (cm/s)	Standard deviation	Average V_y (cm/s)	Standard deviation
D1	10.84	0.13	10.97	0.12	10.96	0.10	10.87	0.16
D2	12.68	0.20	12.29	0.13	12.21	0.27	12.23	0.19
D3	13.36	0.10	12.07	0.17	13.64	0.09	13.51	0.43

Figure 4.2: Effect of Particle Size on Settling Velocity of Acetal in Water at 10°C (ρ= 1.40 g/cm^3; μ =1.30x10^{-2} g/cm.s; Amplitude-2 V_{rms})

Figure 4.2 shows the effect of particle size on the average settling velocity of Acetal sphere in water measured at amplitude of 2 V_{rms}. The results indicate that settling velocity (V_y) increases with increasing particle size while varying sound frequency from 0 to 500 Hz has some effect on V_y for the same size particle. The average settling velocity ranges from 10.84 cm/s to 13.64 cm/s which is below the estimated terminal velocity of 22.4 cm/s, 27.19 cm/s and 36.65 cm/s for the three different particle sizes.

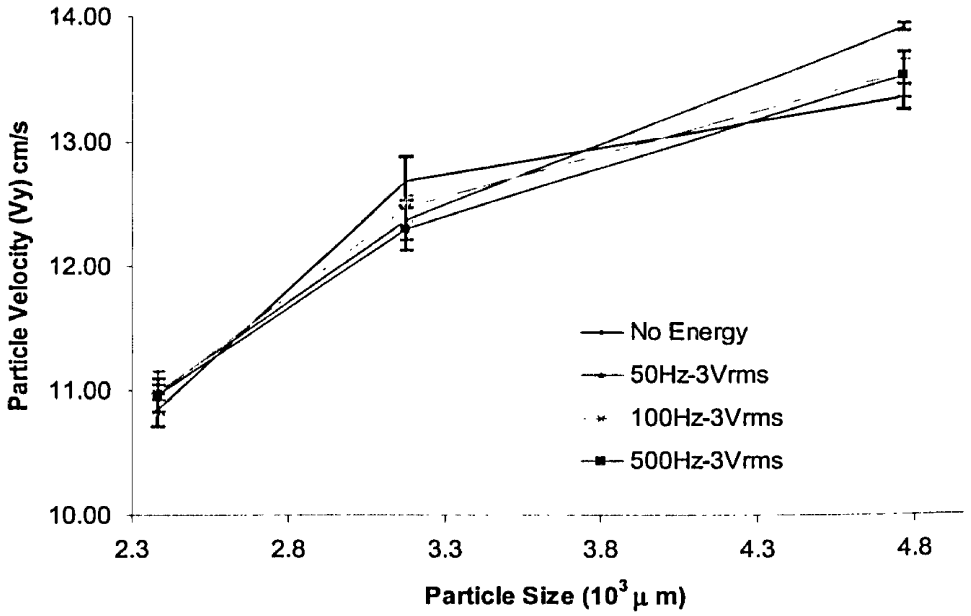

	No Energy		50 Hz		100 Hz		500 Hz	
Size	Average V_y (cm/s)	Standard deviation	Average V_y (cm/s)	Standard deviation	Average V_y (cm/s)	Standard deviation	Average V_y (cm/s)	Standard deviation
D1	10.84	0.13	10.99	0.06	10.98	0.18	10.97	0.13
D2	12.68	0.20	12.37	0.15	12.46	0.11	12.30	0.17
D3	13.36	0.10	13.92	0.03	13.56	0.10	13.54	0.18

Figure 4.3: Effect of Particle Size on Settling Velocity of Acetal in Water at 10°C (ρ= 1.40 g/cm^3; μ =1.30x10^{-2} g/cm.s; Amplitude-3 V_{rms})

Figure 4.3 shows the effect of particle size on the average settling velocity of Acetal sphere in water measured at higher amplitude of 3 V_{rms}. The results show the same trend as those observed for 2 V_{rms} where V_y increases with increasing particle size while varying sound frequency from 0 to 500 Hz has virtually no effect on Vy for the same size particle. The average settling velocity ranges also from 10.84 cm/s to 13.92 cm/s. The effect of amplitude within the range of 2 V_{rms} and 3 V_{rms} on V_y is negligible.

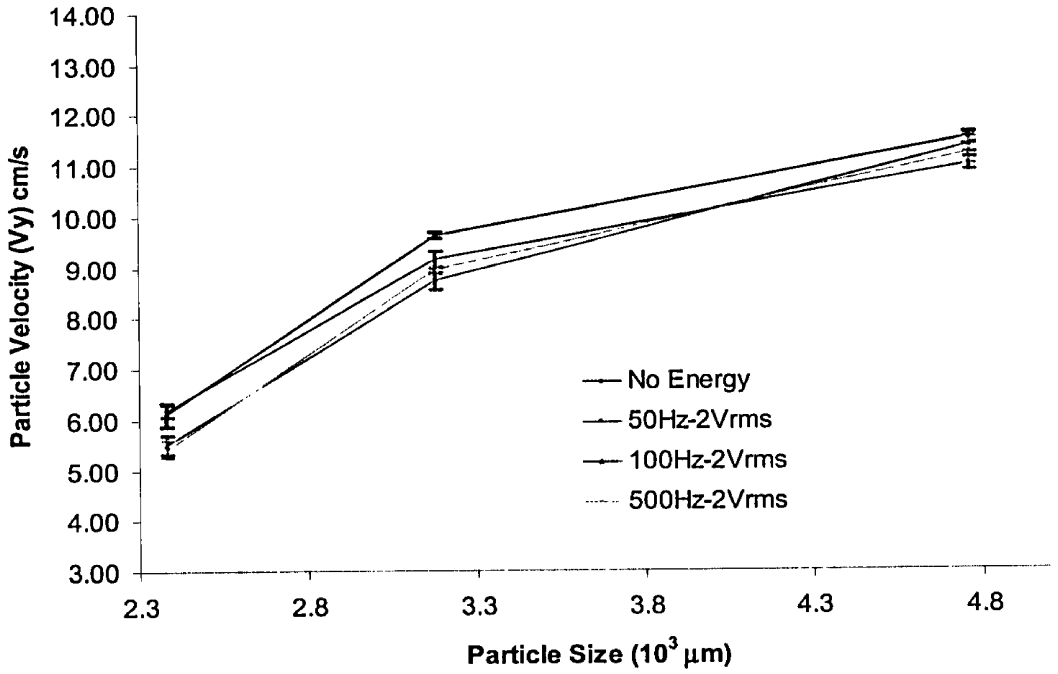

Size	No Energy		50 Hz		100 Hz		500 Hz	
	Average V_y (cm/s)	Standard deviation	Average V_y (cm/s)	Standard deviation	Average V_y (cm/s)	Standard deviation	Average V_y (cm/s)	Standard deviation
D1	6.11	0.23	6.18	0.12	5.50	0.18	5.42	0.17
D2	9.63	0.07	9.16	0.16	8.73	0.17	8.95	0.07
D3	11.51	0.12	11.01	0.12	11.37	0.16	11.23	0.21

Figure 4.4: Effect of Particle Size on Settling Velocity of Acetal in Hydroxypropylcellulose-Water at 10°C ($\mu = 4.57 \times 10^{-2}$ g/cm.s; Amp-2 V_{rms})

Figure 4.4 shows the effect of particle size on the average settling velocity of Acetal sphere in moderate viscosity Hydroxypropylcellulose-water (HPC-water) measured at amplitude of 2 V_{rms}. The results indicate that V_y increases with increasing particle size while varying sound frequency from 0 to 500 Hz has no much effect on V_y for the same size particle. The average settling velocity ranges from 5.42 cm/s to 11.51 cm/s which are about 3 to 5 units lower than those measured in water.

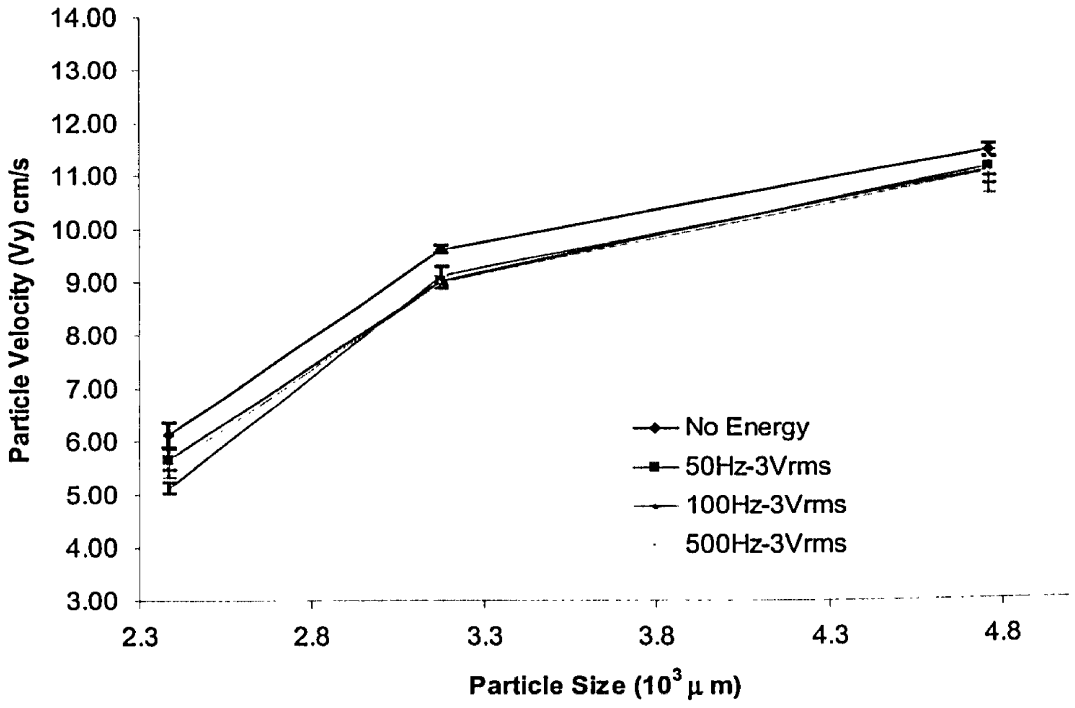

	No Energy		50 Hz		100 Hz		500 Hz	
Size	Average V_y (cm/s)	Standard deviation	Average V_y (cm/s)	Standard deviation	Average V_y (cm/s)	Standard deviation	Average V_y (cm/s)	Standard deviation
D1	6.11	0.23	5.66	0.20	5.13	0.10	5.52	0.20
D2	9.63	0.07	9.02	0.10	9.13	0.15	9.00	0.11
D3	11.51	0.12	11.18	0.18	11.11	0.25	11.09	0.41

Figure 4.5: Effect of Particle Size on Settling Velocity of Acetal in Hydroxypropylcellulose-Water at 10°C ($\mu = 4.57 \times 10^{-2}$ g/cm.s; Amp-3 V_{rms})

Figure 4.5 shows the effect of particle size on the average settling velocity of Acetal sphere in moderate viscosity HPC-water measured at amplitude of 3 V_{rms}. The results indicate that V_y increases with increasing particle size while varying sound frequency from 0 to 500 Hz has virtually no effect on V_y for the same size particle. The average settling velocity ranges from 5.13 cm/s to 11.51 cm/s which are very similar to those measured at 2 V_{rms}.

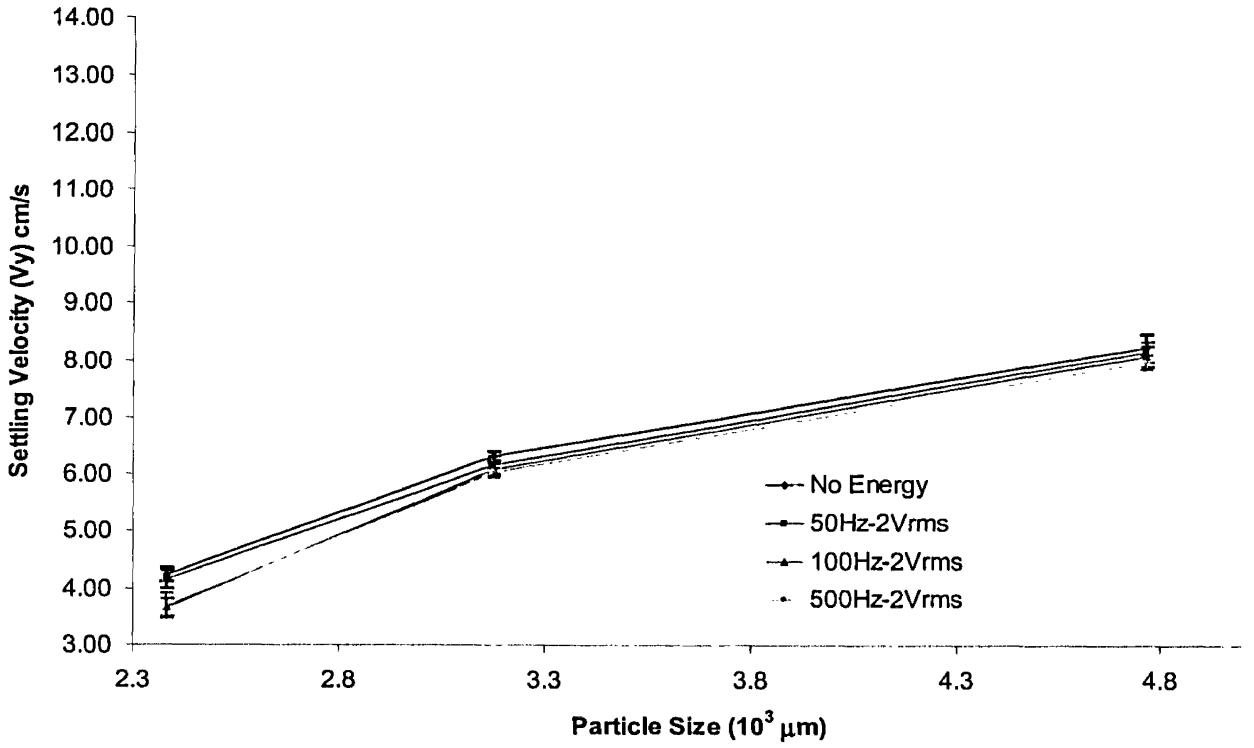

	No Energy		50 Hz		100 Hz		500 Hz	
Size	Average V_y (cm/s)	Standard deviation	Average V_y (cm/s)	Standard deviation	Average V_y (cm/s)	Standard deviation	Average V_y (cm/s)	Standard deviation
D1	4.24	0.11	4.14	0.16	3.66	0.15	3.69	0.22
D2	6.32	0.08	6.17	0.16	6.09	0.10	6.03	0.07
D3	8.24	0.24	8.18	0.18	8.10	0.19	7.99	0.12

Figure 4.6: Effect of Particle Size on Settling Velocity of Acetal in Hydroxypropylcellulose-Water at 10°C ($\mu = 7.02 \times 10^{-2}$ g/cm.s; Amp-2 V_{rms})

Figure 4.6 shows the effect of particle size on the average settling velocity of Acetal sphere in high viscosity HPC-water measured at amplitude of 2 V_{rms}. The results indicate that V_y increases with increasing particle size while varying sound frequency from 0 to 500 Hz has no effect on V_y for the same size particle. The average settling velocity ranges from 3.66 cm/s to 8.24 cm/s which are about 4 to 6 units lower than those measured in water.

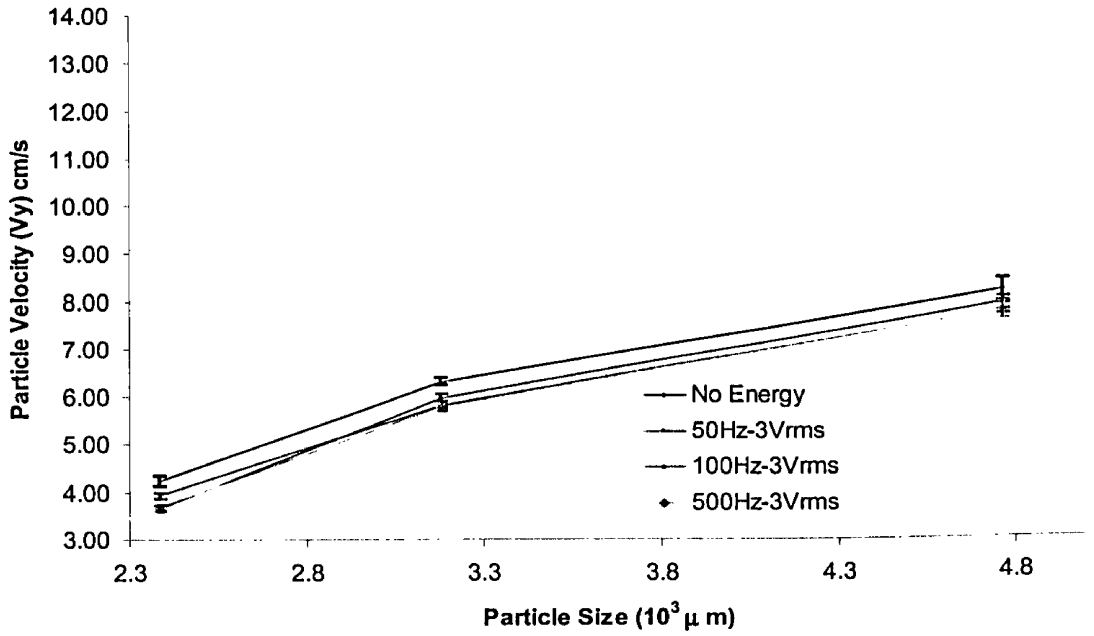

	No Energy		50 Hz		100 Hz		500 Hz	
Size	Average V_y (cm/s)	Standard deviation	Average V_y (cm/s)	Standard deviation	Average V_y (cm/s)	Standard deviation	Average V_y (cm/s)	Standard deviation
D1	4.24	0.11	3.66	0.05	3.94	0.06	3.70	0.06
D2	6.32	0.08	5.99	0.06	5.83	0.07	5.79	0.09
D3	8.24	0.24	7.95	0.13	7.81	0.11	7.80	0.17

Figure 4.7: Effect of Particle Size on Settling Velocity of Acetal in Hydroxypropylcellulose-Water at 10°C ($\mu = 7.02 \times 10^{-2}$ g/cm.s; Amp-3 V_{rms})

Figure 4.7 shows the effect of particle size on the average settling velocity of Acetal sphere in high viscosity HPC-water measured at amplitude of 3 V_{rms}. The results indicate that V_y increases with increasing particle size while varying sound frequency from 0 to 500 Hz has virtually no effect on V_y for the same size particle. The average settling velocity ranges from 3.66 cm/s to 8.24 cm/s which are about 4 to 6 units lower than those measured in water. The effect of changing amplitude within the experimental range of 2 V_{rms} to 3 V_{rms} on settling rate is also shown to be negligible.

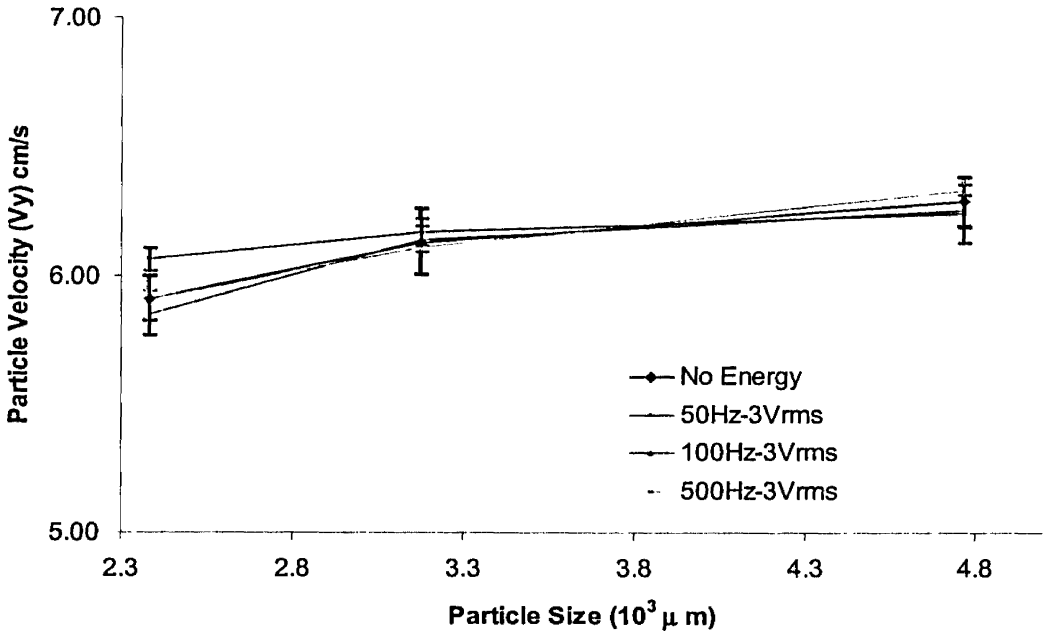

	No Energy		50 Hz		100 Hz		500 Hz	
Size	Average V_y (cm/s)	Standard deviation	Average V_y (cm/s)	Standard deviation	Average V_y (cm/s)	Standard deviation	Average V_y (cm/s)	Standard deviation
D1	5.91	0.09	6.06	0.05	5.85	0.09	5.91	0.03
D2	6.13	0.13	6.17	0.05	6.14	0.05	6.11	0.04
D3	6.29	0.10	6.24	0.11	6.25	0.06	6.33	0.04

Figure 4.8: Effect of Particle Size on Settling Velocity of Nylon in Water at 10°C (ρ= 1.14 g/cm^3; μ =1.307x10^{-2} g/cm.s; Amplitude-2 V_{rms})

Figure 4.8 shows the effect of particle size on the average settling velocity of Nylon sphere in water measured at amplitude of 2Vrms. The results indicate that settling velocity (V_y) does not increases much with increasing particle size while varying sound frequency from 0 to 500 Hz has no effect on V_y for the same size particle. The average settling velocity ranges from 5.85 cm/s to 6.33 cm/s which is below the estimated terminal velocity of 24.9 cm/s, 27.56 cm/s and 36.56 cm/s for the three different particle sizes.

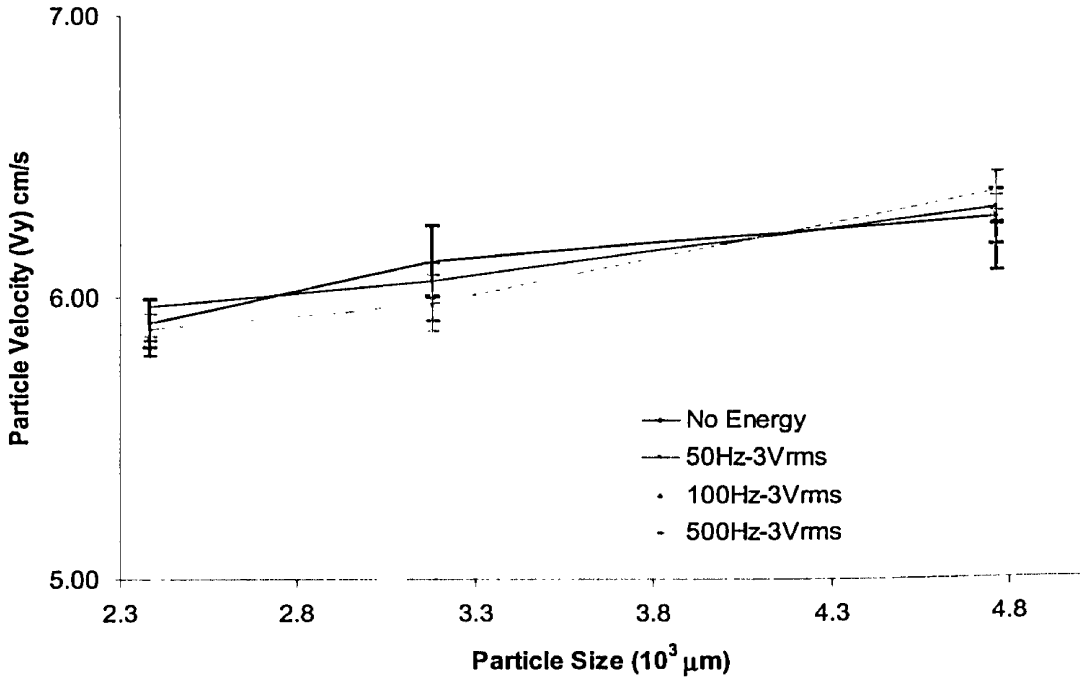

Size	No Energy		50 Hz		100 Hz		500 Hz	
	Average V_y (cm/s)	Standard deviation	Average V_y (cm/s)	Standard deviation	Average V_y (cm/s)	Standard deviation	Average V_y (cm/s)	Standard deviation
D1	5.91	0.09	5.97	0.03	5.82	0.03	5.89	0.03
D2	6.13	0.13	6.06	0.06	6.00	0.08	5.98	0.10
D3	6.29	0.10	6.32	0.05	6.18	0.08	6.38	0.07

Figure 4.9: Effect of Particle Size on Settling Velocity of Nylon in Water at 10°C ($\mu = 1.30 \times 10^{-2}$ g/cm.s; Amplitude-3 V_{rms})

Figure 4.9 shows the effect of particle size on the average settling velocity of Nylon sphere in water measured at higher amplitude of $3V_{rms}$. The results show the same trend as those observed for 2 V_{rms} where V_y does not increases with increasing particle size while varying sound frequency from 0 to 500 Hz has virtually no significant effect on V_y for the same size particle. The average settling velocity ranges also from 5.82 cm/s to 6.38 cm/s. The effect of amplitude within the range of 2 Vrms and 3 V_{rms} on V_y is negligible.

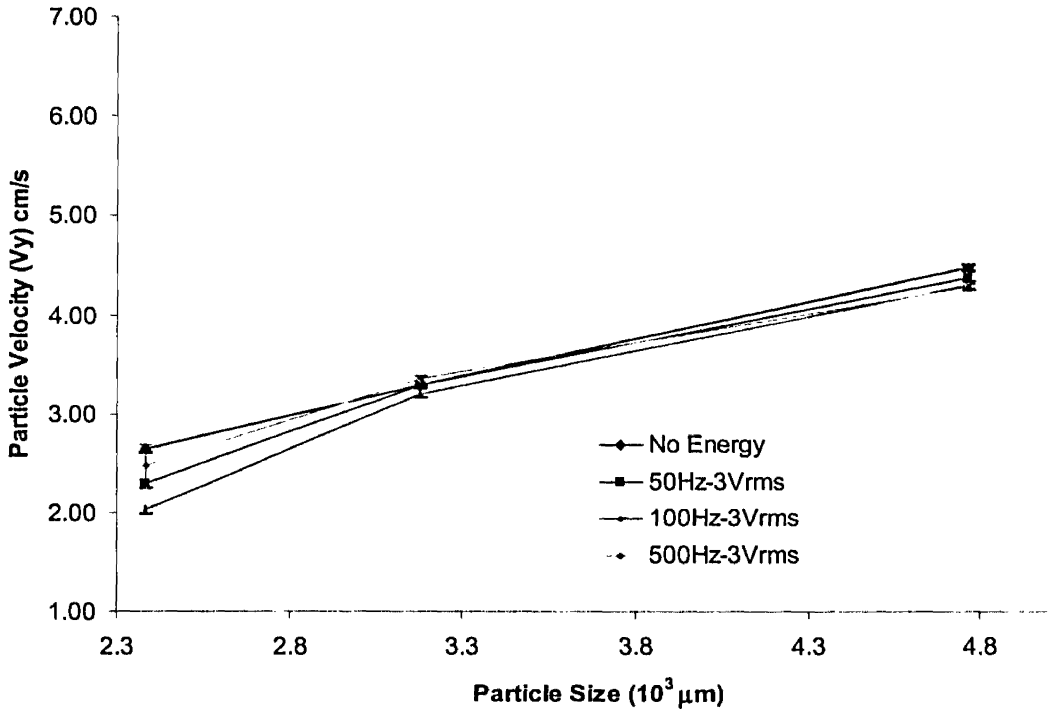

	No Energy		50 Hz		100 Hz		500 Hz	
Size	Average V_y (cm/s)	Standard deviation	Average V_y (cm/s)	Standard deviation	Average V_y (cm/s)	Standard deviation	Average V_y (cm/s)	Standard deviation
D1	2.64	0.04	2.29	0.04	2.02	0.04	2.48	0.21
D2	3.29	0.03	3.30	0.01	3.21	0.04	3.35	0.03
D3	4.47	0.04	4.36	0.03	4.29	0.04	4.28	0.02

Figure 4.10: Effect of Particle Size on Settling Velocity of Nylon in Hydroxypropylcellulose-Water at 10°C ($\mu = 4.57 \times 10^{-2}$ g/cm.s; Amp-2 V_{rms})

Figure 4.10 shows the effect of particle size on the average settling velocity of Nylon sphere in moderate viscosity Hydroxypropylcellulose-water (HPC-water) measured at amplitude of 2 V_{rms}. The results indicate that V_y increases with increasing particle size while varying sound frequency from 0 to 500 Hz has no significant effect on V_y for the two large size particles. The average settling velocity ranges from 2.02 cm/s to 4.47 cm/s which are about 2 to 4 units lower than those measured in water.

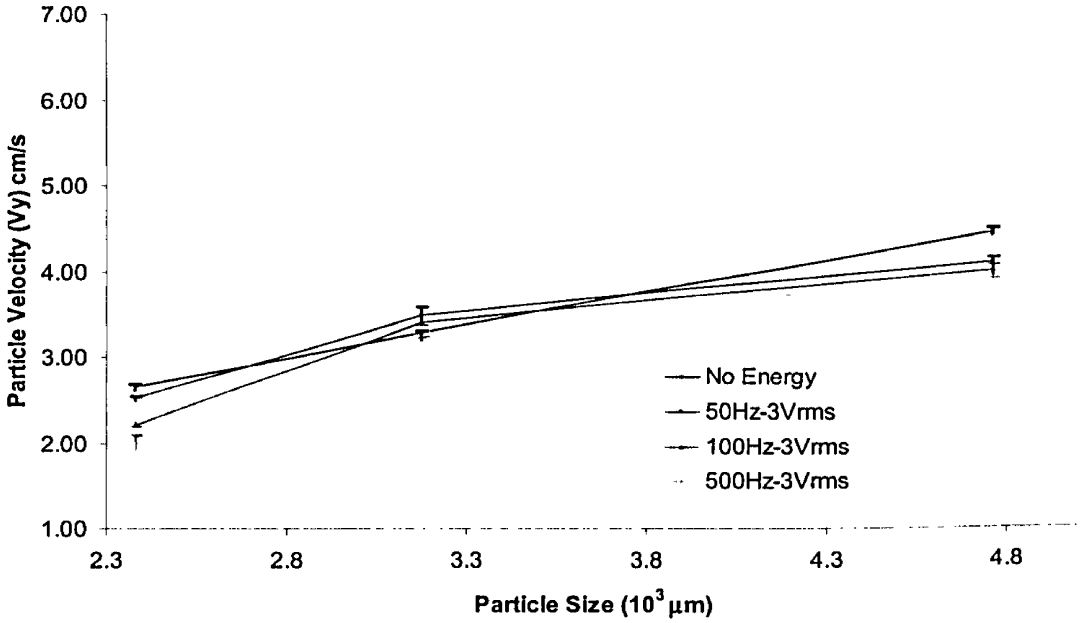

	No Energy		50 Hz		100 Hz		500 Hz	
Size	Average V_y (cm/s)	Standard deviation	Average V_y (cm/s)	Standard deviation	Average V_y (cm/s)	Standard deviation	Average V_y (cm/s)	Standard deviation
D1	2.64	0.04	2.29	0.04	2.02	0.04	2.48	0.21
D2	3.29	0.03	3.30	0.01	3.21	0.04	3.35	0.03
D3	4.47	0.04	4.36	0.03	4.29	0.04	4.28	0.02

Figure 4.11: Effect of Particle Size on Settling Velocity of Nylon in Hydroxypropylcellulose-Water at 10°C (μ= 4.57 x10^{-2} g/cm.s; Amp-3 V_{rms})

Figure 4.11 shows the effect of particle size on the average settling velocity of Nylon sphere in moderate viscosity HPC-water measured at amplitude of 3 V_{rms}. The results indicate that V_y increases with increasing particle size while varying sound frequency from 0 to 500 Hz has no significant effect on V_y for the same size particle. The average settling velocity ranges from 1.99 cm/s to 4.47 cm/s which are very similar to those measured at 2 V_{rms}.

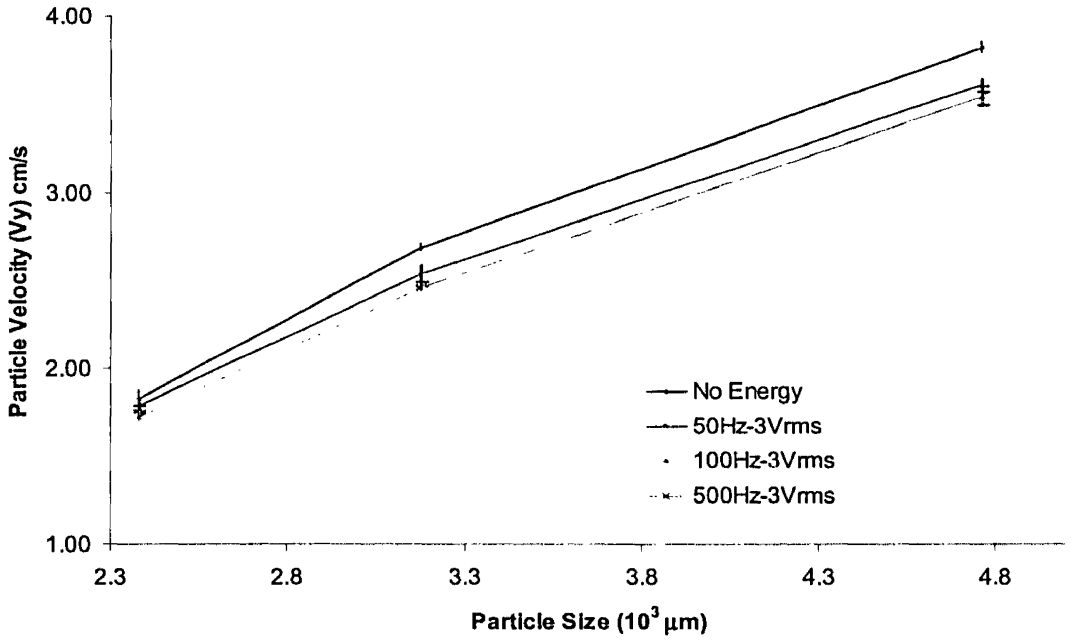

	No Energy		50 Hz		100 Hz		500 Hz	
Size	Average V_y (cm/s)	Standard deviation	Average V_y (cm/s)	Standard deviation	Average V_y (cm/s)	Standard deviation	Average V_y (cm/s)	Standard deviation
D1	2.64	0.04	2.29	0.04	2.02	0.04	2.48	0.21
D2	3.29	0.03	3.30	0.01	3.21	0.04	3.35	0.03
D3	4.47	0.04	4.36	0.03	4.29	0.04	4.28	0.02

Figure 4.12: Effect of Particle Size on Settling Velocity of Nylon in Hydroxypropylcellulose-Water at 10°C ($\mu = 7.02 \times 10^{-2}$ g/cm.s; Amp-2 V_{rms})

Figure 4.12 shows the effect of particle size on the average settling velocity of Nylon sphere in high viscosity HPC-water measured at amplitude of 2 V_{rms}. The results indicate that V_y increases with increasing particle size while varying sound frequency from 50 Hz to 500 Hz has no effect on V_y for the same size particle. The average settling velocity ranges from 1.73 cm/s to 3.83 cm/s which are about 2 to 4 units lower than those measured in water.

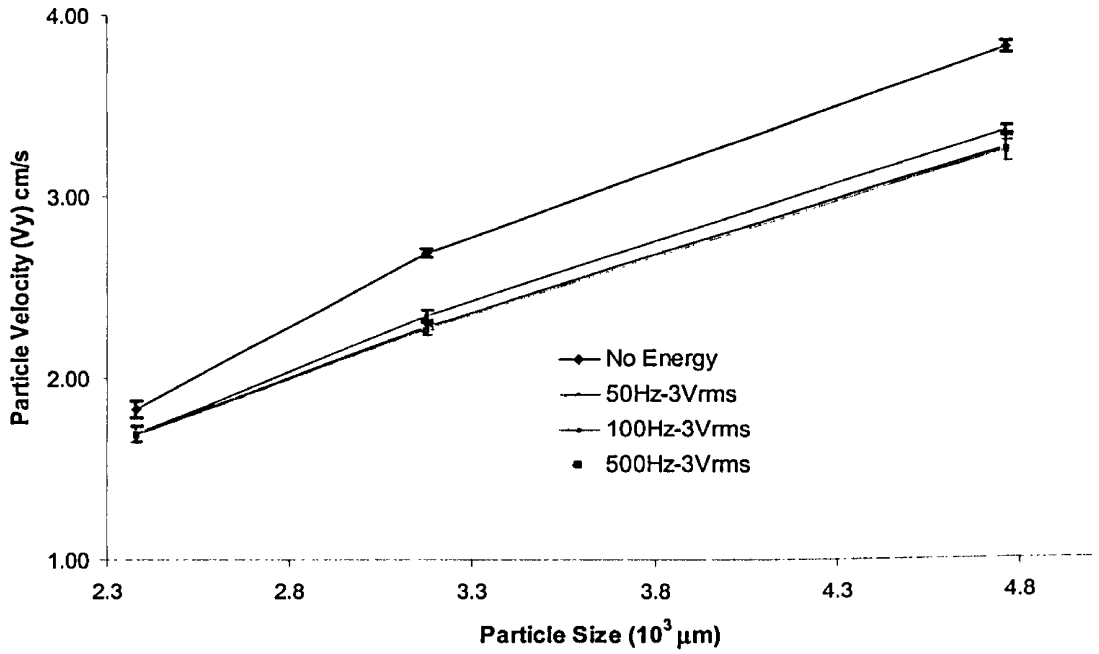

	No Energy		50 Hz		100 Hz		500 Hz	
Size	Average V_y (cm/s)	Standard deviation	Average V_y (cm/s)	Standard deviation	Average V_y (cm/s)	Standard deviation	Average V_y (cm/s)	Standard deviation
D1	2.64	0.04	2.29	0.04	2.02	0.04	2.48	0.21
D2	3.29	0.03	3.30	0.01	3.21	0.04	3.35	0.03
D3	4.47	0.04	4.36	0.03	4.29	0.04	4.28	0.02

Figure 4.13: Effect of Particle Size on Settling Velocity of Nylon in Hydroxypropylcellulose-Water at 10°C ($\mu = 7.02 \times 10^{-2}$ g/cm.s; Amp-3 V_{rms})

Figure 4.13 shows the effect of particle size on the average settling velocity of Nylon sphere in high viscosity HPC-water measured at amplitude of 3 V_{rms}. The results indicate that V_y increases with increasing particle size while varying sound frequency from 50 Hz to 500 Hz has virtually no effect on V_y for the same size particle. The average settling velocity ranges from 1.68 cm/s to 3.83 cm/s which are about 2 to 4 units lower than those measured in water. The effect of changing amplitude within the experimental range of 2 V_{rms} to 3 V_{rms} on settling rate is also shown to be negligible.

The experimental data from the DOE was analyzed using DOE PRO XL software by Air Academy Associates (Digital Computations). In general, the software performs a multiple regression analysis where a mathematical method is used to find the "best fitting" equation for the data set. Regression is the relationship between the mean value of a random variable and the corresponding values of one or more independent variables. It is also a model for predicting one variable from another. It is a statistical analysis assessing the association between two variables. Regression analysis is a method of analysis that enables you to quantify the relationship between two or more variables (X) and (Y) by fitting a line or plane through all the points such that they are evenly distributed about the line or plane. Multiple regression used in this DOE analysis software produces an equation with general format: $y = b_0 + b_1 x_1 + b_2 x_2 + b_3 x_1 x_2 \ldots\ldots$ where b_0 is the constant and b_1, b_2 and b_3 are coefficients for main effect and interaction terms. The equation representing the "best fitting" model can then be used to predict the response(s) given certain input variables.

The first multiple regression analysis which included all the main factors, namely diameter, viscosity, density, amplitude and frequency showed that amplitude and frequency were statistically insignificant. The regression was then recomputed without the insignificant factors and a final analysis was obtained as shown in Table 4.3.1.

In Table 4.3.1, Coeff is the coefficient of the effect of the independent variables; P(2 Tail) is the measure of the significance of an effect, less than 0.05 is considered

significant; R^2 is the measure of the fit of the regression model. An R^2 value of 1 means the model has a perfect fit; Adj R^2 is the R^2 adjusted for the number of observations and terms in the model; Std Error can be used as an estimate of the standard deviation of Y; if F is greater than 6 it indicates a significant model for prediction. Sig F less than 0.05 indicates a significant model for prediction. F_{LOF} greater than 6 indicates that the model is lacking its fit of the data. Sig F_{LOF} less than 0.05 indicates that the model is lacking its fit of the data. SS, df, and MS are the sum of the squares, degree of freedom and mean of squares respectively.

Table 4.3.1 Regression Model with Actual (Uncoded) Coefficients

Y-hat Model		Velocity			
Factor	Name	Coeff	P(2 Tail)	Tol	Active
Const		-12.909	0.0000		
A	Diameter	-0.00126	0.0736	0.0040	X
B	Density	12.640	0.0000	0.0608	X
E	Viscosity	56.256	0.0105	0.0074	X
AA		-0.0000005	0.0000	0.0066	X
AB		0.00411	0.0000	0.0091	X
AE		0.01216	0.0000	0.0610	X
BE		-177.93	0.0000	0.0100	X
EE		506.67	0.0000	0.0363	X
	R^2	0.9822			
	Adj R^2	0.9809			
	Std Error	0.4890			
	F	798.6328			
	Sig F	0.0000			
	F_{LOF}	46.9893			
	Sig F_{LOF}	0.0000			
	Source	SS	df	MS	
	Regression	1527.8	8	191.0	
	Error	27.7	116	0.2	
	$Error_{Pure}$	5.6	107	0.1	
	$Error_{LOF}$	22.1	9	2.5	
	Total	1555.5	124		

Table 4.3.2 shows the predictions of the resultant model for a high and low setting of the input parameters.

Table 4.3.2 Multiple Regression model prediction with Low and High Input Settings

Factor	Name	Low	High	Exper
A	Diameter	2381	4763	2000
B	Density	1.14	1.4	1.2
C	Frequency	0	500	1000
D	Amplitude	0	3	1.5
E	Viscosity	0.01307	0.0702	0.041635
Multiple Response Prediction				
			99% Confidence Interval	
	Y-hat	S-hat	Lower Bound	Upper Bound
Velocity	3.0640	0.4890	1.597	4.531
Factor	Name	Low	High	Exper
A	Diameter	2381	4763	3571
B	Density	1.14	1.4	1.27
C	Frequency	0	500	250
D	Amplitude	0	3	1.5
E	Viscosity	0.01307	0.0702	0.041635
Multiple Response Prediction				
			99% Confidence Interval	
	Y-hat	S-hat	Lower Bound	Upper Bound
Velocity	6.8108	0.4991	5.313	8.308

The regression analysis generated a series of regression coefficients relative to each input variable (density, viscosity, and diameter and the interaction terms). When each variable was plotted against the corresponding coefficients, a Pareto chart as shown in Figure 4.14 was created. A Pareto chart is a special type of bar chart where the coefficients are arranged in descending order. Coded coefficients are used to normalize the effects. The chart shows that Density has the strongest effect followed closely by Viscosity and to a lesser extent by Diameter on settling velocity.

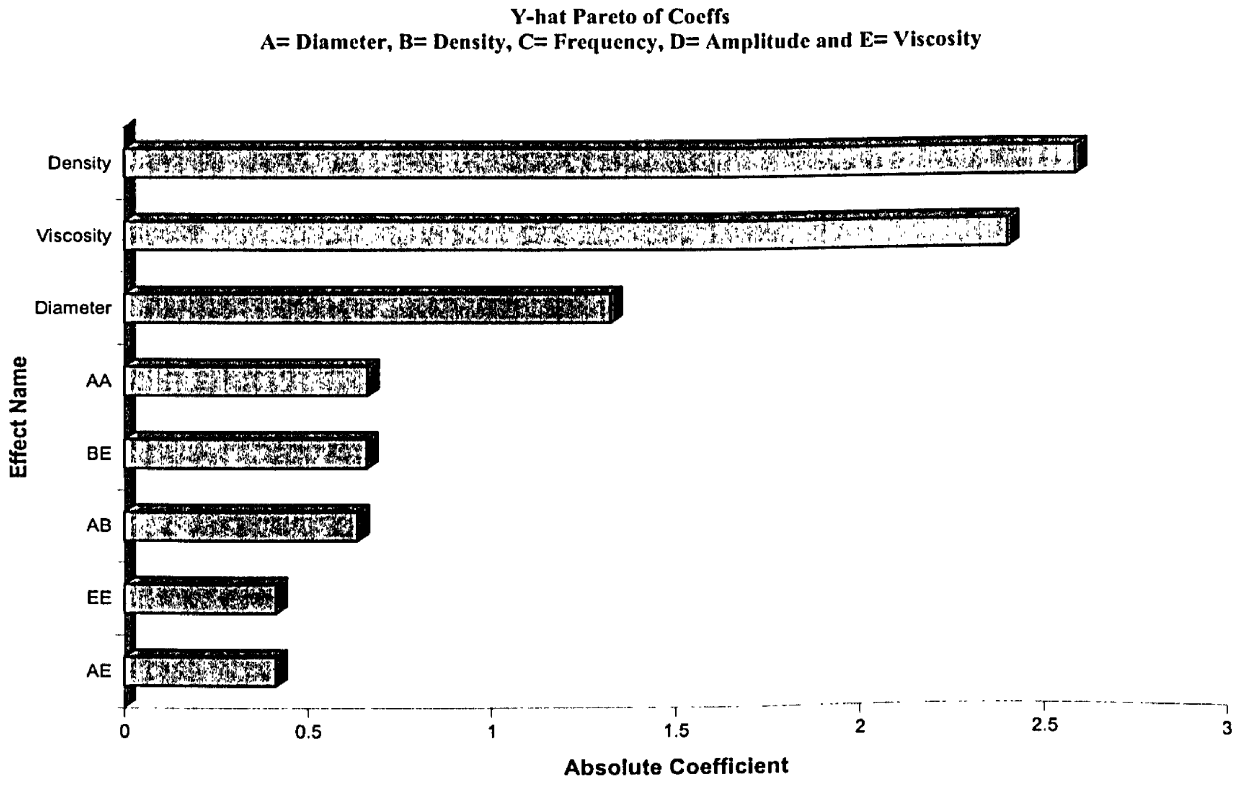

Figure 4.14 Pareto chart

Table 4.4 DOE Regression Model Coefficients

Coeff	Factor
Constant	
-12.909	
-0.00126	D
12.64	ρ
56.256	η
-0.0000005	D^2
0.00411	$D\rho$
0.01216	$D\eta$
-177.93	$p\eta$
506.67	η^2

Table 4.4 shows the regression model coefficients for predicting settling velocity as given by the following equation:

$$V = -12.909 - 0.00126D + 12.64\rho + 56.256\eta - 5 \times 10^{-7}D^2 + 0.00411D\rho + 0.01216D\eta - 177.93\rho\eta + 506.67\eta^2 \qquad 4.1$$

Where V is velocity in cm/s, D is diameter in microns, ρ is density in g/cm^3 and η is viscosity in g/cm.s.

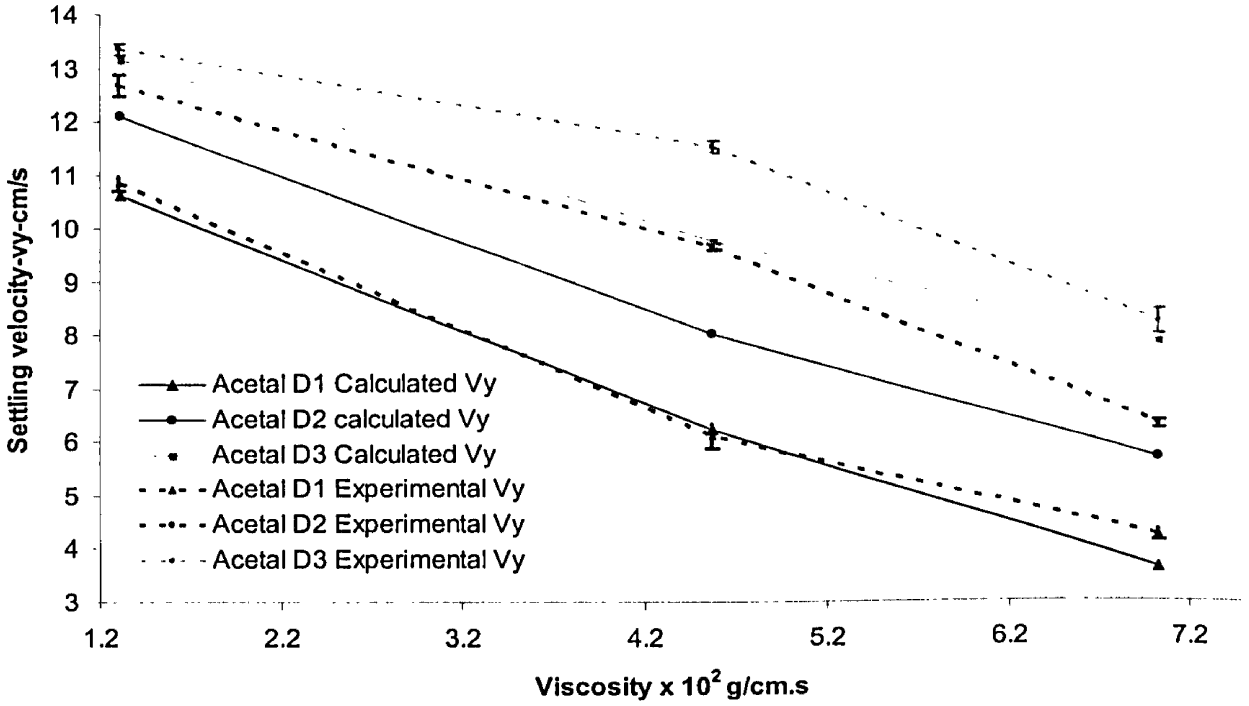

Size:	D1		D2		D3	
VISCOSITY (10^{-2} g/cm.s)	Average V_y (cm/s)	Standard deviation	Average V_y (cm/s)	Standard deviation	Average V_y (cm/s)	Standard deviation
1.30	10.84	0.13	12.68	0.20	13.36	0.10
4.57	6.11	0.23	9.63	0.07	11.51	0.12
7.02	4.24	0.11	6.32	0.08	8.24	0.24

Figure 4.15: Effect of Viscosity on Settling Velocity for Acetal Particle
Calculated Velocity vs Experimental Velocity

Figure 4.15 compares the experimental values of V_y measured in the absence of sound energy with the calculated values obtained from the regression model.

For Acetal particle with density of 1.40 g/cm^3, V_y decreases with increasing viscosity for all particle sizes. It is interesting to note that the calculated V_y matches the experimental data very closely with the smallest diameter particle having the best agreement. As the

viscosity goes up, resistance to flow or the viscous drag force on the particle increases causing V_y to decrease.

D1, D2, and D3 in the legend are the diameters of the spheres; 2.38 x 10^3 μm, 3.17 x 10^3 μm, and 4.67 x 10^3 μm respectively.

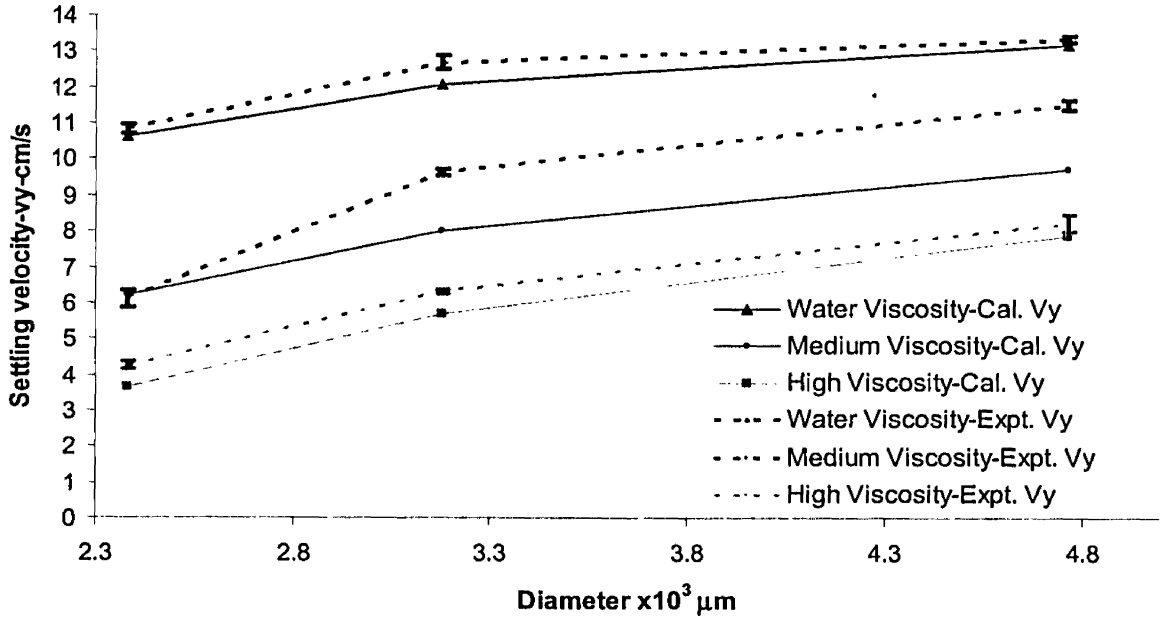

Viscosity: μ1			μ2		μ3	
DIAMETER (10^3 μm)	Average V_y (cm/s)	Standard deviation	Average V_y (cm/s)	Standard deviation	Average V_y (cm/s)	Standard deviation
2.38	10.84	0.13	6.11	0.23	4.24	0.11
3.18	12.68	0.20	9.63	0.07	6.32	0.08
4.76	13.36	0.10	11.51	0.12	8.24	0.24

Figure 4.16: Effect of Size on Settling Velocity for Acetal Particle
Calculated Velocity vs Experimental Velocity

Figure 4.16 compares the experimental values of V_y measured in the absence of sound energy with the calculated values obtained from the regression analysis of the experimental data. For Acetal particle with density of 1.40 g/cm^3, V_y increases with

increasing diameter. The calculated V_y values are in good agreement with the experimental data for all viscosity range. From equation 2.14, the settling velocity is a function of the particle diameter, D_P, as shown in this equation: $V=\left[\frac{8\,D_r}{\pi C_D \rho_f D_P^{\,2}}\right]^{\frac{1}{2}}$

Settling velocity is proportional to D_p which is consistent with the trend shown in Figure 4.15.

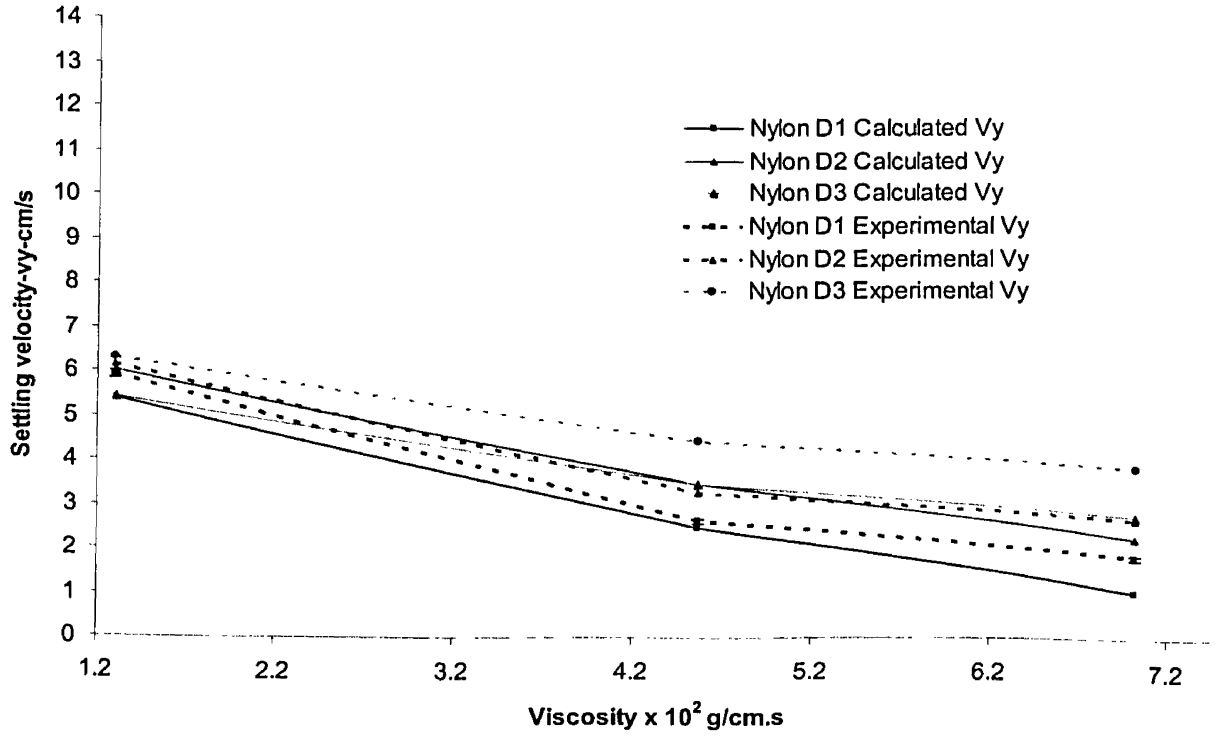

Size:	D1		D2		D3	
VISCOSITY (10^{-2} g/cm.s)	Average V_y (cm/s)	Standard deviation	Average V_y (cm/s)	Standard deviation	Average V_y (cm/s)	Standard deviation
1.30	5.91	0.09	6.13	0.13	6.29	0.10
4.57	2.64	0.04	3.29	0.03	4.47	0.04
7.02	1.83	0.05	2.69	0.02	3.83	0.03

Figure 4.17: Effect of Viscosity on Settling Velocity for Nylon Particle
Calculated Velocity vs Experimental Velocity

Figure 4.17 compares the experimental values of V_y measured in the absence of sound energy with the calculated values obtained from the regression analysis of the experimental data.

For Nylon particle with density of 1.14 g/cm^3, V_y decreases with increasing viscosity for all particle sizes. The calculated Vy values are in good agreement with the experimental data. For the same reason given to Figure 15, V_y goes down as viscosity goes up.

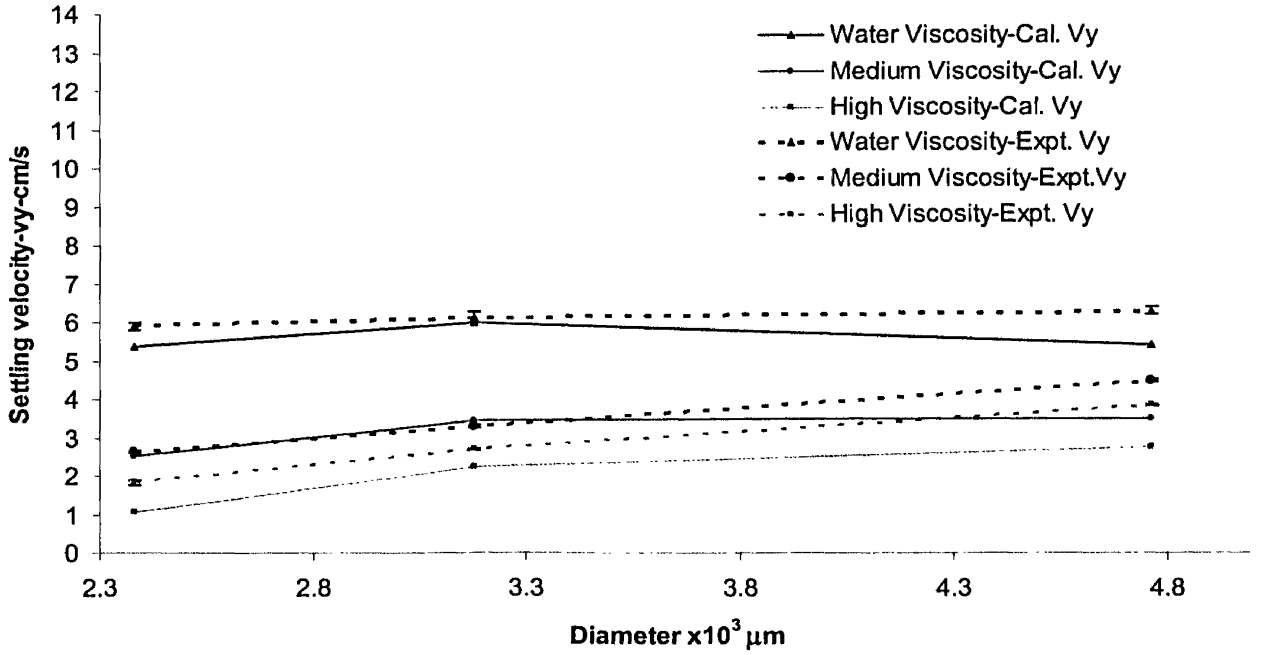

Figure 4.18: Effect of Size on Settling Velocity for Nylon Particle
Calculated Velocity vs Experimental Velocity

DIAMETER (10^3 µm)	Average V_y (cm/s)	Standard deviation	Average V_y (cm/s)	Standard deviation	Average V_y (cm/s)	Standard deviation
2.38	5.91	0.09	2.64	0.04	1.83	0.05
3.18	6.13	0.13	3.29	0.03	2.69	0.02
4.76	6.29	0.10	4.47	0.04	3.83	0.03

Figure 4.18 shows good agreement between the calculated and measured V_y values for Nylon particles of three sizes measured without the sound waves.

Figures 4.19 to 4.22 show the effects of DOE factors on particle settling velocity measured in the presence of sound waves. The calculated values predicted by the regression model were also compared with the experimental data.

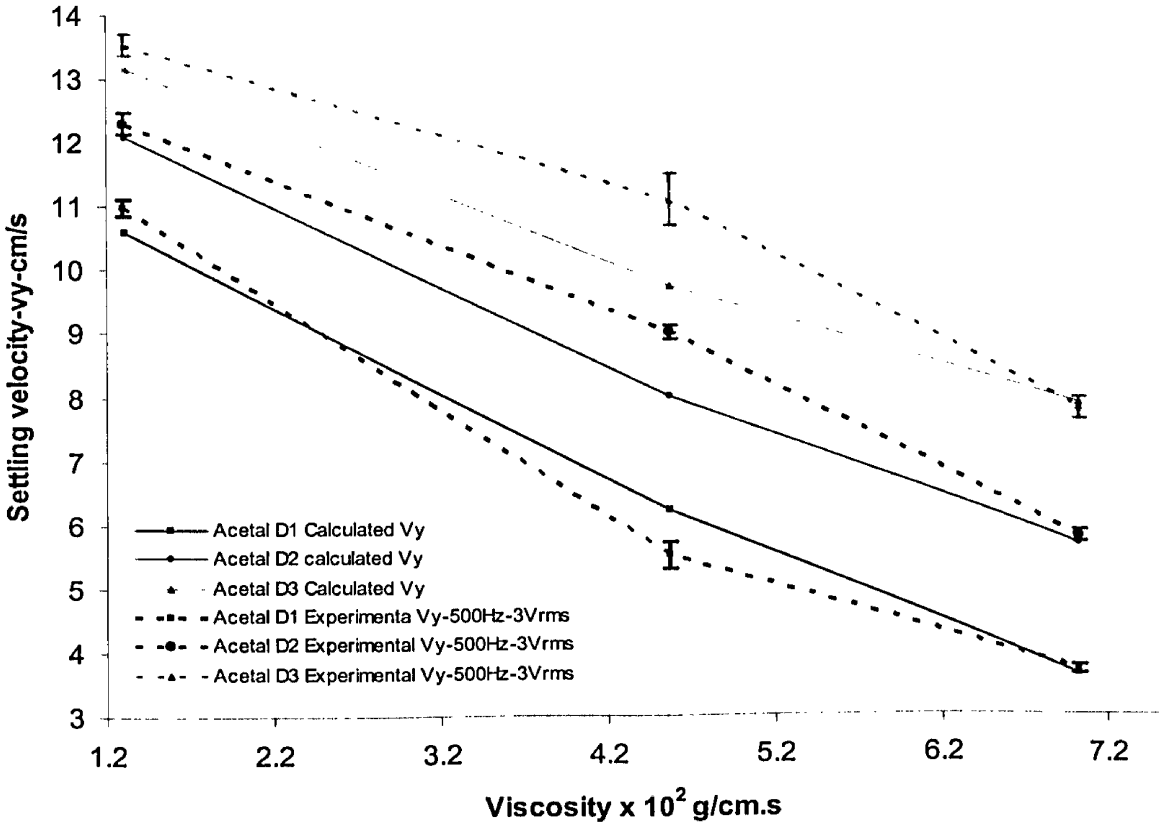

Size: D1			D2		D3	
VISCOSITY (10^{-2} g/cm.s)	Average V_y (cm/s)	Standard deviation	Average V_y (cm/s)	Standard deviation	Average V_y (cm/s)	Standard deviation
1.30	10.97	0.13	12.30	0.17	13.54	0.18
4.57	5.52	0.20	9.00	0.11	11.09	0.41
7.02	3.70	0.06	5.79	0.09	7.80	0.17

Figure 4.19: Effect of Viscosity on Settling Velocity for Acetal Particle
Calculated Velocity vs Experimental Velocity with 500 Hz-3 Vrms

Figure 4.19 shows the effect of viscosity on settling velocity measured at 500 Hz – 3 V_{rms} sound waves for three Acetal particles. Both model predictions and measured values are in good agreement showing V_y decreases with increasing viscosity.

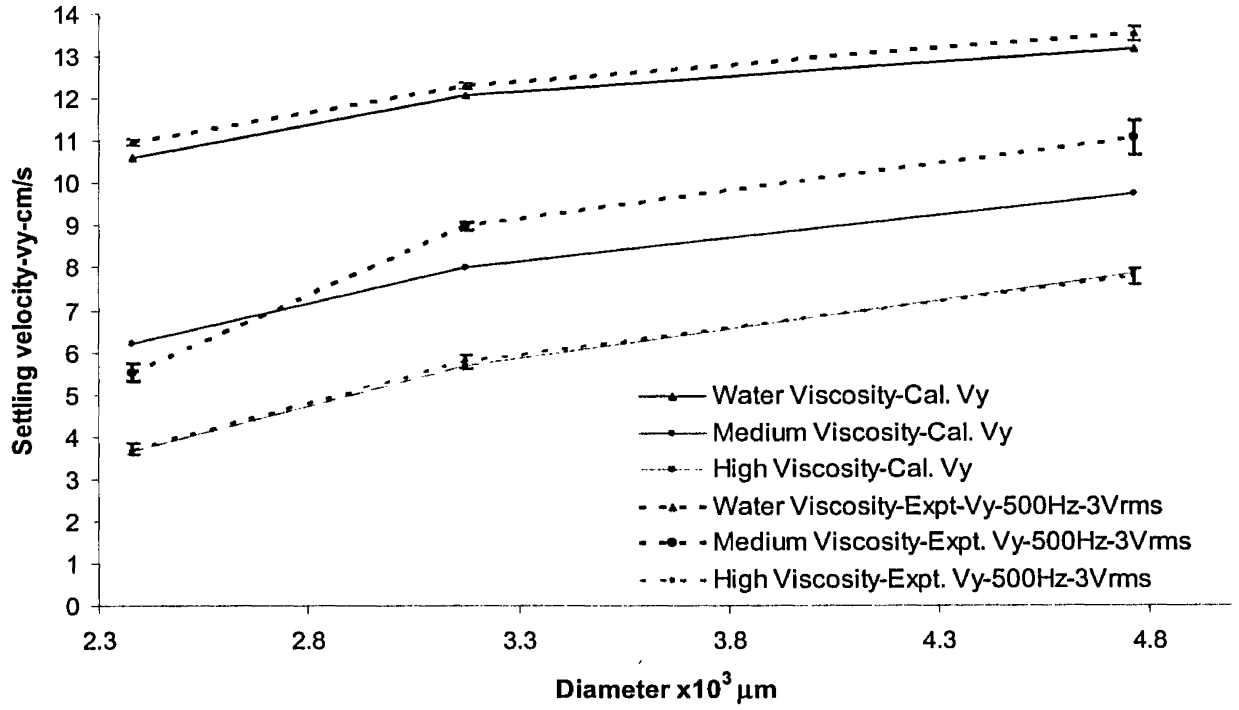

DIAMETER (10^3 µm)	Average V_y (cm/s)	Standard deviation	Average V_y (cm/s)	Standard deviation	Average V_y (cm/s)	Standard deviation
2.38	10.97	0.13	5.52	0.20	3.70	0.06
3.18	12.30	0.17	9.00	0.11	5.79	0.09
4.76	13.54	0.18	11.09	0.41	7.80	0.17

Figure 4.20: Effect of Size on Settling Velocity for Acetal Particle
Calculated Velocity vs Experimental Velocity with 500 Hz-3 V_{rms}

Figure 4.20 illustrates the correlation between Acetal particle diameter and settling velocity. As particle size increases, the settling velocity goes up with the lowest viscosity being at the highest level. Again, the model predictions are in good agreement with the experimental values.

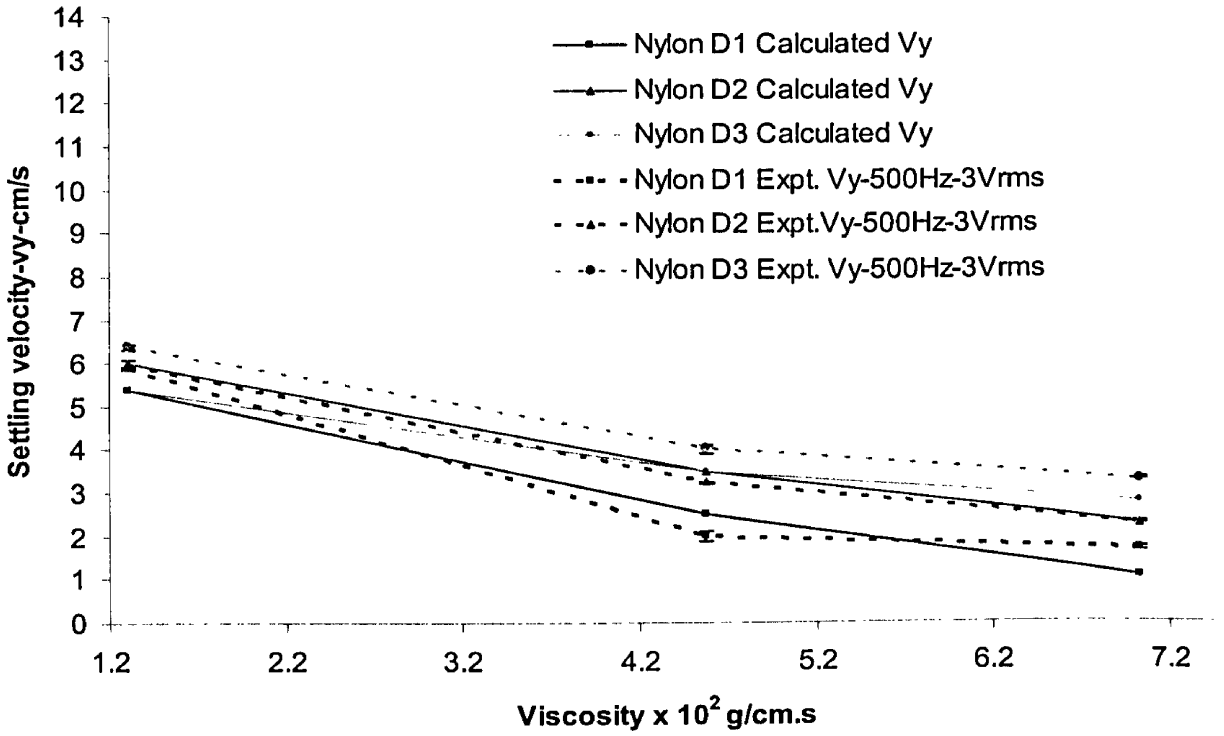

Size: D1			D2		D3	
VISCOSITY (10^{-2} g/cm.s)	Average V_y (cm/s)	Standard deviation	Average V_y (cm/s)	Standard deviation	Average V_y (cm/s)	Standard deviation
1.30	5.89	0.03	5.98	0.10	6.38	0.07
4.57	1.99	0.11	3.22	0.03	4.00	0.08
7.02	1.68	0.03	2.27	0.03	3.29	0.02

Figure 4.21: Effect of Viscosity on Settling Velocity for Nylon Particle
Calculated Velocity vs Experimental Velocity with 500Hz-3V_{rms}

Figure 4.21 depicts the decreasing velocity trend with increasing viscosity for Nylon particles. It is also noted that the settling velocities were all lower than those of Acetal particles by approximately 4 to 8 cm/s due largely to its lower density.

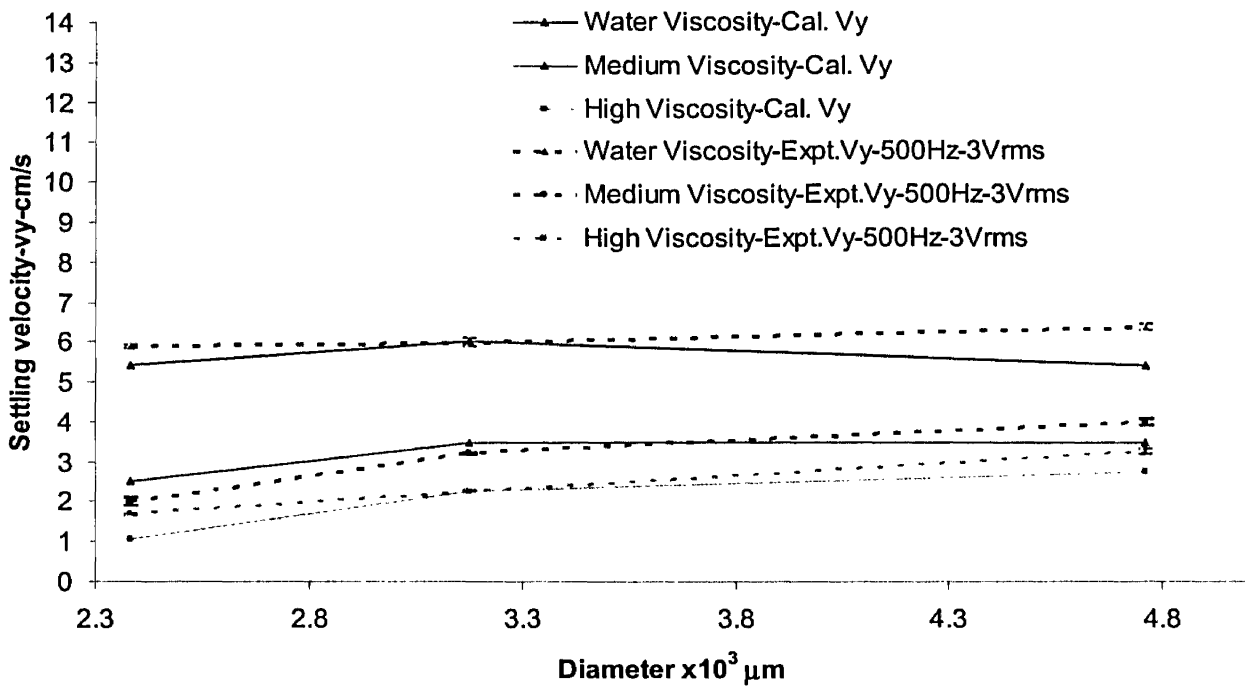

DIAMETER (10^3 µm)	Average V_y (cm/s)	Standard deviation	Average V_y (cm/s)	Standard deviation	Average V_y (cm/s)	Standard deviation
2.38	5.89	0.03	1.99	0.11	1.68	0.03
3.18	5.98	0.10	3.22	0.03	2.27	0.03
4.76	6.38	0.07	4.00	0.08	3.26	0.06

Figure 4.22: Effect of Size on Settling Velocity for Nylon Particle
Calculated Velocity vs Experimental Velocity with 500 Hz-3 V_{rms}

Figure 4.22 shows that increase in particle diameter has a weak effect on settling velocity for Nylon particle of relatively lower density. Again, the regression model shows good prediction when compared to the experimental values.

Conclusion

The effects of sonic energy waves on the settling velocity of small particles in water were studied. A design of experiment (DOE) with five variables (frequency, amplitude, diameter, density and viscosity) at two or three levels was conducted to obtain the particle settling velocity as the response. The DOE data were analyzed both experimentally and by a statistical multiple regression software. It was concluded that when sound frequency and amplitude in the range of 0 to 500 Hz and 2 V_{rms} to 3 V_{rms} respectively were applied to plastic particles of three different diameters (2,380 μm, 3,170 μm and 4,760 μm) and two different densities (1.14 g/cm^3 and 1.40 g/cm^3), their effects on the particle settling velocity in HPC solutions of three different viscosities (1.30 x 10^{-2} g/cm.s, 4.57 x 10^{-2} g/cm.s and 7.02 x 10^{-2} g/cm.s) were insignificant. The regression analysis gave the following equation:

$$V = -12.909 - 0.00126D + 12.64\rho + 56.256\eta - 5 \times 10^{-7}D^2 + 0.00411D\rho + 0.01216D\eta - 177.93\rho\eta + 506.67\eta^2$$

where V is velocity in cm/s, D is diameter in microns, ρ is density in g/cm^3 and η is viscosity in g/cm.s. The calculated values based on the above equation are in good agreement with the experimental data. The Pareto chart shows that particle density has the largest effect followed closely by viscosity of the fluid medium and to a lesser extent by particle diameter on the settling velocity. The settling velocity increases with increasing density, decreasing viscosity and increasing diameter. For Acetal particles with density of 1.40 g/cm^3, the settling velocity spans the range of about 4 to 14 cm/s. Comparatively, for Nylon particles with a lower density of 1.14 g/cm^3, the settling rate covers the range of about 2 to 6 cm/s. It is important to note that given the relatively short

dimension of the settling tank; the particles never reached the respective terminal velocities (see Appendix B).

Recommandations

- Decrease the particle size down to a toner size range of 5 to 10 μm.
- Use a longer holding tank or cylinder to reach the terminal velocity of the particles.
- Apply sound wave from different angles or placements inside the container.

References

Aboobaker, N., Meegoda, J.N., and Blackmore, D. (2001). "Analysis of fractionation of sediments caused by an acoustic field." *Proc., Int. Conf. on Computer Methods and Advances in Geomechanics, Desai, eds.,* Vol. 1, Balkema, Rotterdam, The Netherlands, 775-780.

Allen T., 1981 "Particle size measurement, 3rd edition".

Arnold, H. D., 1911, Limitations imposed by slip and inertia terms upon Stokes' law for the motion of spheres through liquids, Philosophical Mag., 22, 755-775.

(As cited by Galehouse, 1971).

Danilov, S. D., and Mironov, M. A. (1984). "Radition pressure force acting on a small particle in asound field." *Sov. Phy. Acoust., 30(4), 280-283.*

Embleton, T. F. W., "Mean Force on a Sphere in a Spherical Sound Field. I *(Theoretical)," Acoustical Society of America,* Vol. 26, pp. *40-45,* 1954.

Galehouse Jon S.,1971, Sedimentation Analysis, San Francisco State College, San Francisco, California, US.

French, A. P. (1971). Vibrations and waves, W. W. Norton, New York.

Gor'kov, L. P., "On the Forces Acting on a Small Particle in an Acoustic Field in an Ideal Fluid," Soviet Phys.-Doklady, Vol. 6, pp. 773-775, 1962.

Gould, R. K., Coakley, W., Terrence, G., and Martin, A. (1991). "Upper sound pressure limits on particle concentration in fields of ultrasonic standing wave at megahertz frequencies." Ultrasonics, 34(4), 239-243.

Johnson, D. A., Feke, D.L., " Methodology for fractionation Suspended Particles using Ultrasonic Standing Wave and Divided Flow Fields," *Separation Technology,* Vol. 5, pp. 251-258,1995.

King, V. Louis, Macdonald, F.R.S., "On the Acoustic Radiation Pressure on Spheres," Proc. R. Soc. London Ser. A 147, pp. 2 12-240, 1934.Klein D., "Absolute Sound Intensity in Liquids by Spherical Torsion Pendula," *Acoustic Society of America,* Vol. 9, pp. 3 12-320, 1938.

Kundt, A., and Lehmann, O., "Longitudinal Vibrations and Acoustic Figures in Cylindrical Columns of Liquids," Annal. Phys. Chem., Vol. 153, No. 1, 1874.

K.S. Suslick (1998) in Kirk-Othmer Encyclopedia of Chemical Technology; 4th Ed. J. Wiley & Sons: New York, 1998, vol. 26, 517-541.

Mason, T. J., "Practical Sonochemistry: User's Guide to Application in Chemistry and Chemical Engineering, Ellis Horwood, Chichester, 1991.

Nyborg, W. L., "Radiation Pressure on a Small Sphere," *Acoustical Society of America,* Vol. 42, pp. 947-952, 1967.

Porath-Furedi, US Patent No. 4,055,491 (Method and apparatus for separating particulate matter from a fluid, Issued on November 18, 1997).

R. Clift, J.R. Grace, and M.E. Weber *(Bubbles, Drops, and Particles,* Academic Press, 1978).

Richard Holland, *Design of Resonant Piezoelectric Devices*, the Colonial Press Inc., 1969.

Rudnick, K., "Measurements of the Acoustic Radiation Pressure on a Sphere in a Standing Wave Field," *Acoustical Society of America,* Vol. 62, pp. 20-22, 1977.

S.S. Phull, A.P. Newman, J.P. lorimer, B. Pollet, T.J. Mason "The development and evaluation of ultrasound in the biocidal treatment of water," Ultrasonics Sonochemistry 4(1997) 157-164.

Watson, J. R. 1971. Ultrasonic Vibration as a Method of Soil Dispersion. Soils and Fertilizers 34, 127-134.

Weyssenhoff,.J.,1920 , Betrachtungen uber den Gultigkeitsbereich der Stokesschen and der Stokes-Cunninghamschen Formel, Annalen der Physik, 62, 1-45. (As cited by Galehouse, 1971).

Yosioka K., and Kawasima Y., "Acoustic Radiation Pressure on a Compressible Sphere," *Acoustics,* Vol. 5, pp. 167-173, 1955.

8. Appendices

8.1 Appendix A

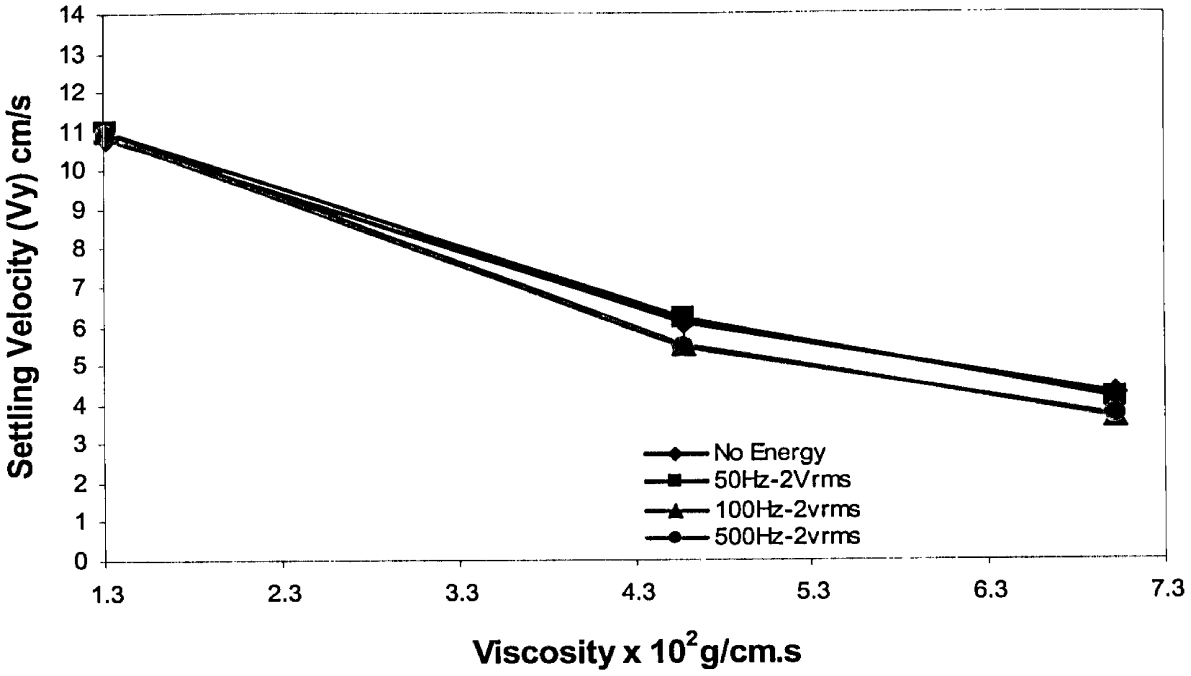

Figure 1A: Effect of Viscosity on Settling Velocity of Acetal in Water at 10^0C (ρ = 1.40g/cm^3; Amplitude-2 V_{rms}; Particle Size=2.38x10^3 μm)

Figure 1A shows the effect of viscosity on the average settling velocity of Acetal sphere in water, in moderate and in high viscosity hydroxypropylcellulose-water (HPC-water) measured at amplitude of 2 V_{rms}. The results indicate that settling velocity (V_y) decreases with increasing the viscosity while varying sound frequency from 0 to 500 Hz has less effect on V_y for the same size particle. The average settling velocity ranges from 3.66 cm/s to 10.97 cm/s. This shows that the settling velocity was lowered 3 times by increasing the viscosity of water approximately 5.4 times.

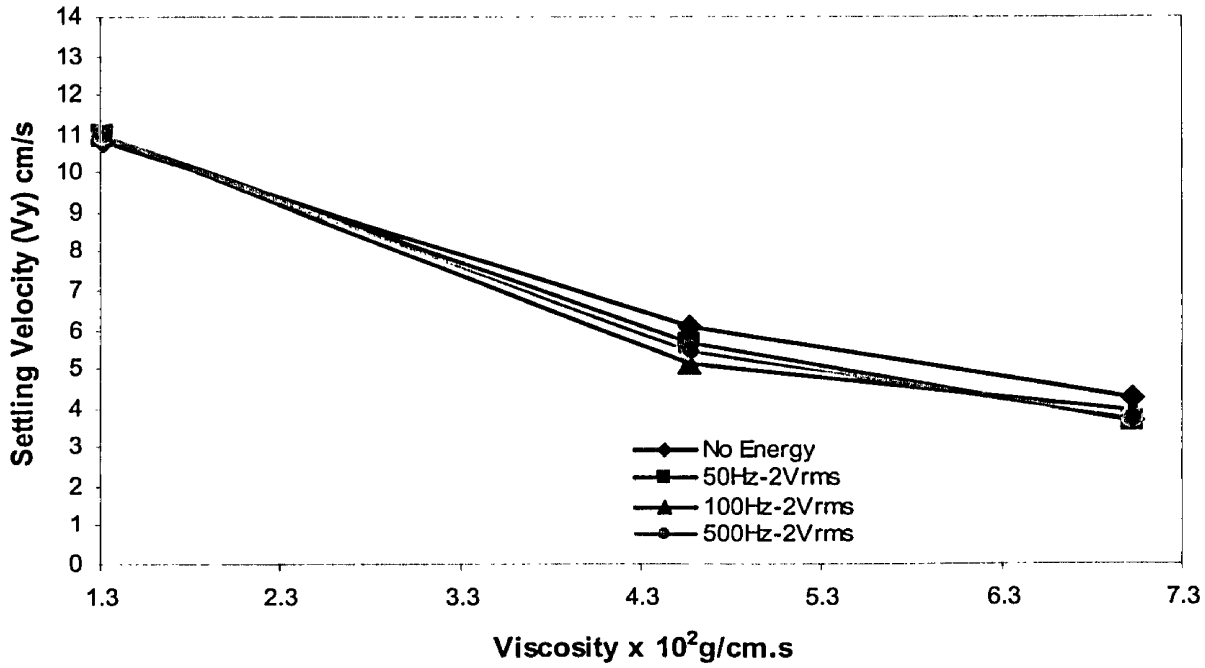

Figure 2A: Effect of Viscosity on Settling Velocity of Acetal in Water at 10^0C (ρ = 1.40g/cm^3; Amplitude-3 V_{rms}; Particle Size=2.38x10^3 μm)

Figure 2A shows the effect of viscosity on the average settling velocity of Acetal sphere in water, in moderate and in high viscosity hydroxypropylcellulose-water (HPC-water) measured at amplitude of 3 V_{rms}. The results indicate that settling velocity (V_y) decreases with increasing the viscosity while varying sound frequency from 0 to 500 Hz has less effect on V_y for the same size particle. The average settling velocity ranges from 3.66 cm/s to 10.99 cm/s. This shows that the settling velocity was lowered 3 times by increasing the viscosity of water approximately 5.4 times. Increasing the amplitude from 2 V_{rms} to 3 V_{rms} does not affect the settling velocity of the particle.

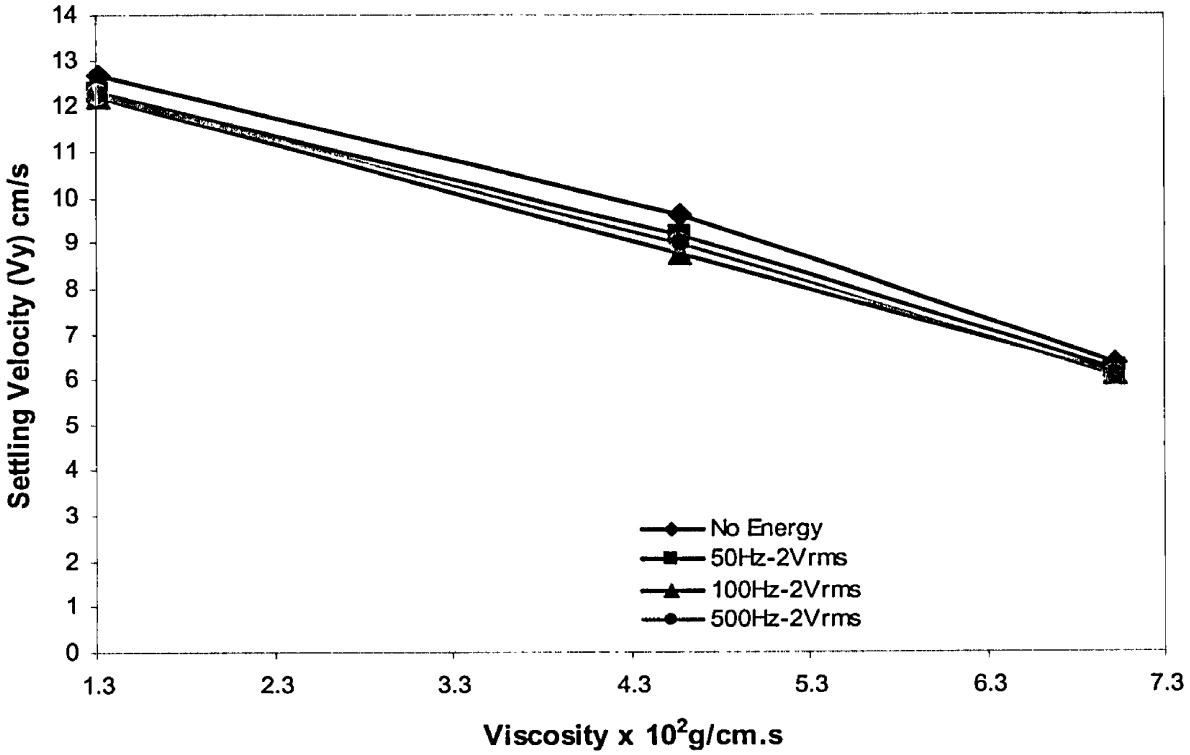

Figure 3A: Effect of Viscosity on Settling Velocity of Acetal in Water at 10^0C ($\rho = 1.40 g/cm^3$; Amplitude-2 V_{rms}; Particle Size= 3.17×10^3 μm)

Figure 3A shows the effect of viscosity on the average settling velocity of Acetal sphere in water, in moderate and in high viscosity hydroxypropylcellulose-water (HPC-water) measured at amplitude of 2 V_{rms}. The results indicate that settling velocity (V_y) decreases with increasing the viscosity while varying sound frequency from 0 to 500 Hz has less effect on V_y for the same size particle. The average settling velocity ranges from 6.09 cm/s to 12.68 cm/s. This shows that the settling velocity was lowered 2 times by increasing the viscosity of water approximately 5.4 times.

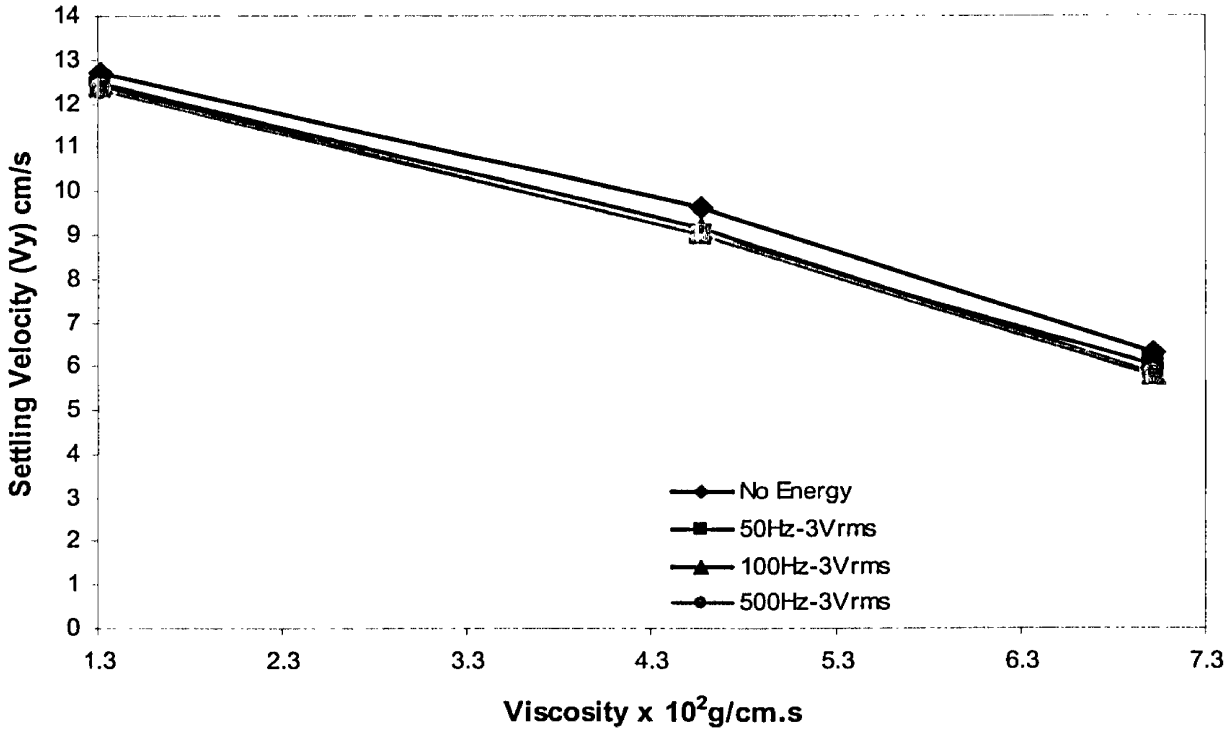

Figure 4A: Effect of Viscosity on Settling Velocity of Acetal in Water at 10^0C (ρ = 1.40g/cm^3; Amplitude-3 V_{rms}; Particle Size= 3.17 x10^3 μm)

Figure 4A shows the effect of viscosity on the average settling velocity of Acetal sphere in water, in moderate and in high viscosity hydroxypropylcellulose-water (HPC-water) measured at amplitude of 3 V_{rms}. The results indicate that settling velocity (V_y) decreases with increasing the viscosity while varying sound frequency from 0 to 500 Hz has less effect on V_y for the same size particle. The average settling velocity ranges from 5.79 cm/s to 12.46 cm/s. This shows that the settling velocity was lowered two times by increasing the viscosity of water approximately 5.4 times. Increasing the amplitude from 2 V_{rms} to 3 V_{rms} does not affect the settling velocity of the particle.

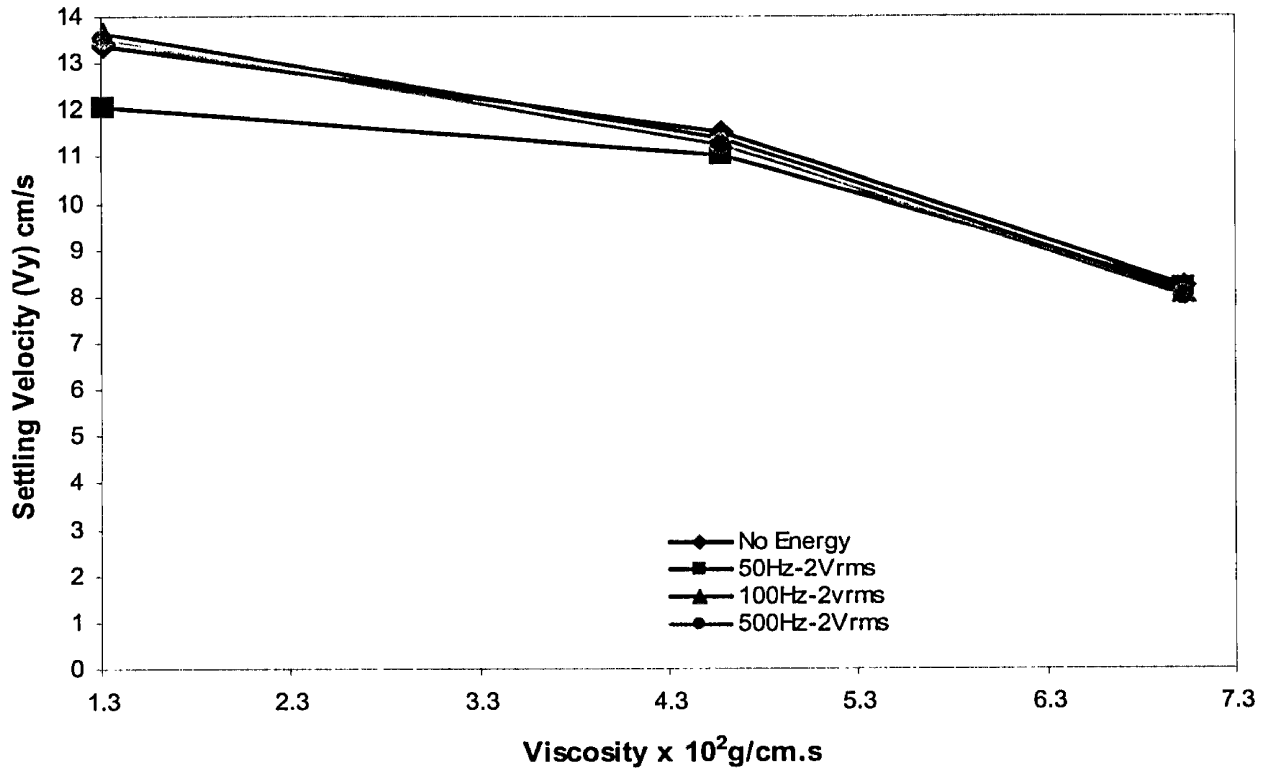

Figure 5A: Effect of Viscosity on Settling Velocity of Acetal in Water at 10^0C (ρ = 1.40g/cm^3; Amplitude-2 V_{rms}; Particle Size= 4.67 x10^3 μm)

Figure 5A shows the effect of viscosity on the average settling velocity of Acetal sphere in water, in moderate and in high viscosity hydroxypropylcellulose-water (HPC-water) measured at amplitude of 2 V_{rms}. The results indicate that settling velocity (V_y) decreases with increasing the viscosity while varying sound frequency from 0 to 500 Hz has no significant effect on V_y for the same size particle. The average settling velocity ranges from 8.1 cm/s to 13.64 cm/s. This shows that the settling velocity was lowered approximately 1.7 times by increasing the viscosity of water approximately 5.4 times.

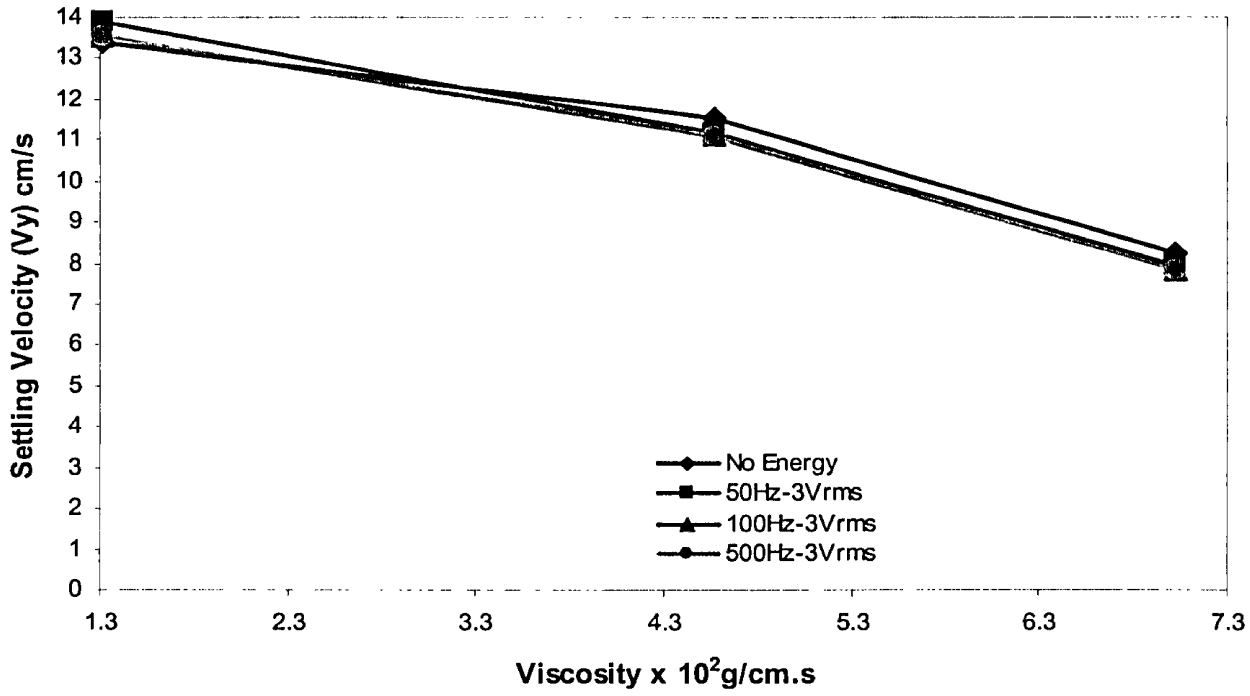

Figure 6A: Effect of Viscosity on Settling Velocity of Acetal in Water at 10^0C ($\rho = 1.40 g/cm^3$; Amplitude-3 V_{rms}; Particle Size= 4.67×10^3 μm)

Figure 6A shows the effect of viscosity on the average settling velocity of Acetal sphere in water, in moderate and in high viscosity hydroxypropylcellulose-water (HPC-water) measured at amplitude of 3 V_{rms}. The results indicate that settling velocity (V_y) decreases with increasing the viscosity while varying sound frequency from 0 to 500 Hz has no significant effect on V_y for the same size particle. The average settling velocity ranges from 7.8 cm/s to 13.92 cm/s. This shows that the settling velocity was lowered approximately 1.8 times by increasing the viscosity of water approximately 5.4 times. Increasing the amplitude from 2 V_{rms} to 3 V_{rms} does not affect the settling velocity of the particle.

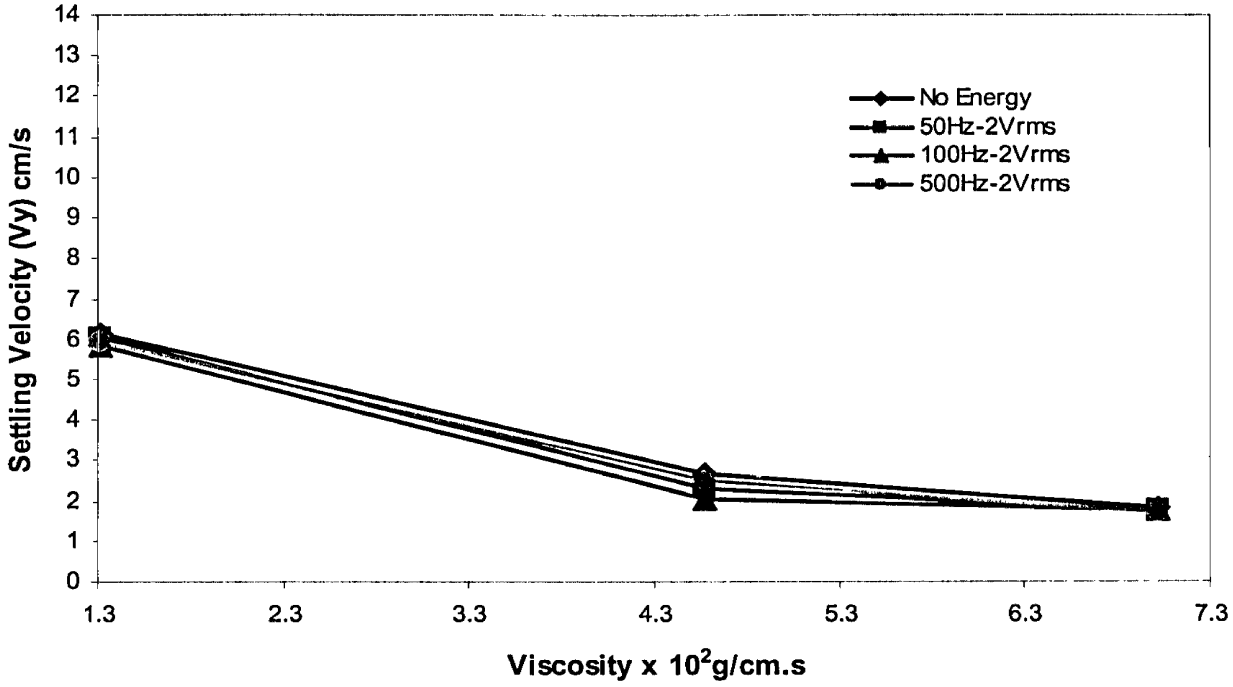

Figure 7A: Effect of Viscosity on Settling Velocity of Nylon in Water at 10^0C (ρ = 1.14 g/cm^3; Amplitude-2 V_{rms}; Particle Size= 2.38 x10^3 μm)

Figure 7A shows the effect of viscosity on the average settling velocity of Nylon sphere in water, in moderate and in high viscosity Hydroxypropylcellulose-water (HPC-water) measured at amplitude of 2 V_{rms}. The results indicate that settling velocity (V_y) decreases with increasing the viscosity while varying sound frequency from 0 to 500 Hz has no significant effect on V_y for the same size particle except at the mid viscosity where the figure shows some variation. The average settling velocity ranges from 1.73 cm/s to 6.05 cm/s. This shows that the settling velocity was lowered approximately 3.5 times by increasing the viscosity of water approximately 5.4 times.

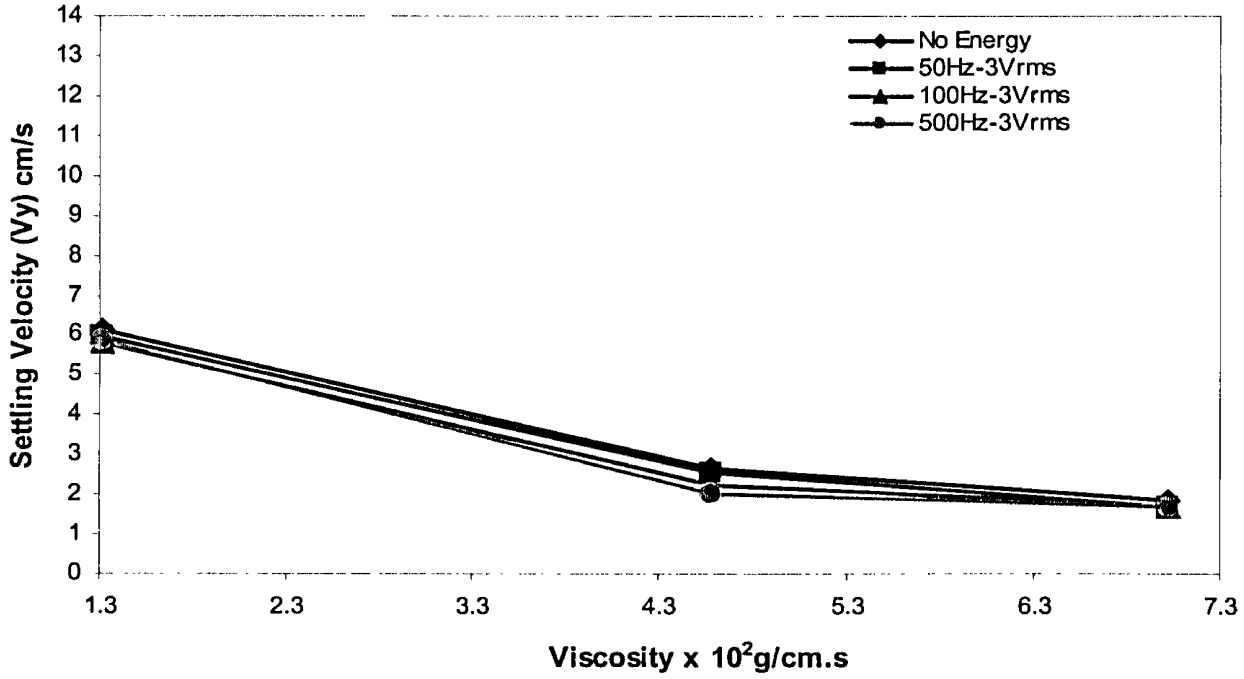

Figure 8A: Effect of Viscosity on Settling Velocity of Nylon in Water at 10^0C (ρ = 1.14 g/cm^3; Amplitude-3 V_{rms}; Particle Size= 2.38 x10^3 μm)

Figure 8A shows the effect of viscosity on the average settling velocity of Nylon sphere in water, in moderate and in high viscosity hydroxypropylcellulose-water (HPC-water) measured at amplitude of 3 V_{rms}. The results indicate that settling velocity (V_y) decreases with increasing the viscosity while varying sound frequency from 0 to 500 Hz has no significant effect on V_y for the same size particle except at the mid viscosity where the figure shows some variation. The average settling velocity ranges from 1.69 cm/s to 5.97 cm/s. This shows that the settling velocity was lowered approximately 3.5 times by increasing the viscosity of water approximately 5.4 times. Increasing the amplitude from 2 V_{rms} to 3 V_{rms} does not affect the settling velocity of the particle.

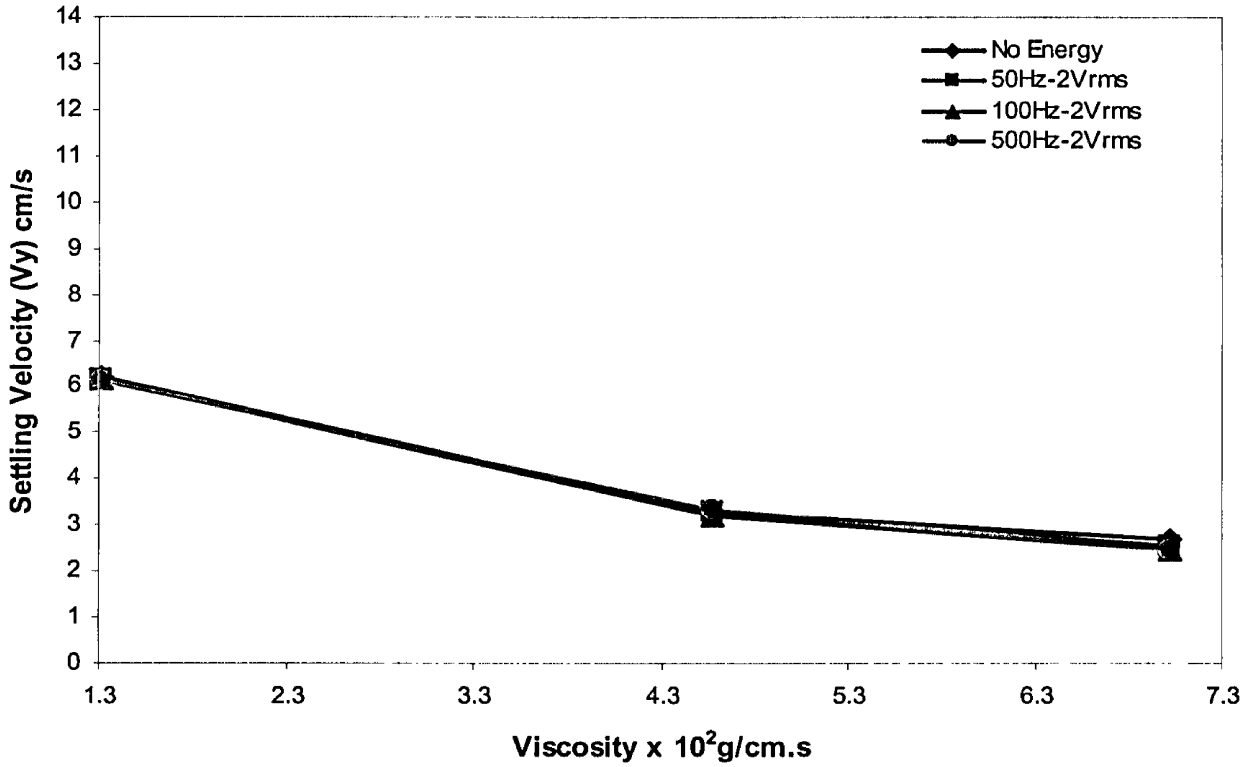

Figure A9: Effect of Viscosity on Settling Velocity of Nylon in Water at 10^0C (ρ = 1.14 g/cm^3; Amplitude-2 V_{rms}; Particle Size= 3.17 x10^3 μm)

Figure 9A shows the effect of viscosity on the average settling velocity of Nylon sphere in water, in moderate and in high viscosity hydroxypropylcellulose-water (HPC-water) measured at amplitude of 2 V_{rms}. The results indicate that settling velocity (V_y) decreases with increasing the viscosity while varying sound frequency from 0 to 500 Hz has no significant effect on V_y for the same size particle except at the high viscosity where the figure shows some variation. The average settling velocity ranges from 2.48 cm/s to 6.2 cm/s. This shows that the settling velocity was lowered approximately 2.5 times by increasing the viscosity of water approximately 5.4 times.

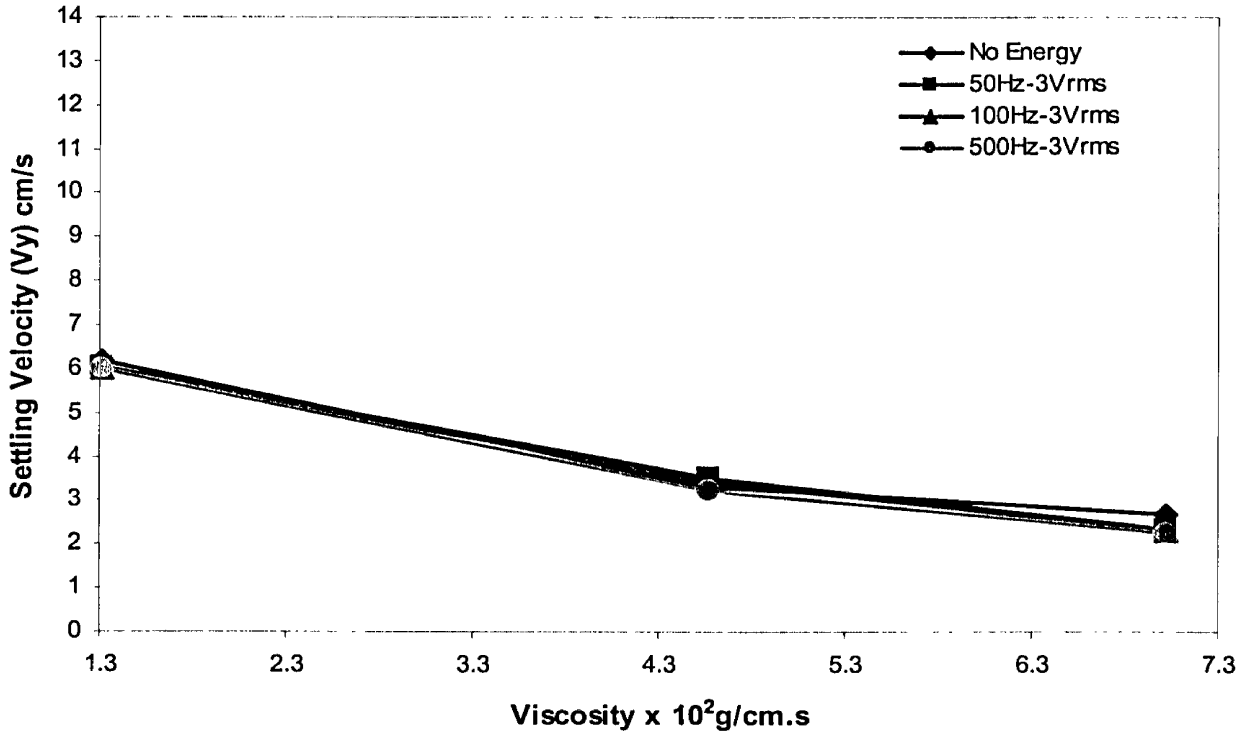

Figure 10A: Effect of Viscosity on Settling Velocity of Nylon in Water at 10^0C (ρ = 1.14 g/cm^3; Amplitude-3 V_{rms}; Particle Size= 3.17 x10^3 μm)

Figure 10A shows the effect of viscosity on the average settling velocity of Nylon sphere in water, in moderate and in high viscosity hydroxypropylcellulose-water (HPC-water) measured at amplitude of 3 V_{rms}. The results indicate that settling velocity (V_y) decreases with increasing the viscosity while varying sound frequency from 0 to 500 Hz has no significant effect on V_y for the same size particle except at the high viscosity where the figure shows some variation. The average settling velocity ranges from 2.27 cm/s to 6.11 cm/s. This shows that the settling velocity was lowered approximately 2.7 times by increasing the viscosity of water approximately 5.4 times. Increasing the amplitude from 2 V_{rms} to 3 V_{rms} does not affect much about the settling velocity of the particle.

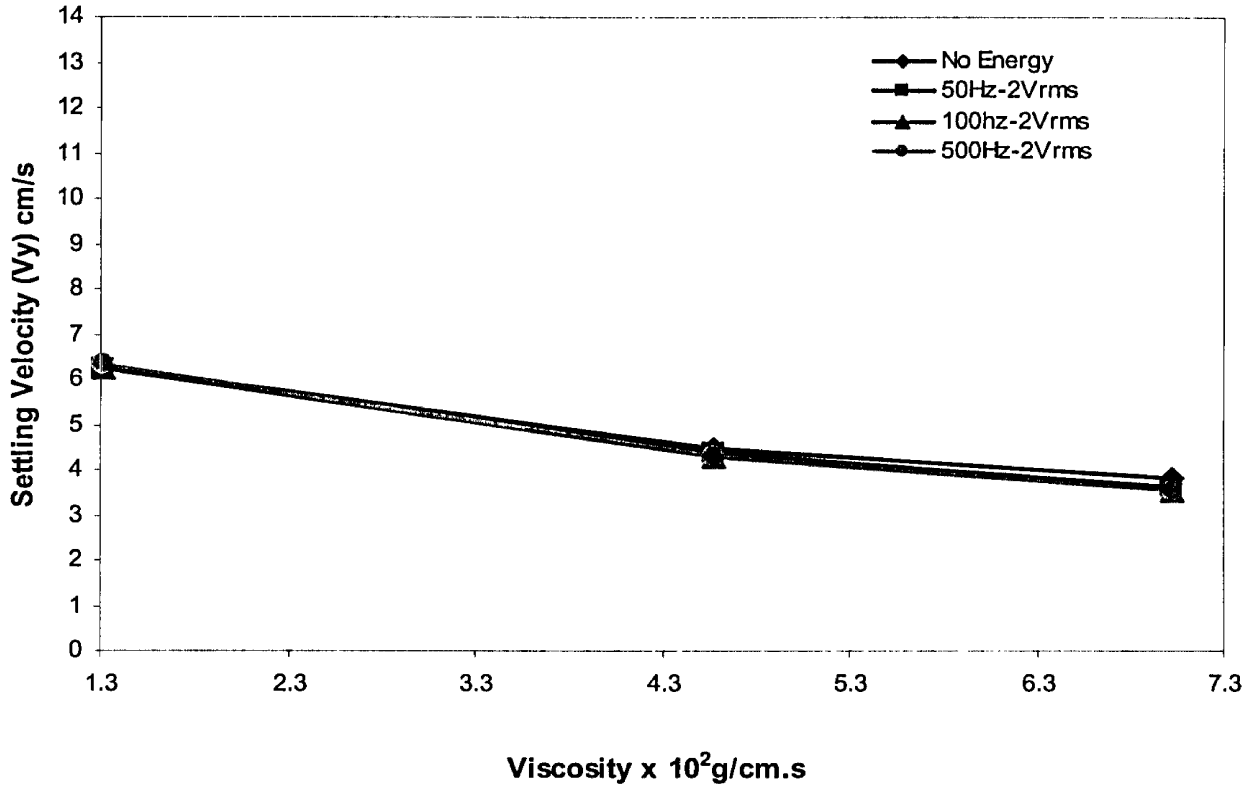

Figure 11A: Effect of Viscosity on Settling Velocity of Nylon in Water at 10^0C (ρ = 1.14 g/cm^3; Amplitude-2 V_{rms}; Particle Size= 4.76 x10^3 μm)

Figure 11A shows the effect of viscosity on the average settling velocity of Nylon sphere in water, in moderate and in high viscosity hydroxypropylcellulose-water (HPC-water) measured at amplitude of 2 V_{rms}. The results indicate that settling velocity (V_y) decreases with increasing the viscosity while varying sound frequency from 0 to 500 Hz has no significant effect on V_y for the same size particle except at the high viscosity where the figure shows some variation. The average settling velocity ranges from 3.55 cm/s to 6.29 cm/s. This shows that the settling velocity was lowered approximately 1.8 times by increasing the viscosity of water approximately 5.4 times.

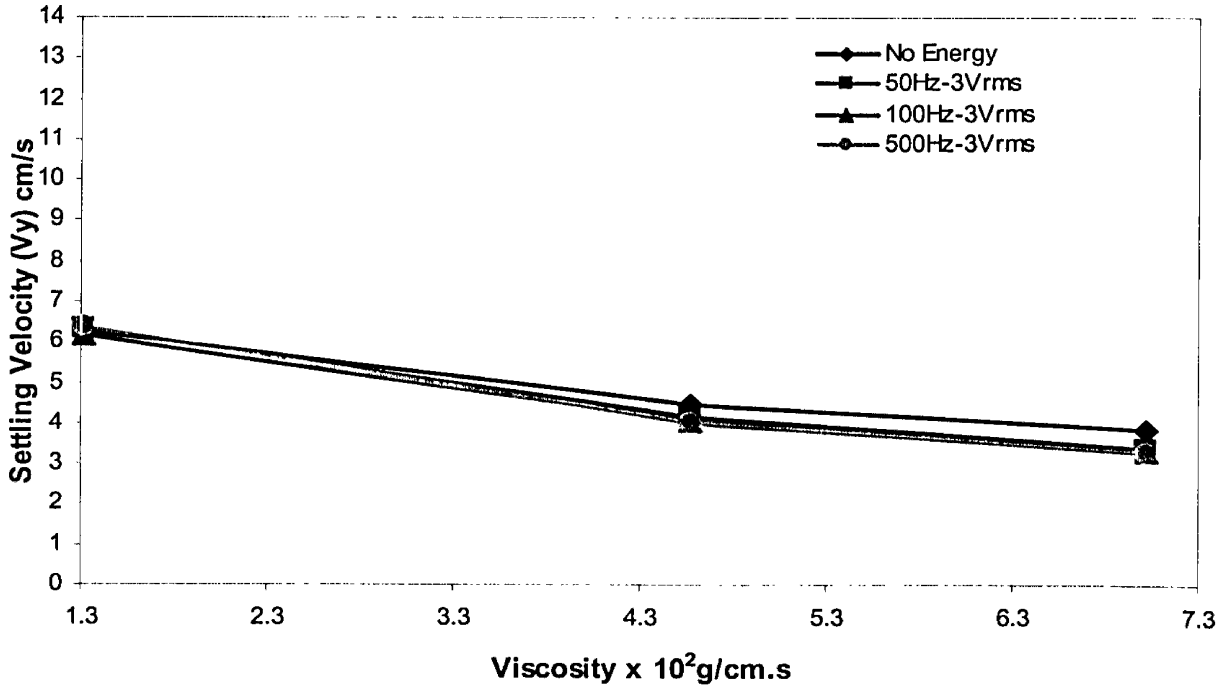

Figure 12A: Effect of Viscosity on Settling Velocity of Nylon in Water at 10^0C (ρ = 1.14 g/cm^3; Amplitude-3 V_{rms}; Particle Size= 4.76 x10^3 μm)

Figure 12A shows the effect of viscosity on the average settling velocity of Nylon sphere in water, in moderate and in high viscosity hydroxypropylcellulose-water (HPC-water) measured at amplitude of 3 V_{rms}. The results indicate that settling velocity (V_y) decreases with increasing the viscosity while varying sound frequency from 0 to 500 Hz has no significant effect on V_y for the same size particle except at the high viscosity where the figure shows some variation. The average settling velocity ranges from 3.31 cm/s to 6.38 cm/s. This shows that the settling velocity was lowered approximately 1.9 times by increasing the viscosity of water approximately 5.4 times. Increasing the amplitude from 2 V_{rms} to 3 V_{rms} does not affect much about the settling velocity of the particle.

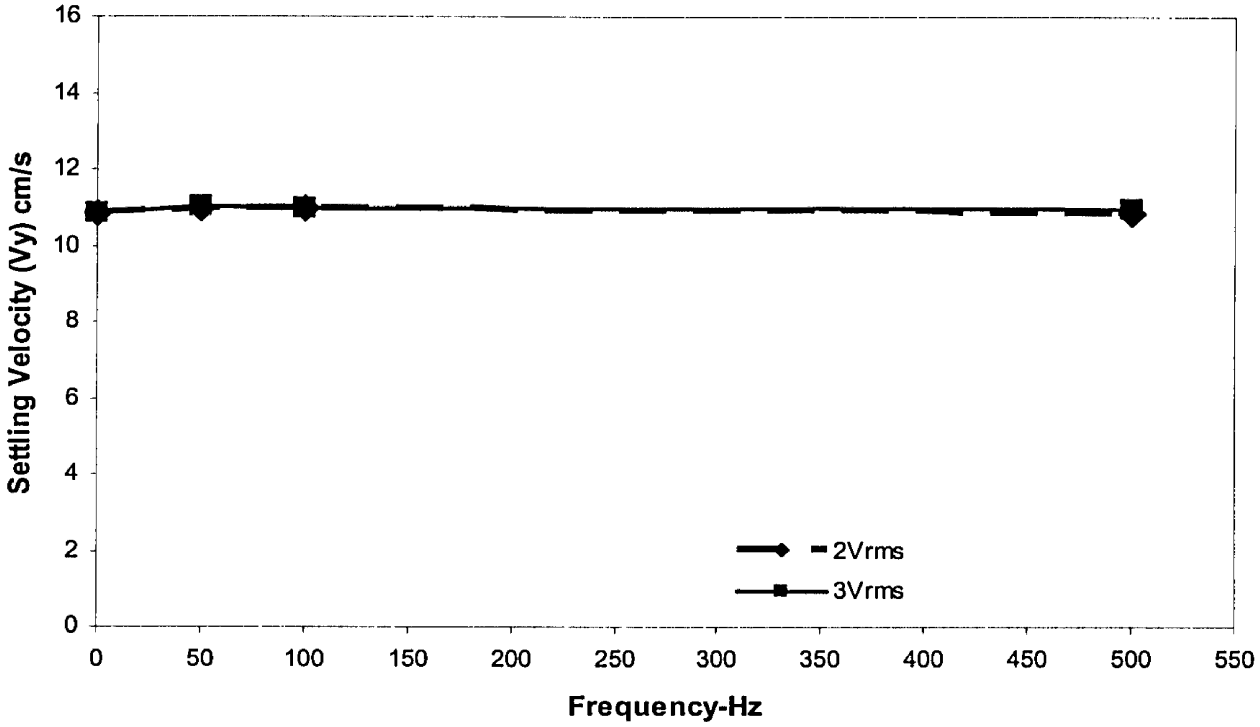

Figure 13A: Effect of Frequency on Settling Velocity of Acetal in Water at 10^0C (ρ = 1.40 g/cm^3; μ = 1.30x10^{-2} g/cm.s; Particle Size = 2.38 x10^3 μm)

Figure 13A shows the effect of acoustic frequency on the average settling velocity of Acetal sphere in water measured at different amplitudes of 2 V_{rms} and 3 V_{rms}. The results indicate that the effect of the frequency on settling velocity is not consistent since this figure is showing the lowest velocity as the one with zero frequency. It does not show a good trend.

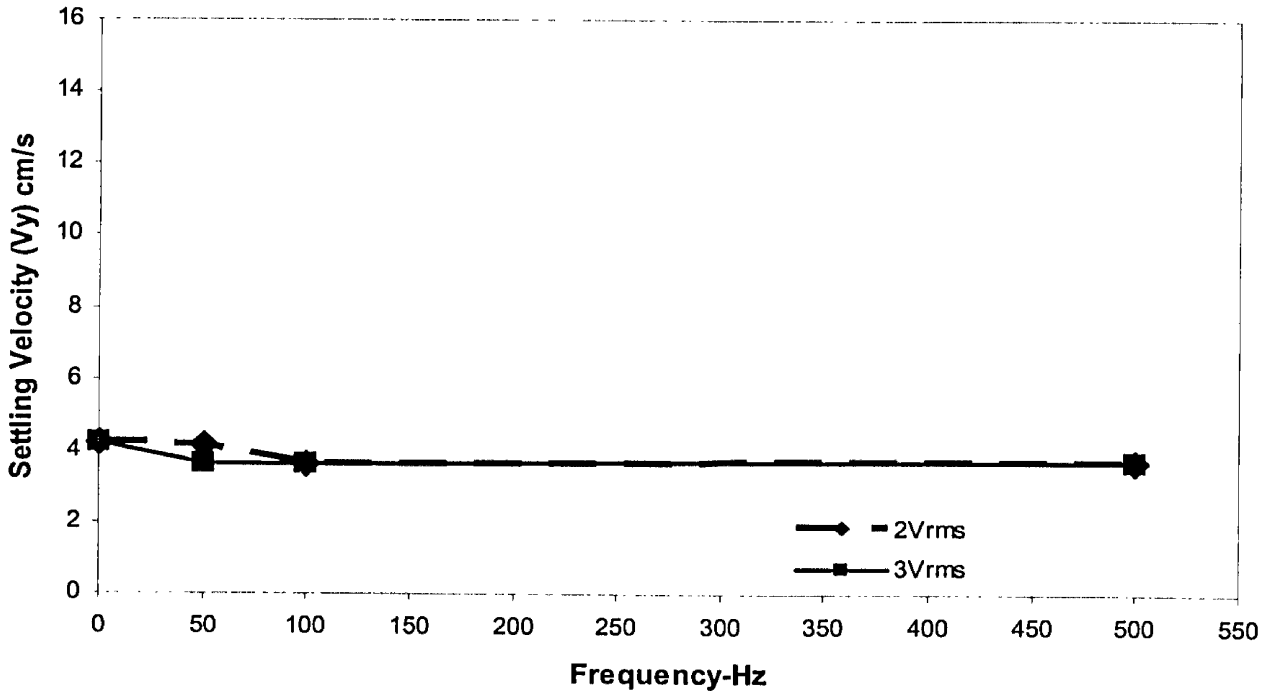

Figure 14A: Effect of Frequency on Settling Velocity of Acetal in HPC-Water at 10^0C ($\mu = 7.02 \times 10^{-2}$ g/cm.s; Particle Size = 2.38×10^3 μm)

Figure 14A shows the effect of acoustic frequency on the average settling velocity of Acetal sphere in a high viscosity hydroxypropylcellulose-water (HPC-water) measured at different amplitudes of 2 V_{rms} and 3 V_{rms}. The results indicate that the settling velocity is slightly low at 100 Hz. It does not show a good trend.

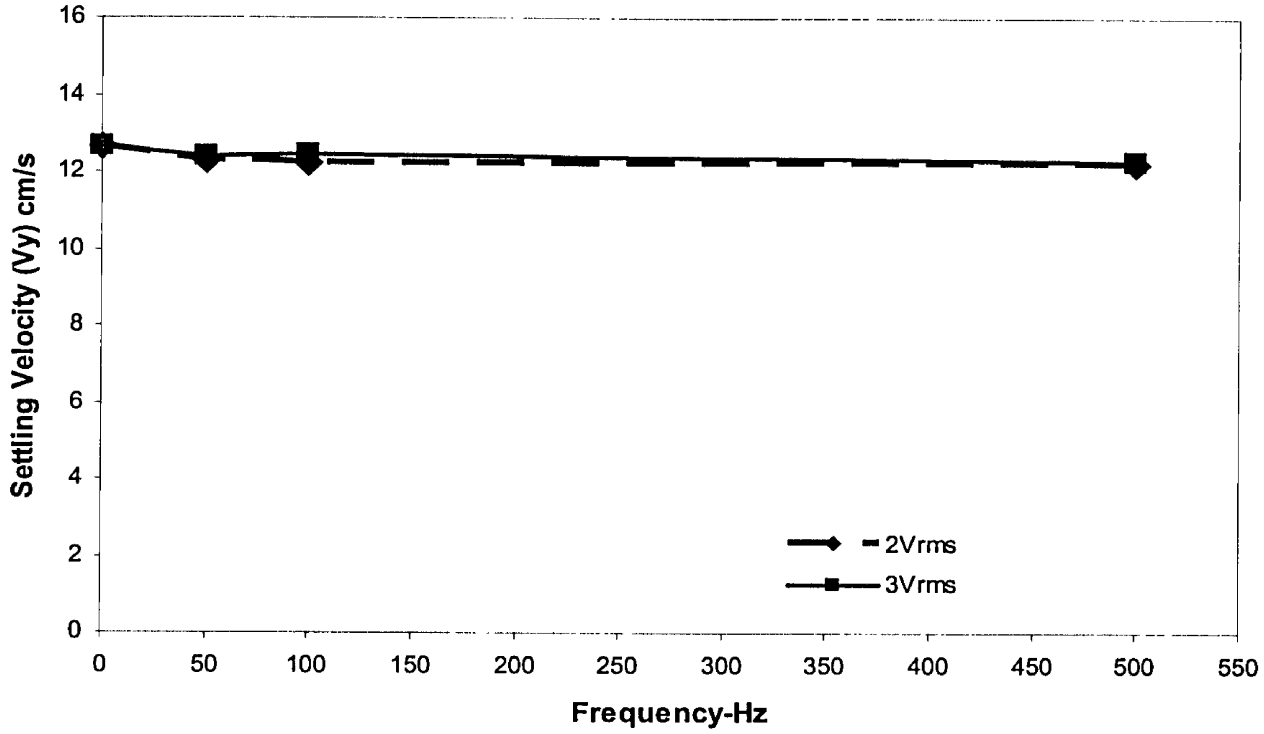

Figure 15A: Effect of Frequency on Settling Velocity of Acetal in Water at 10^0C (ρ = 1.40 g/cm^3; μ = 1.30x10^{-2} g/cm.s; Particle Size = 3.17 x10^3 μm)

Figure 15A shows the effect of acoustic frequency on the average settling velocity of Acetal sphere in water measured at different amplitudes of 2 V_{rms} and 3 V_{rms}. The results indicate that the settling velocity is not showing any change when applied to sound energy.

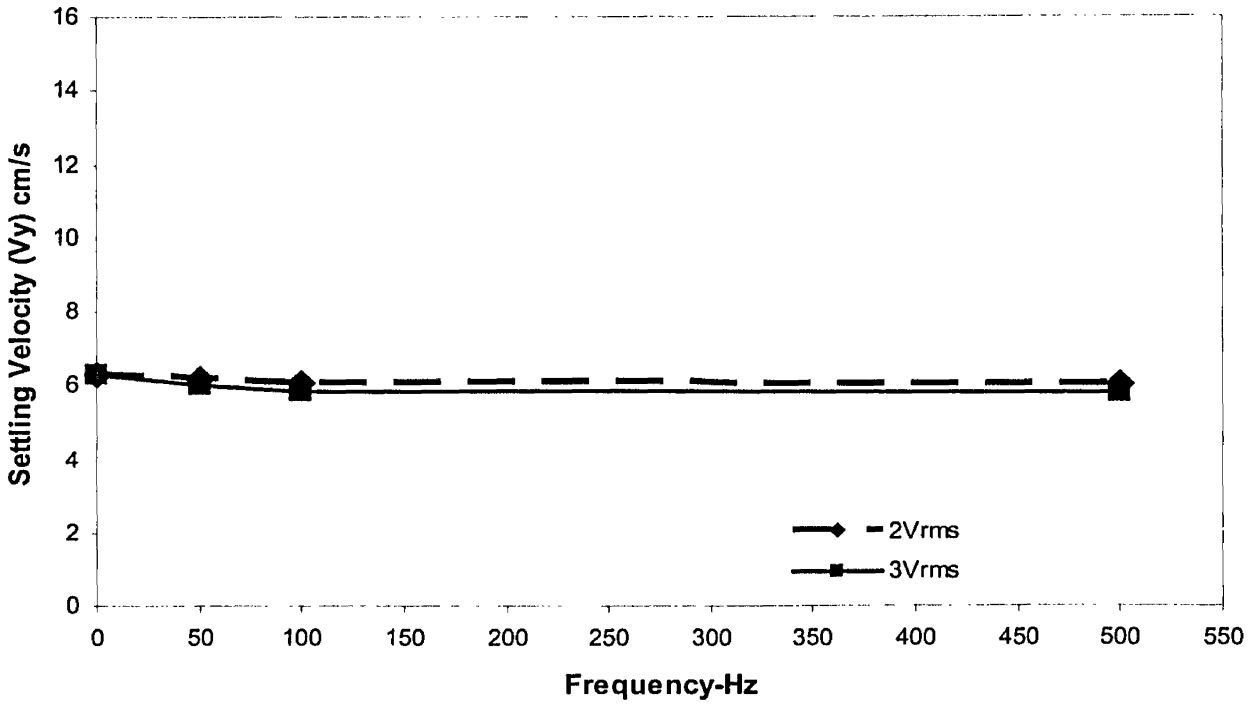

Figure 16A: Effect of Frequency on Settling Velocity of Acetal in HPC-Water at 10^0C (μ = 7.02 x10^{-2} g/cm.s; Particle Size = 3.17 x10^3 μm)

Figure16A shows the effect of acoustic frequency on the average settling velocity of Acetal sphere in a high viscosity hydroxypropylcellulose-water (HPC-water) measured at different amplitudes of 2 V_{rms} and 3 V_{rms}. The results indicate that the settling velocity is slightly low at 100 Hz.

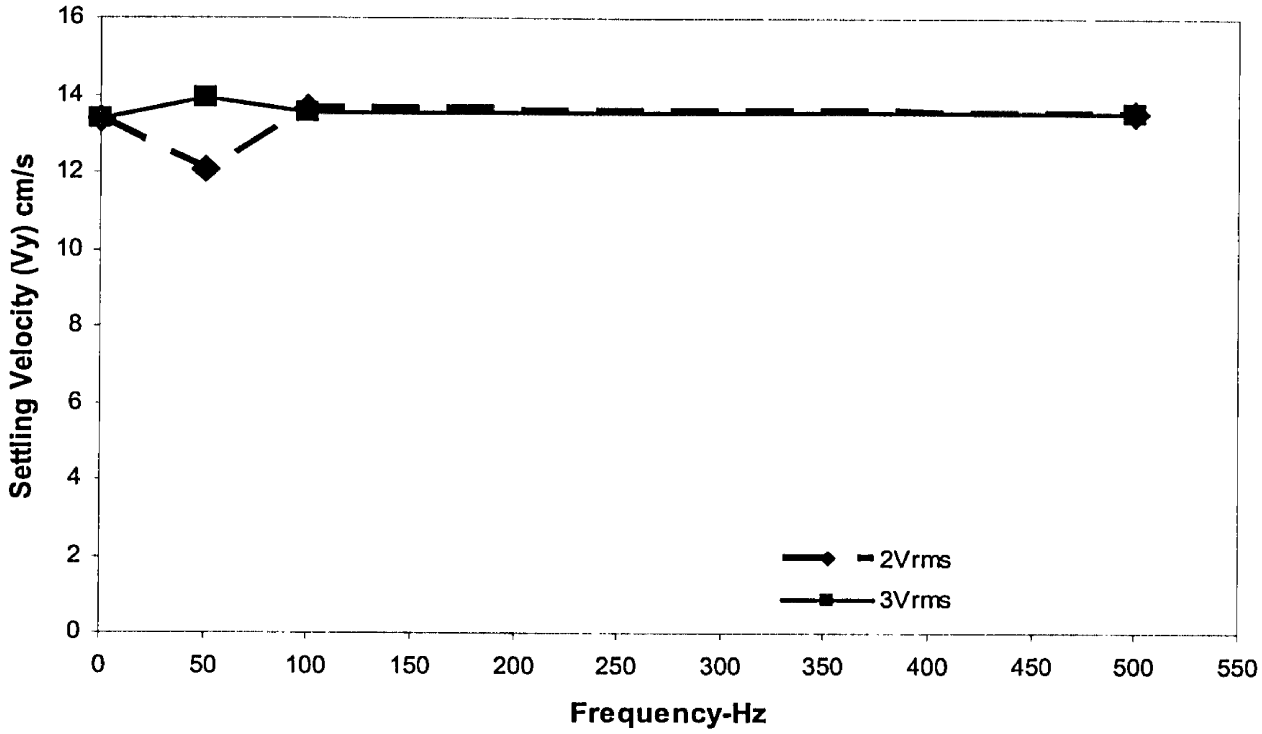

Figure17A: Effect of Frequency on Settling Velocity of Acetal in Water at 10^0C (ρ = 1.40 g/cm^3; μ = 1.30x10^{-2} g/cm.s; Particle Size = 4.76 x10^3 μm)

Figure 17A shows the effect of acoustic frequency on the average settling velocity of Acetal sphere in water measured at different amplitudes of 2 V_{rms} and 3 V_{rms}. The results indicate that the settling velocity is slightly low at 50 Hz. It does not show a good trend.

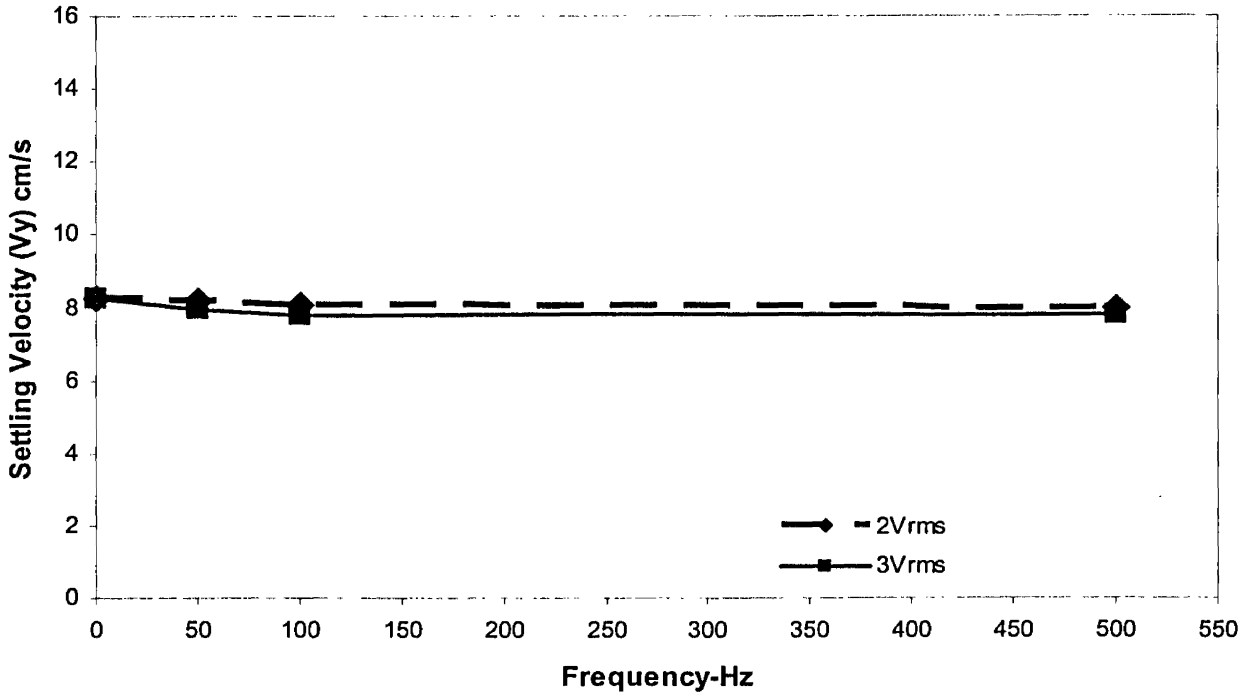

Figure 18A: Effect of Frequency on Settling Velocity of Acetal in HPC-Water at 10^0C ($\mu = 7.02 \times 10^{-2}$ g/cm.s; Particle Size = 4.76×10^3 μm)

Figure 18A shows the effect of acoustic frequency on the average settling velocity of Acetal sphere in a high viscosity hydroxypropylcellulose-water (HPC-water) measured at different amplitudes of 2 V_{rms} and 3 V_{rms}. The results indicate that the settling velocity is slightly low at 100 Hz and 500 Hz.

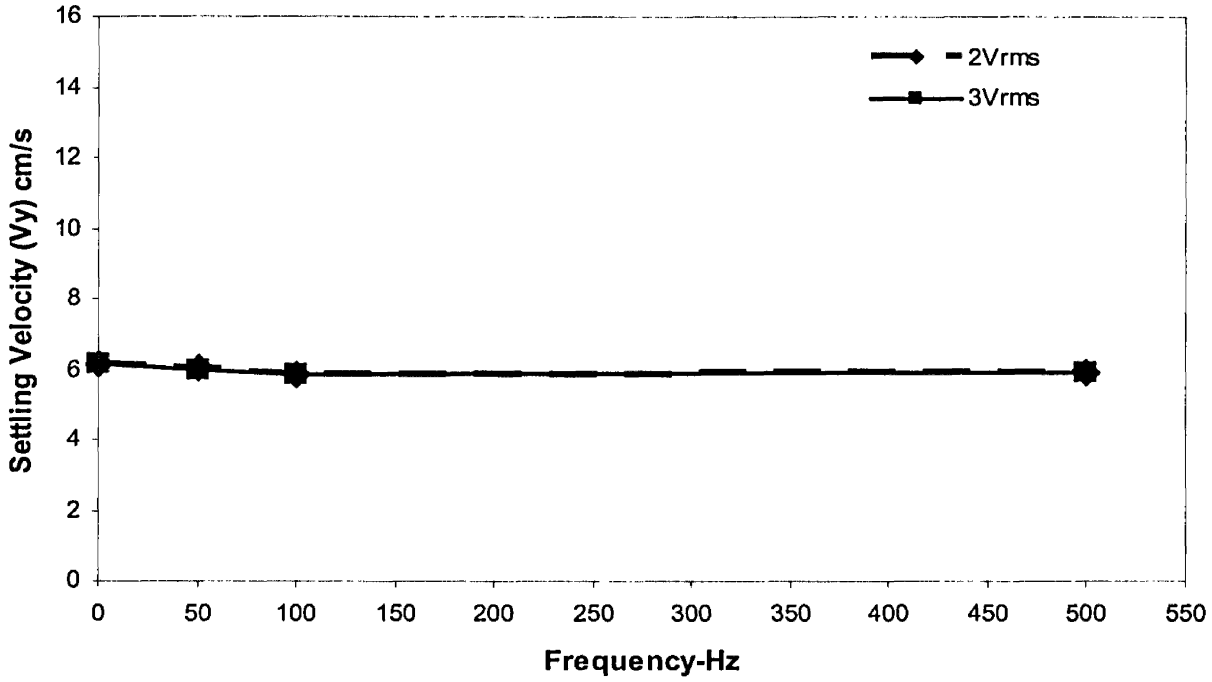

Figure 19A: Effect of Frequency on Settling Velocity of Nylon in Water at 10^0C (ρ = 1.14 g/cm^3; μ = 1.30x10^{-2} g/cm.s; Particle Size = 2.38 x10^3 μm)

Figure 19A shows the effect of acoustic frequency on the average settling velocity of Nylon sphere in water measured at different amplitudes of 2 V_{rms} and 3 V_{rms}. The results indicate that the settling velocity was slightly dropped at 100 Hz and 500 Hz.

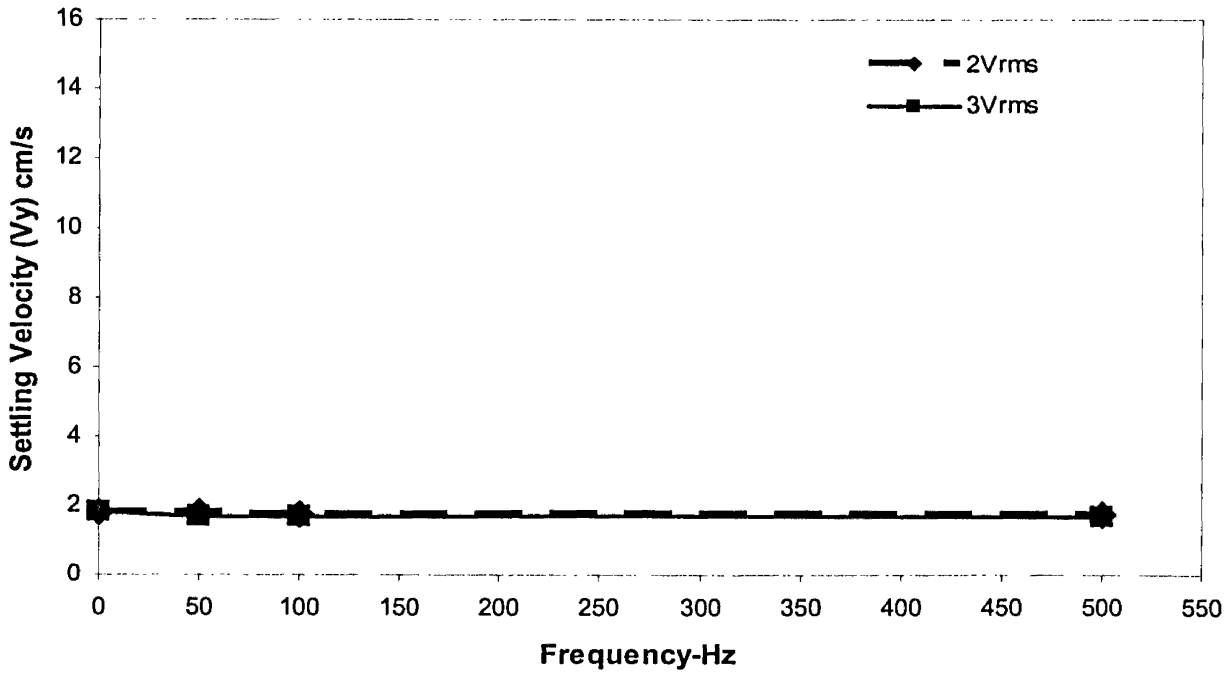

Figure 20A: Effect of Frequency on Settling Velocity of Nylon in HPC-Water at 10^0C ($\mu = 7.02 \times 10^{-2}$ g/cm.s; Particle Size = 2.38×10^3 μm)

Figure 20A shows the effect of acoustic frequency on the average settling velocity of Nylon sphere in a high viscosity hydroxypropylcellulose-water (HPC-water) measured at different amplitudes of 2 V_{rms} and 3 V_{rms}. The results indicate that there is no significant difference between the settling velocities at 50 Hz, 100 Hz and 500 Hz.

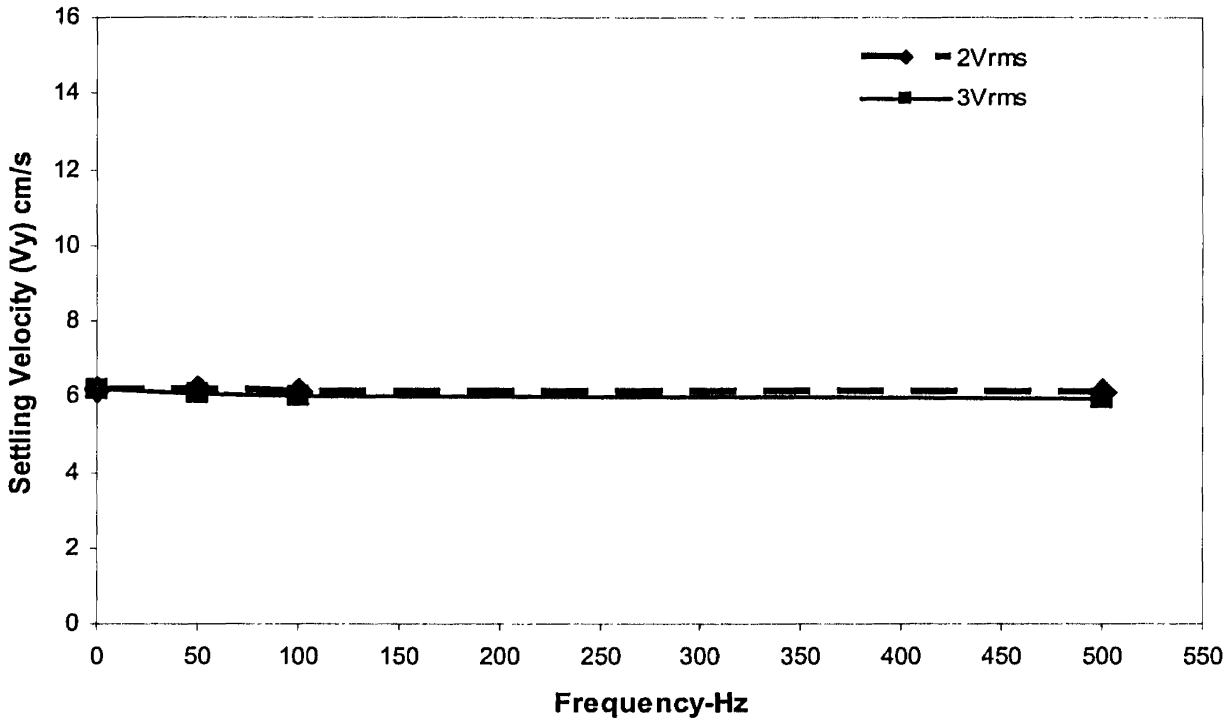

Figure 21A: Effect of Frequency on Settling Velocity of Nylon in Water at 10^0C (ρ = 1.14 g/cm^3; μ = 1.30x10^{-2} g/cm.s; Particle Size = 3.17 x10^3 μm)

Figure 21A shows the effect of acoustic frequency on the average settling velocity of Nylon sphere in water measured at different amplitudes of 2 V_{rms} and 3 V_{rms}. The results are similar to those of figure 20A.

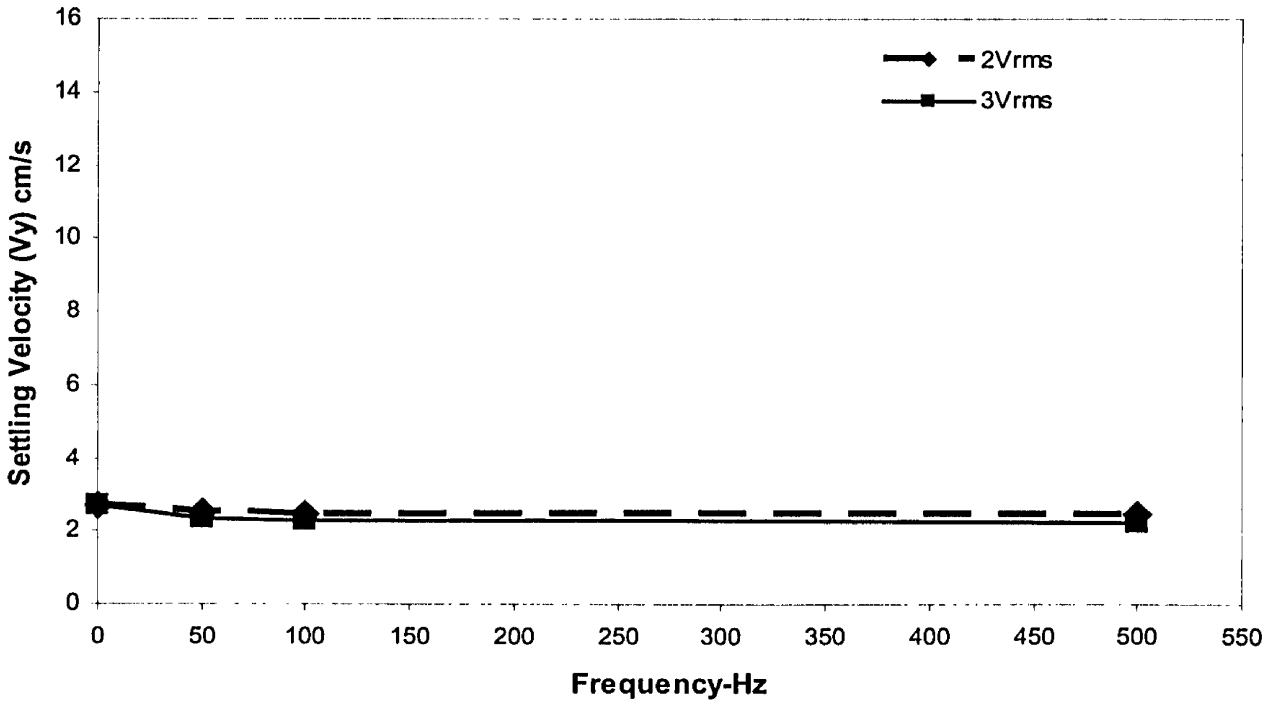

Figure 22A: Effect of Frequency on Settling Velocity of Nylon in HPC-Water at 10^0C ($\mu = 7.02 \times 10^{-2}$ g/cm.s; Particle Size = 3.17×10^3 μm)

Figure 22A shows the effect of acoustic frequency on the average settling velocity of Nylon sphere in a high viscosity hydroxypropylcellulose-water (HPC-water) measured at different amplitudes of 2 V_{rms} and 3 V_{rms}. The results are similar to those of figure 21A.

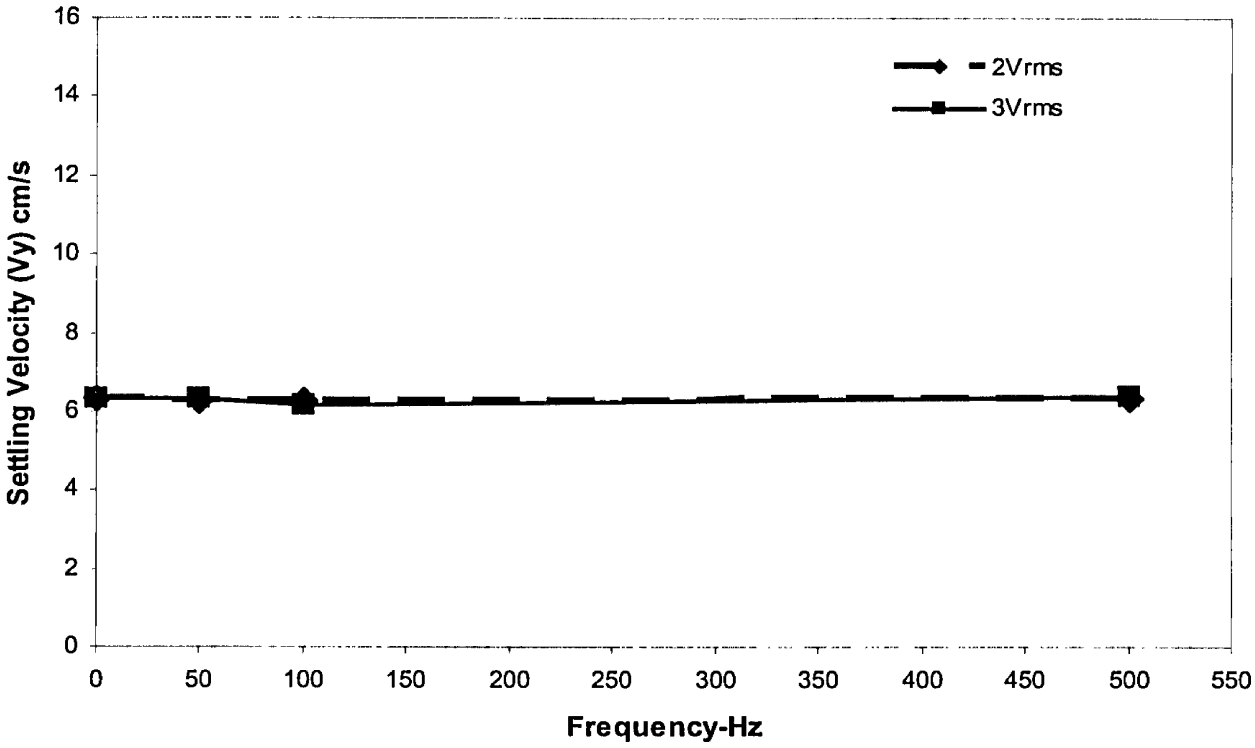

Figure 23A: Effect of Frequency on Settling Velocity of Nylon in Water at 10^0C (ρ = 1.14 g/cm^3; μ = 1.30x10^{-2} g/cm.s; Particle Size = 4.76 x10^3 μm)

Figure 23A shows the effect of acoustic frequency on the average settling velocity of Nylon sphere in water measured at different amplitudes of 2 V_{rms} and 3 V_{rms}. The results are similar to those of figure A22.

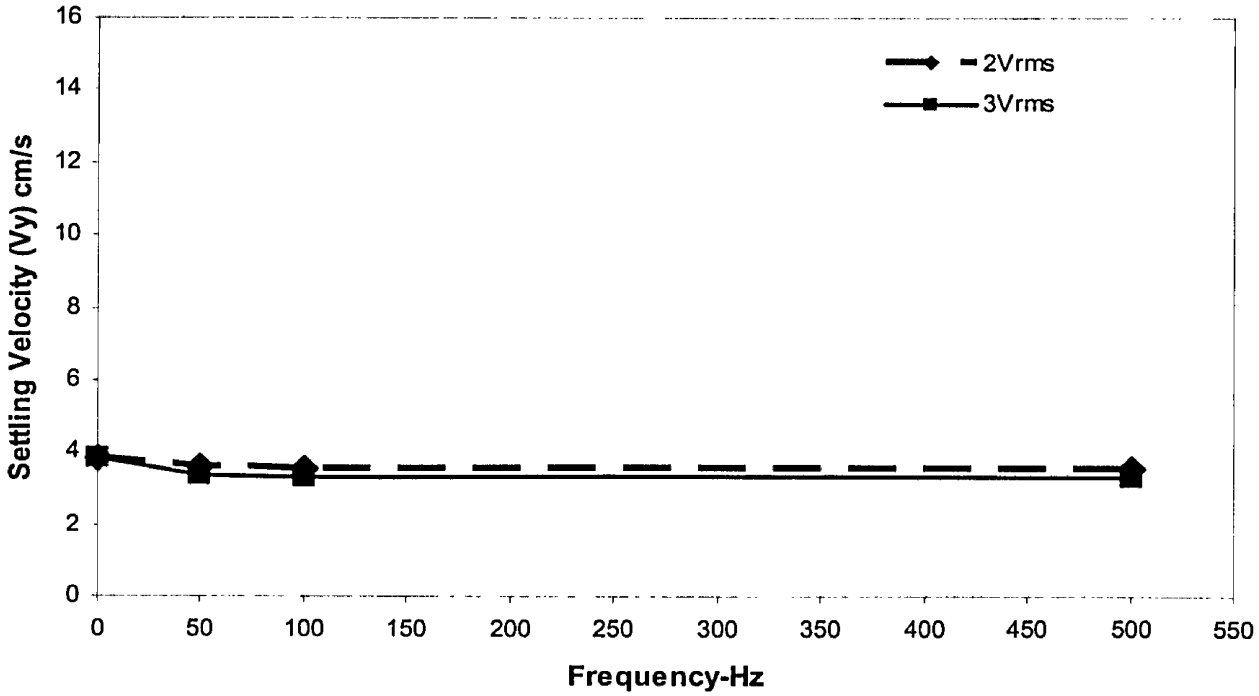

Figure 24A: Effect of Frequency on Settling Velocity of Nylon in HPC-Water at 10^0C ($\mu = 7.02 \times 10^{-2}$ g/cm.s; Particle Size = 4.76×10^3 μm)

Figure 24A shows the effect of acoustic frequency on the average settling velocity of Nylon sphere in a high viscosity hydroxypropylcellulose-water (HPC-water) measured at different amplitudes of 2 $V_{rms}$and 3 V_{rms}. The results indicate that there is no significant difference between the settling velocities of the particle at the frequencies of 50 Hz, 100 Hz and 500Hz.

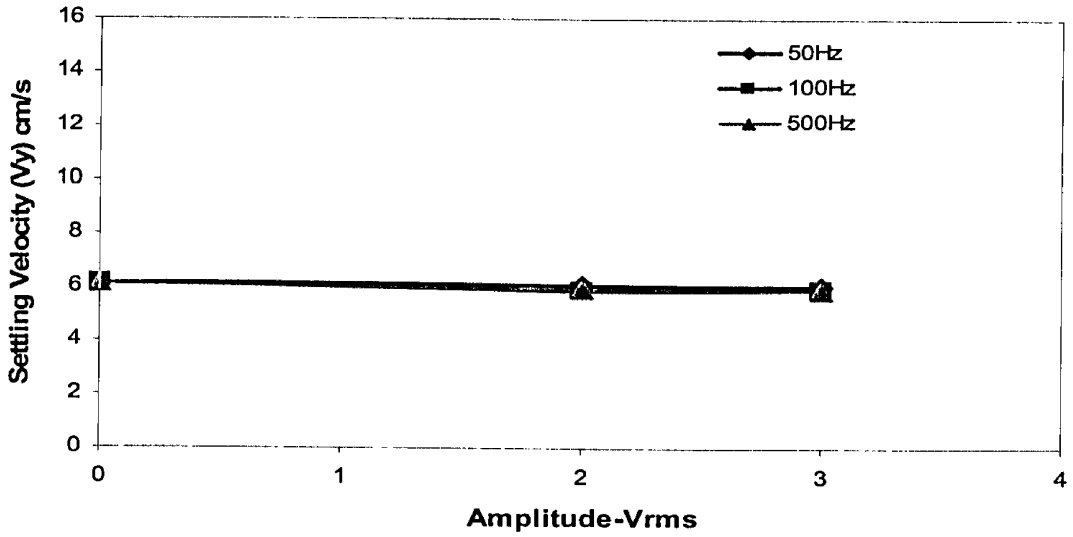

Figure 25A: Effect of Acoustic Amplitude on Settling Velocity of Nylon in Water at 10^0C (ρ = 1.14 g/cm^3; μ = 1.30x10^{-2} g/cm.s; Particle Size = 2.38 x10^3 μm)

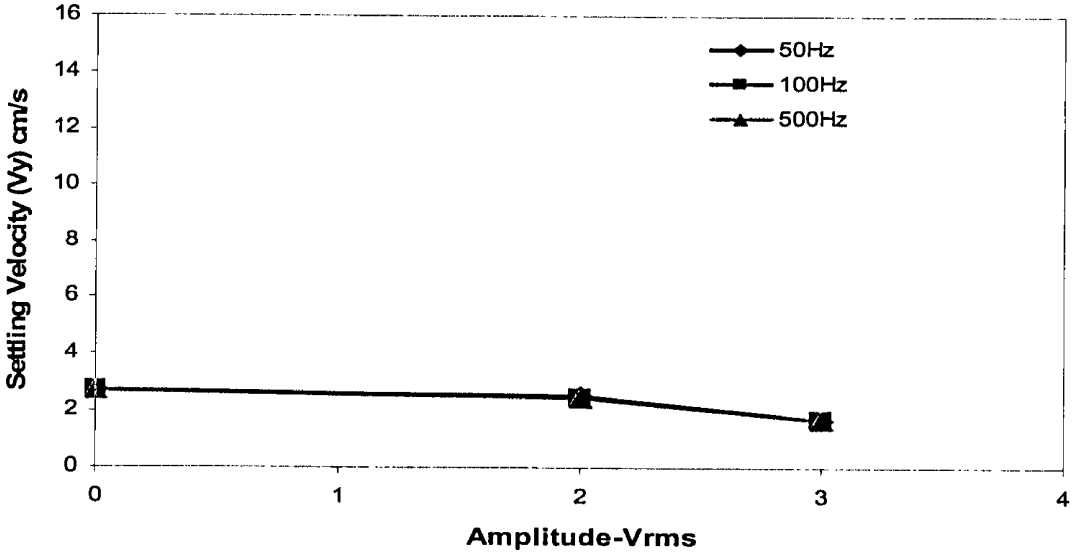

Figure 26A: Effect of Acoustic Amplitude on Settling Velocity of Nylon in HPC-Water at 10^0C (μ = 7.02 x10^{-2} g/cm.s; Particle Size = 2.38 x10^3 μm)

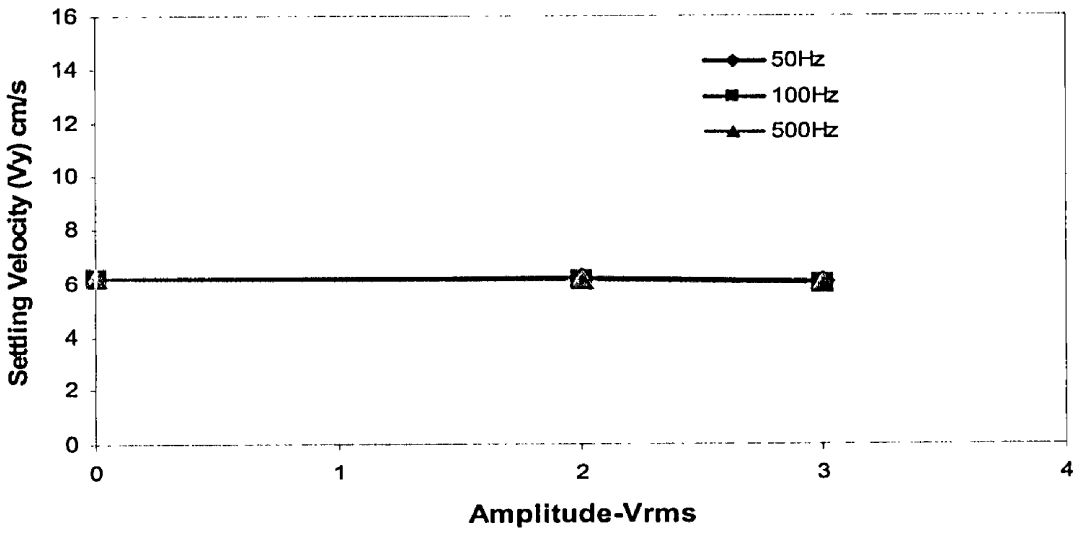

Figure 27A: Effect of Acoustic Amplitude on Settling Velocity of Nylon in Water at 10^0C (ρ = 1.14 g/cm^3; μ = 1.30x10^{-2} g/cm.s; Particle Size = 3.17 x10^3 μm)

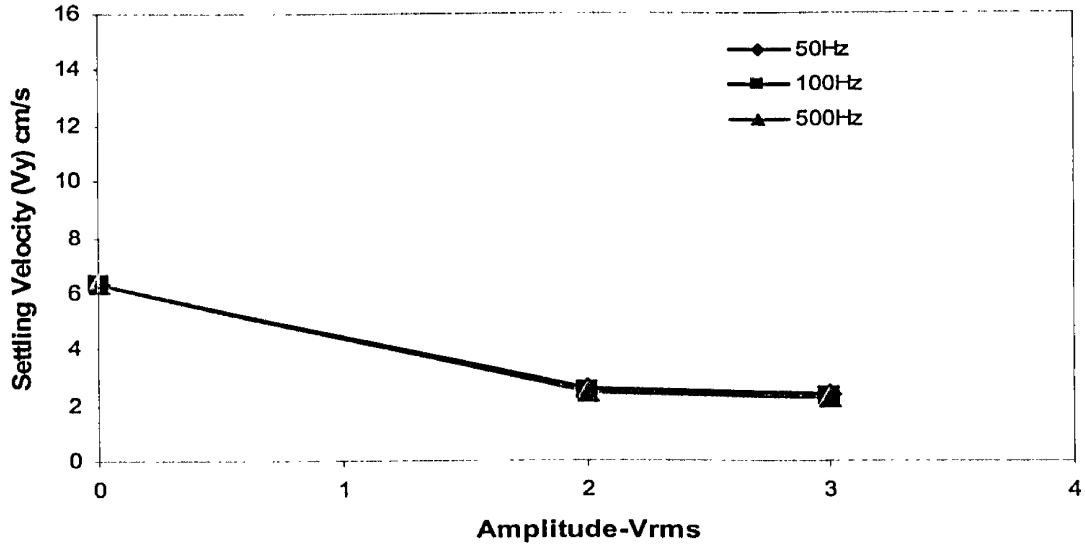

Figure 28A: Effect of Acoustic Amplitude on Settling Velocity of Nylon in HPC-Water at 10^0C (μ = 7.02 x10^{-2} g/cm.s; Particle Size = 3.17 x10^3 μm)

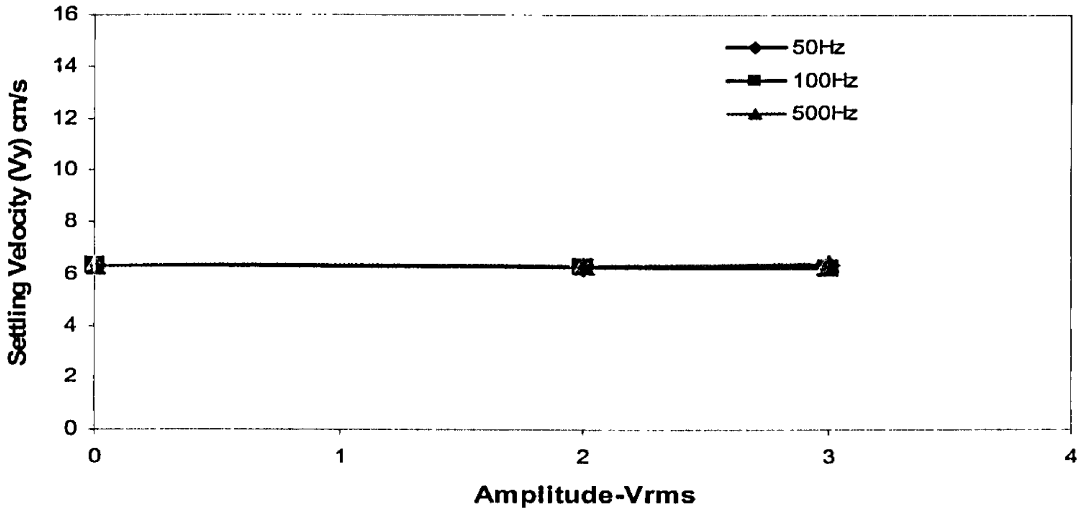

Figure 29A: Effect of Acoustic Amplitude on Settling Velocity of Nylon in Water at 10^0C (ρ = 1.14 g/cm^3; μ = 1.30x10^{-2} g/cm.s; Particle Size = 4.76 x10^3 μm)

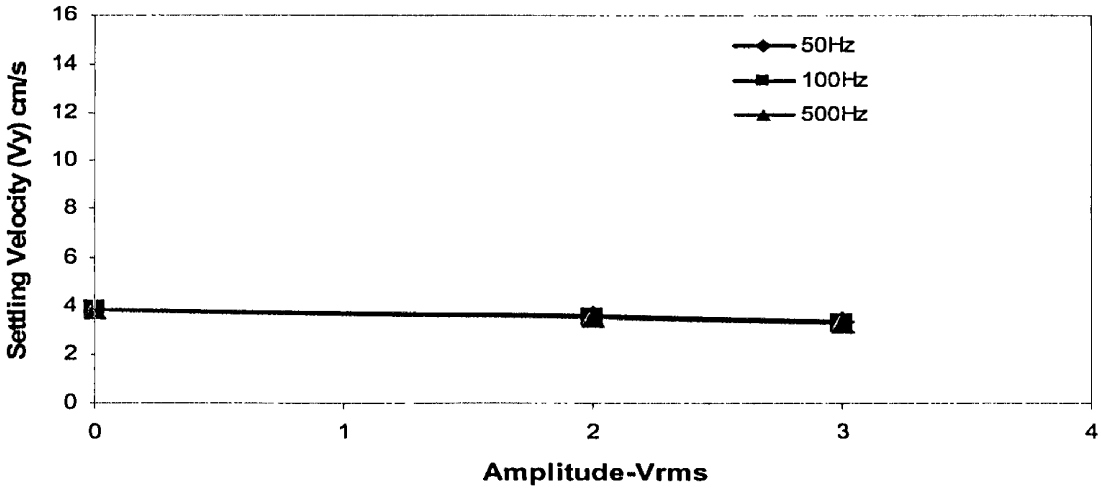

Figure 30A: Effect of Acoustic Amplitude on Settling Velocity of Nylon in HPC-Water at 10^0C (μ = 7.02 x10^{-2} g/cm.s; Particle Size = 4.76 x10^3 μm)

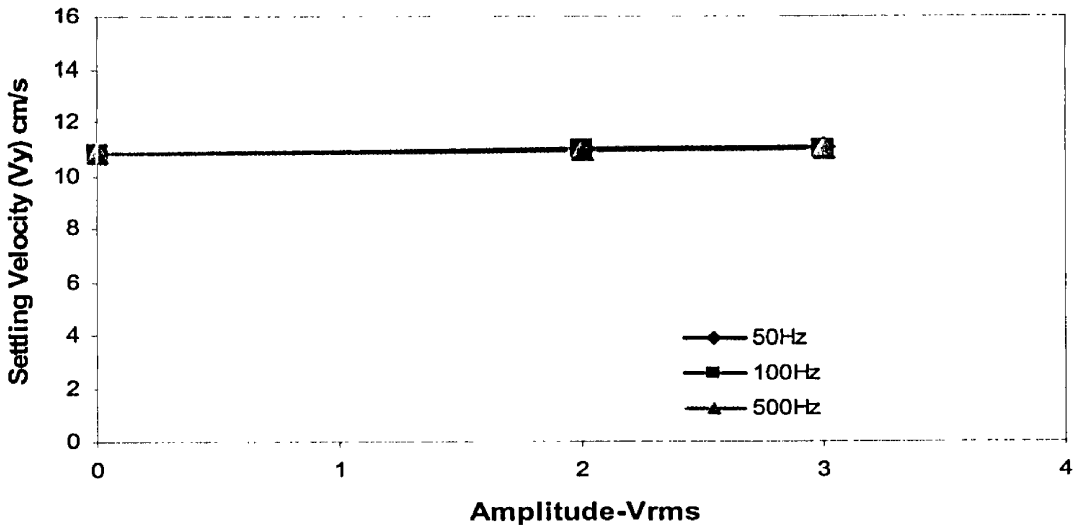

Figure 31A: Effect of Acoustic Amplitude on Settling Velocity of Acetal in Water at 10^0C (ρ = 1.40 g/cm^3; μ = 1.30x10^{-2} g/cm.s; Particle Size = 2.38 x10^3 μm)

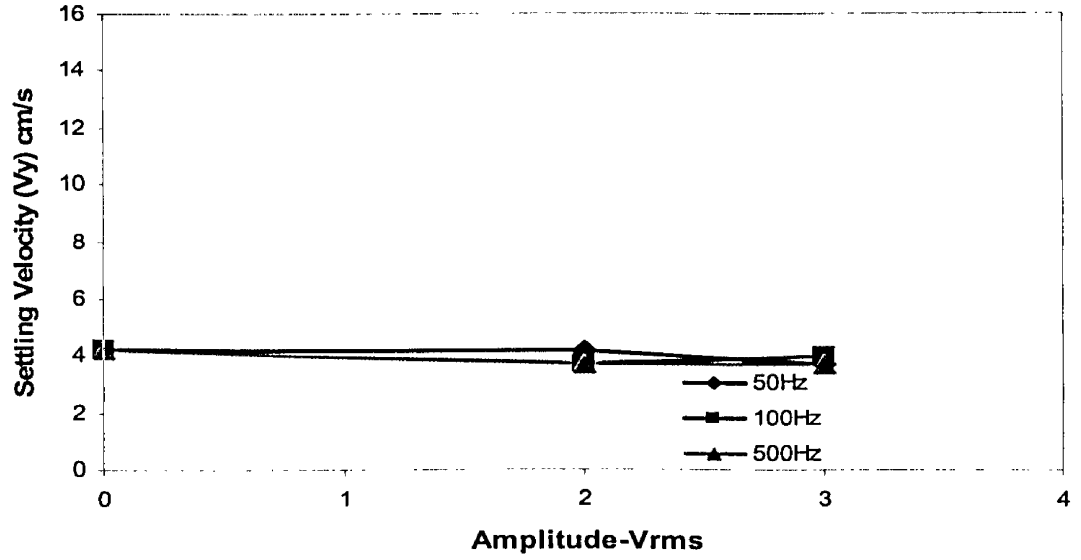

Figure 32A: Effect of Acoustic Amplitude on Settling Velocity of Acetal in HPC-Water at 10^0C (μ = 7.02 x10^{-2} g/cm.s; Particle Size = 2.38 x10^3 μm)

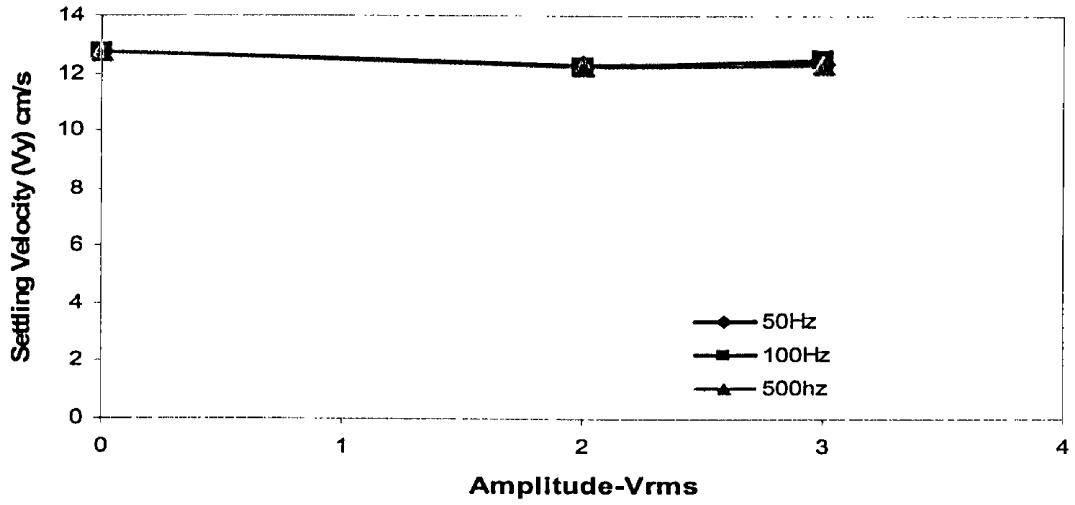

Figure 33A: Effect of Acoustic Amplitude on Settling Velocity of Acetal in Water at 10^0C (ρ = 1.40 g/cm^3; μ = 1.30x10^{-2} g/cm.s; Particle Size = 3.17 x10^3 μm)

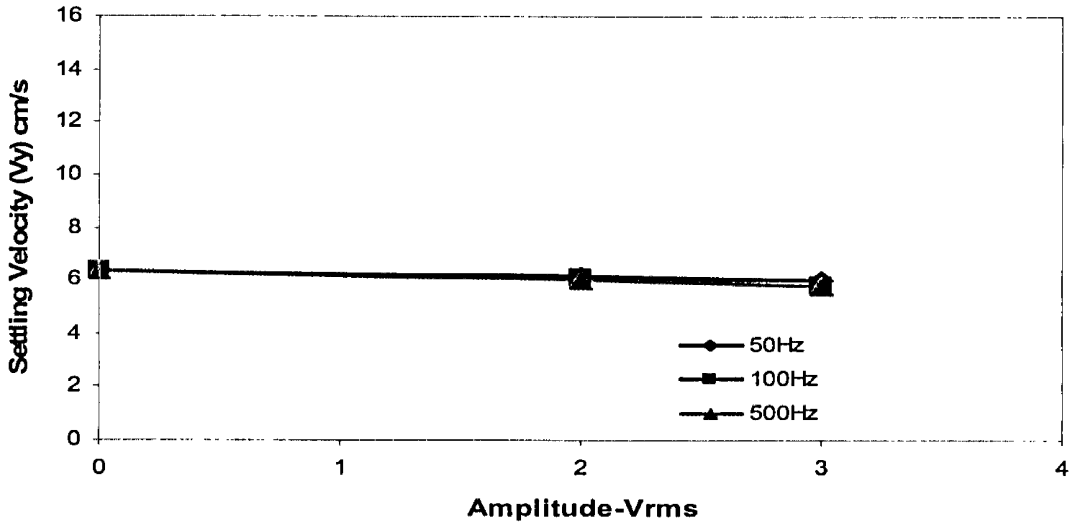

Figure 34A: Effect of Acoustic Amplitude on Settling Velocity of Acetal in HPC-Water at 10^0C (μ = 7.02 x10^{-2} g/cm.s; Particle Size = 3.1 x10^3 μm)

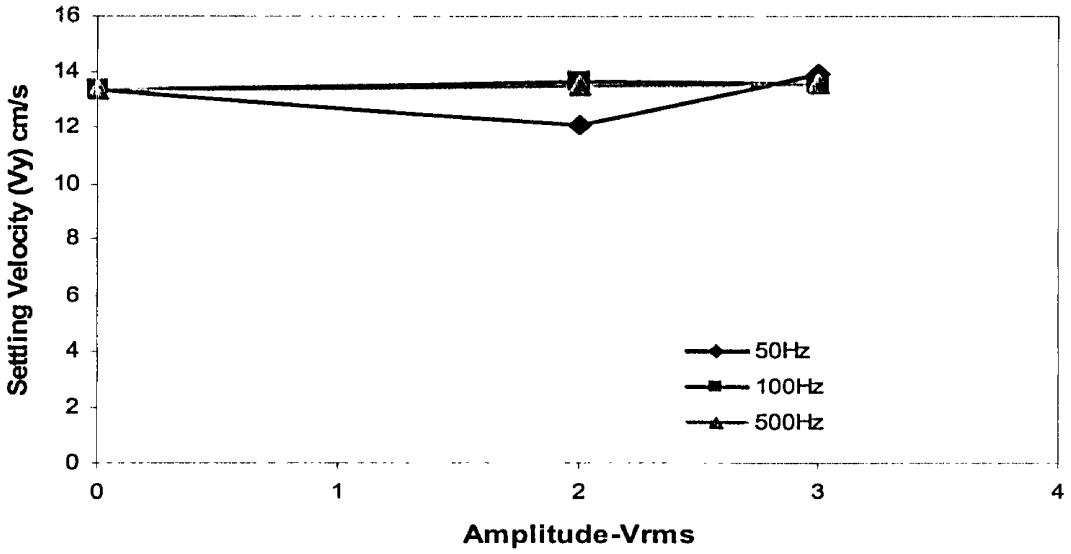

Figure 35A: Effect of Acoustic Amplitude on Settling Velocity of Acetal in Water at 10^0C (ρ = 1.40 g/cm^3; μ = 1.30x10^{-2} g/cm.s; Particle Size = 4.76 x10^3 μm)

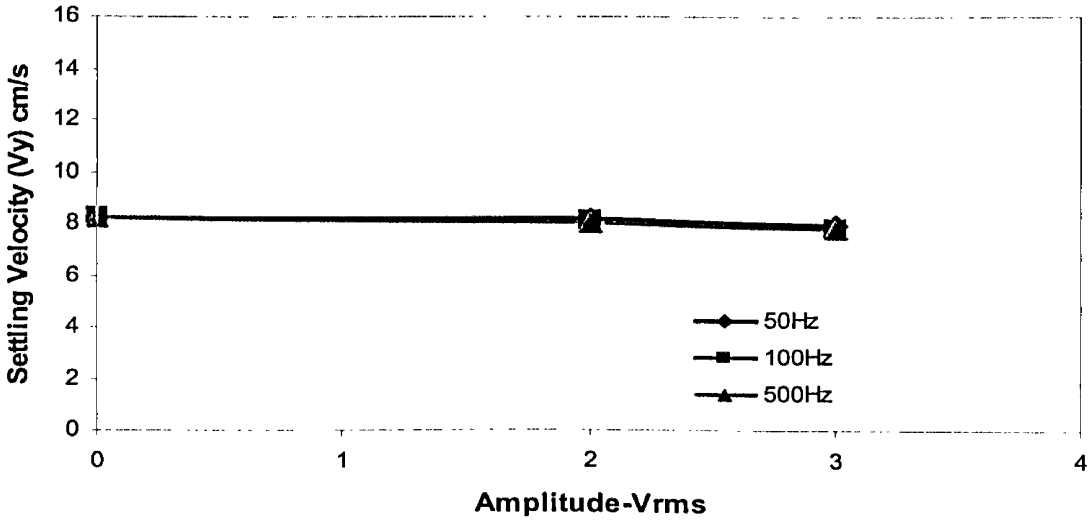

Figure 36A: Effect of Acoustic Amplitude on Settling Velocity of Acetal in HPC-Water at 10^0C (μ = 7.02 x10^{-2} g/cm.s; Particle Size = 4.76 x10^3 μm)

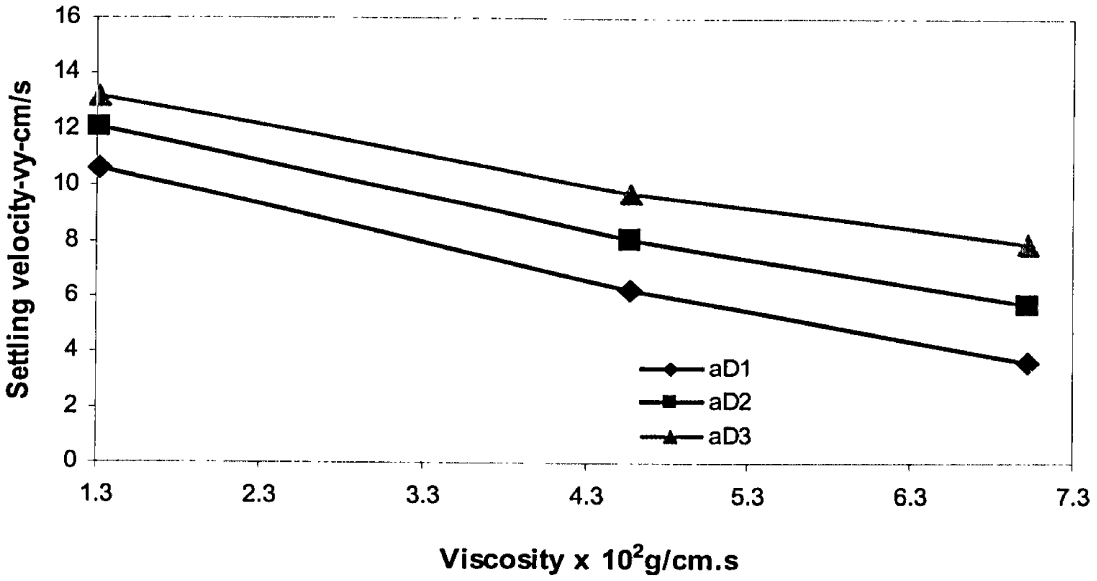

Figure 37A: Calculated Analysis - Effect of Viscosity -Acetal Spheres

Where aD1, aD2, and aD3 are the diameters of Acetal particles

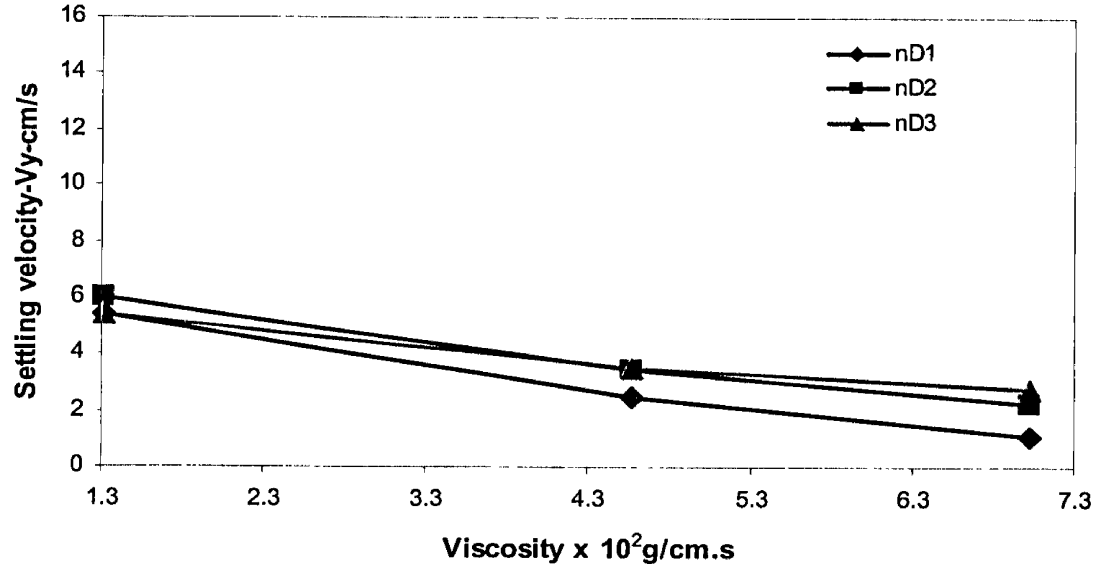

Figure 38A: Calculated Analysis - Effect of Viscosity -Nylon Spheres

Where nD1, nD2, and nD3 are the diameters of Nylon particles

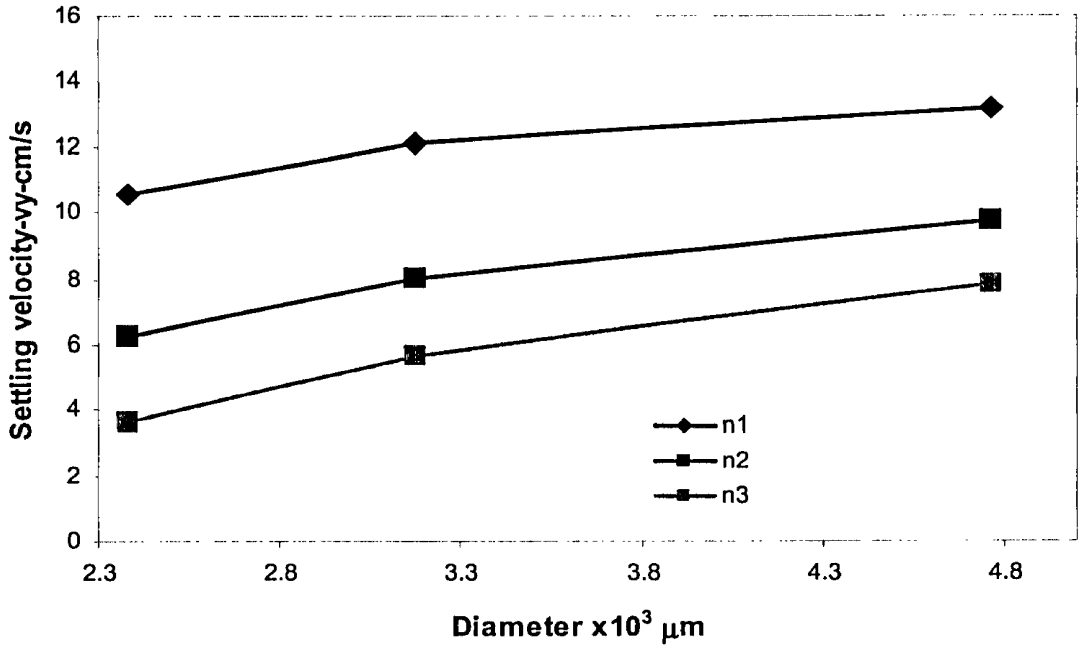

Figure 39A: Calculated Analysis - Effect of Size -Acetal Spheres

Where n1, n2, and n3 are the viscosities of the medium.

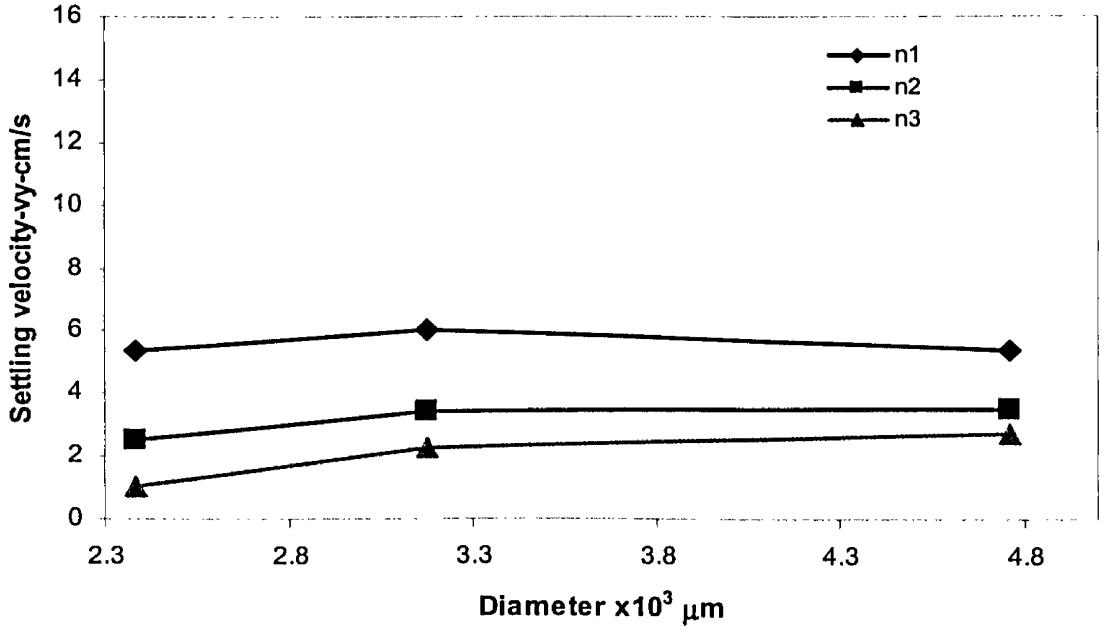

Figure 40A: Calculated Analysis - Effect of Size -Nylon Spheres

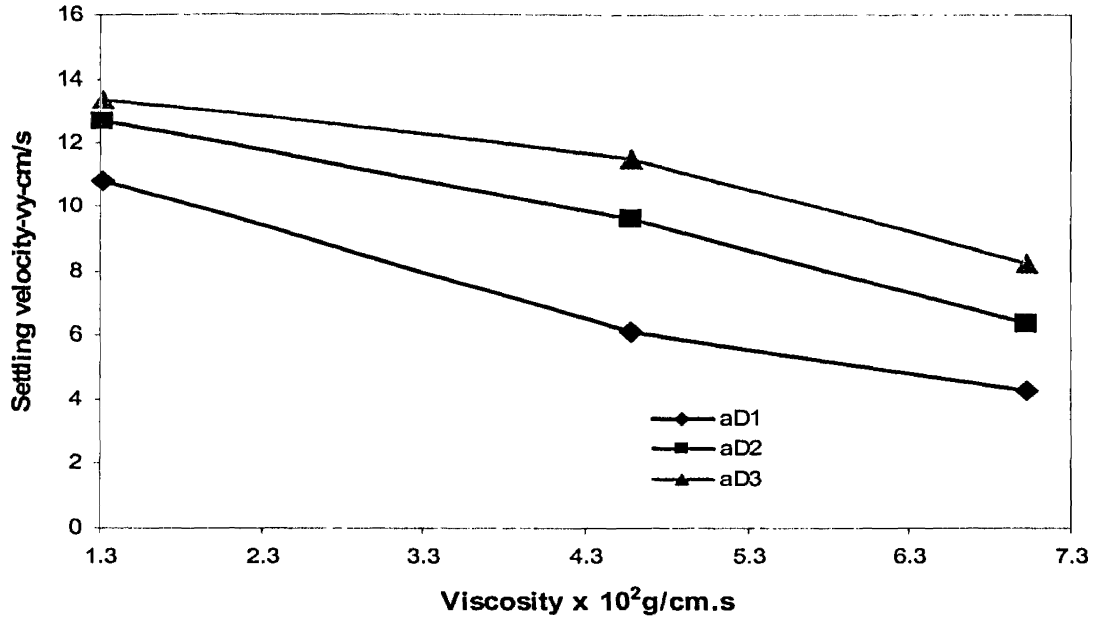

Figure 41A: Experimental Analysis - Effect of viscosity - Acetal Spheres

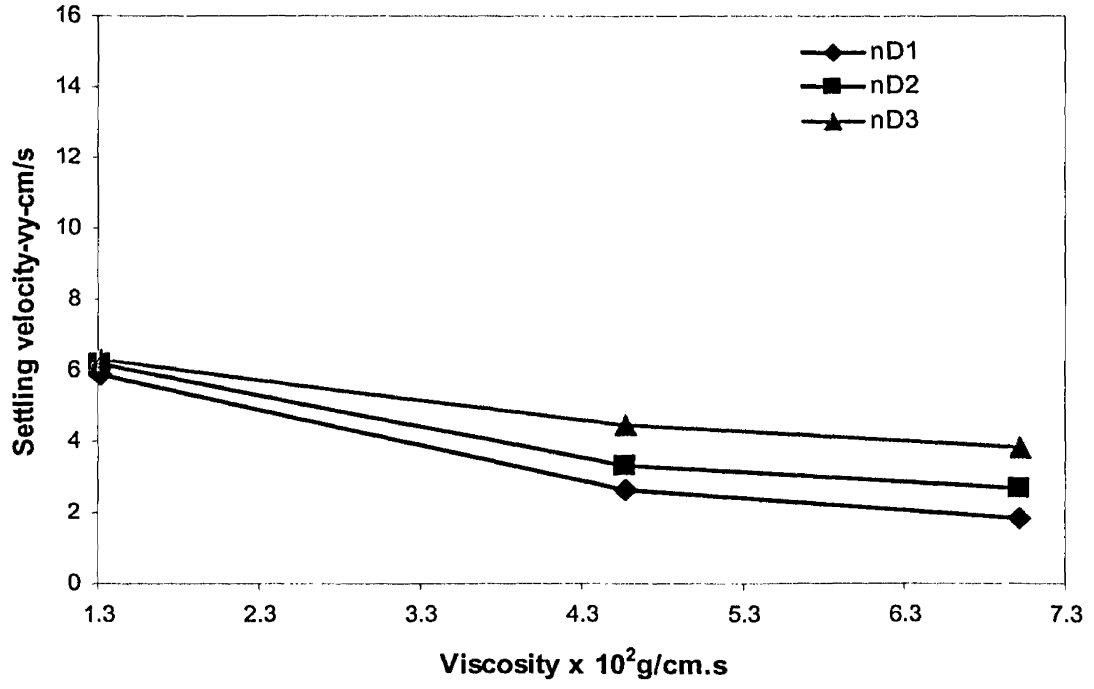

Figure 42A: Experimental Analysis - Effect of viscosity - Nylon Spheres

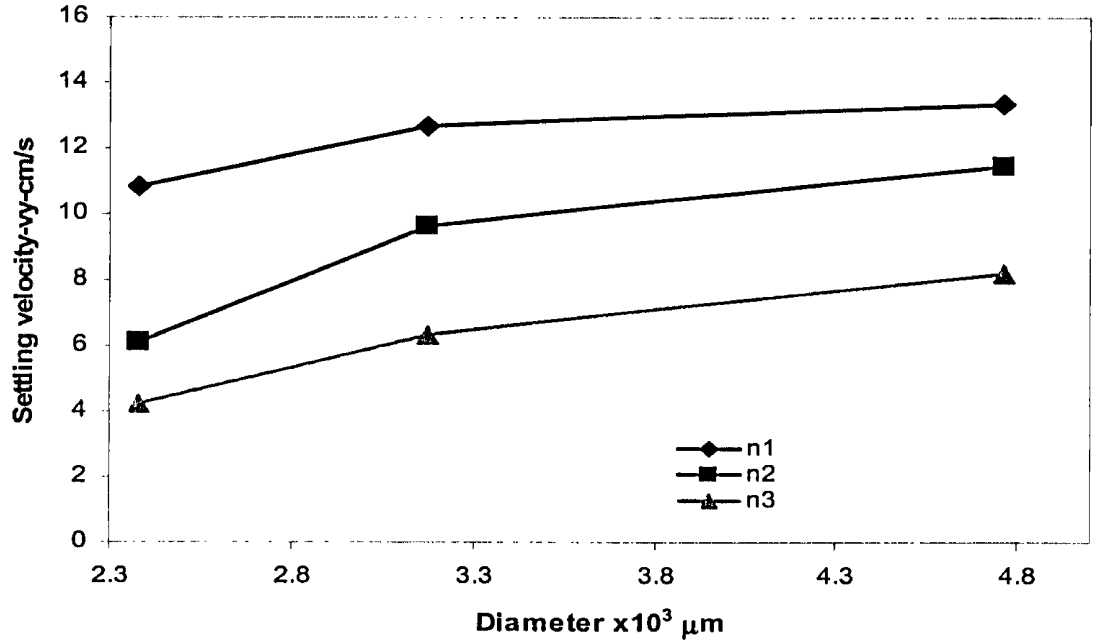

Figure 43A: Experimental Analysis - Effect of Size -Acetal Spheres

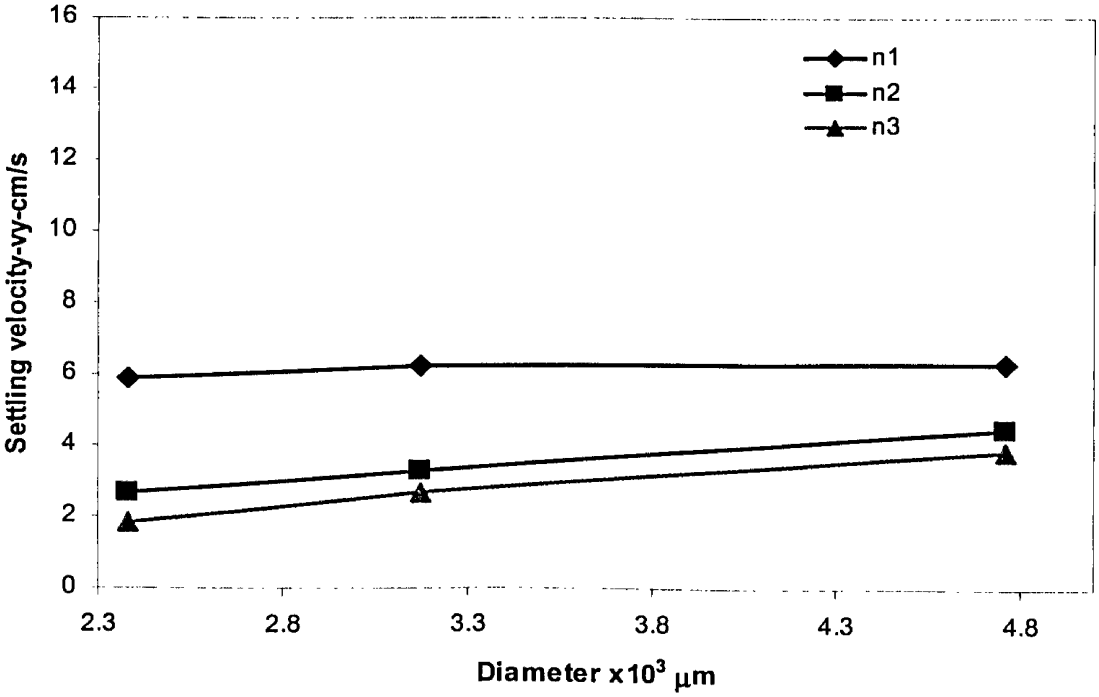

Figure 44A: Experimental Analysis - Effect of Size -Nylon Spheres

8.2 Appendix B (See attached CD)